nature astronomy

Article

https://doi.org/10.1038/s41550-024-02472-9

Abundant ammonia and nitrogen-rich soluble organic matter in samples from asteroid (101955) Bennu

Received: 25 July 2024

Accepted: 16 December 2024

Published online: 29 January 2025

Check for updates

A list of authors and their affiliations appears at the end of the paper

Organic matter in meteorites reveals clues about early Solar System chemistry and the origin of molecules important to life, but terrestrial exposure complicates interpretation. Samples returned from the B-type asteroid Bennu by the Origins, Spectral Interpretation, Resource Identification, and Security–Regolith Explorer mission enabled us to study pristine carbonaceous astromaterial without uncontrolled exposure to Earth's biosphere. Here we show that Bennu samples are volatile rich, with more carbon, nitrogen and ammonia than samples from asteroid Ryugu and most meteorites. Nitrogen-15 isotopic enrichments indicate that ammonia and other N-containing soluble molecules formed in a cold molecular cloud or the outer protoplanetary disk. We detected amino acids (including 14 of the 20 used in terrestrial biology), amines, formaldehyde, carboxylic acids, polycyclic aromatic hydrocarbons and N-heterocycles (including all five nucleobases found in DNA and RNA), along with ~10,000 N-bearing chemical species. All chiral non-protein amino acids were racemic or nearly so, implying that terrestrial life's left-handed chirality may not be due to bias in prebiotic molecules delivered by impacts. The relative abundances of amino acids and other soluble organics suggest formation and alteration by low-temperature reactions, possibly in NH_3-rich fluids. Bennu's parent asteroid developed in or accreted ices from a reservoir in the outer Solar System where ammonia ice was stable.

Primitive asteroids—those whose bulk chemistry was established in the protoplanetary disk—record processes that occurred during the formation and evolution of the early Solar System. The transport and delivery of organic compounds from these bodies could have been a source of molecules available for the emergence of life on Earth and potentially elsewhere.

Carbonaceous chondrite (CC) meteorites are samples of primitive carbon-rich bodies. In particular, the CI, CM, CR, CY and $C2_{ung}$ (Ivuna-like, Mighei-like, Renazzo-like, Yamato-like and ungrouped-type-2, respectively) CCs have experienced moderate to extensive aqueous alteration (reactions with liquid water) in their parent bodies and typically contain ~1–3 wt% total carbon, with rare instances up to ~5 wt% (ref. 1). Organic carbon is primarily found in structurally complex insoluble organic matter and a diverse mixture of soluble organic matter (SOM) that contains prebiotic organic molecules (ref. 2 and the references therein). However, it is often unclear which Solar System objects are the parent bodies of CCs[3]. Furthermore, they experience alteration upon exposure to the terrestrial environment[4], making interpretation challenging. The Origins, Spectral Interpretation, Resource Identification, and Security–Regolith Explorer (OSIRIS-REx) mission collected pristine material from the well-characterized surface of primitive B-type asteroid (101955) Bennu and delivered it to Earth under controlled conditions to minimize contamination and protect against atmospheric entry effects[5].

Spacecraft observations made in proximity to Bennu corroborated preflight predictions[6,7] of a carbon-rich composition, including strong

e-mail: daniel.p.glavin@nasa.gov

https://doi.org/10.1038/s41550-024-02472-9

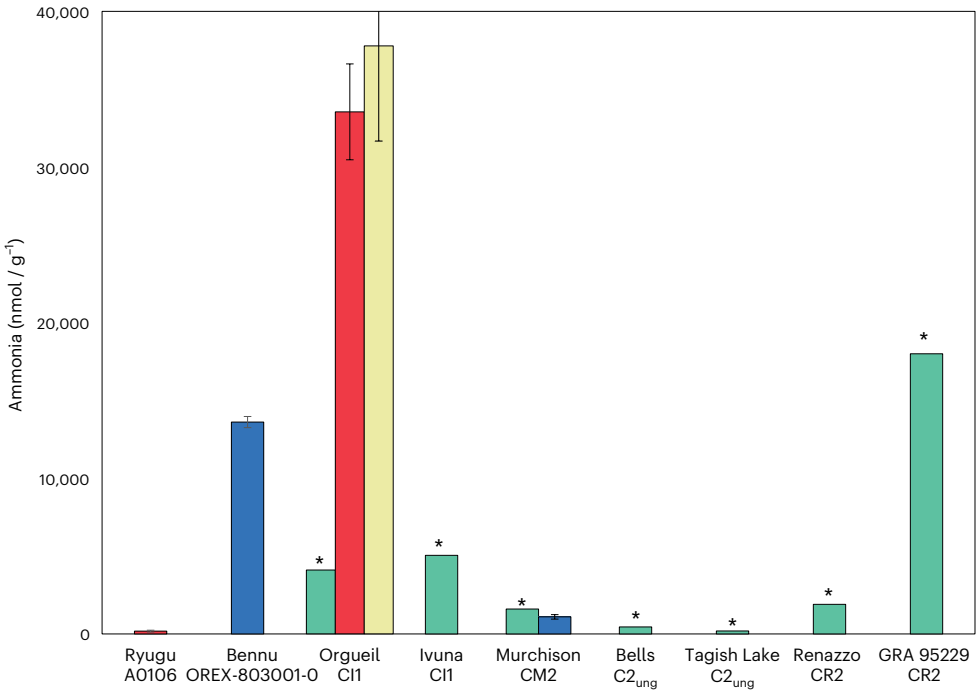

Fig. 1 | Concentrations of free ammonia measured in the extracts of Bennu (sample OREX-803001-0), Ryugu (sample A0106) and selected CCs. Data from this study (Extended Data Table 2) for the hot-water extracts of Bennu and Murchison (blue bars); data from hot-water extracts of Ryugu and Orgueil[21] (red bars); data from cold-water leachates of Orgueil[22] (yellow bar); and data from water and dichloromethane:methanol (9:1 v/v) extracts of Orgueil, Ivuna, Murchison, Bells, Tagish Lake (lithology not specified), Renazzo and GRA 95229 (ref. 16) (green bars). Data is presented as mean values ± the standard error of the mean. Estimated concentration of free ammonia is indicated by an asterisk taken from the data shown in Fig. 1a in ref. 16 and did not include errors. The large difference in ammonia concentrations measured in the Orgueil meteorite extracts could be due to differences in the extraction and analytical methods used[16,21,22] and/or sample heterogeneity.

aliphatic and aromatic organic carbon features at 3.4 µm, consistent with carbon abundances up to ~2.5 wt% and a low-temperature (<100 °C) aqueous alteration history[8,9]. A much weaker spectral feature observed at 3.1 µm could be consistent with some NH-bearing phases[9], such as ammonium salts or N-rich organic matter. The remote sensing data also confirmed that Bennu is a rubble pile[7], consisting of reaccumulated fragments of a larger, catastrophically disrupted asteroid (hereafter, parent body).

The spacecraft collected regolith (unconsolidated granular material) from as deep as ~0.5 m in Hokioi crater[10], which is thought to be a recent impact site on Bennu based on its redder than average spectral slope[11], and it delivered a total sample mass of 121.6 g to Earth[5]. Early laboratory analyses found C contents of 4.5–4.7 wt% and N contents of 0.23–0.25 wt% (ref. 5). The regolith's hydrated mineralogy[5] suggests that Bennu's parent body accreted ices, which condensed from the outer protoplanetary disk.

Given Bennu's compositional resemblance to aqueously altered CIs and CMs[5–9], we hypothesized[12] that the samples would contain a similar suite of organic compounds—including molecules found in biology, such as protein amino acids with left-handed enantiomeric excesses[13], carboxylic acids, purines, pyrimidines and their precursors—and similar abundances and distributions of SOM. To test these hypotheses and explore the implications for Bennu's parent body, we analysed organic matter in four aggregate (unsorted bulk) Bennu samples: two samples consisting of mostly fine particles (<100 µm) retrieved from spillover onto the avionics deck of the sample return canister[5,12] and two samples containing a mixture of fine and intermediate (100–500 µm) particles removed from inside the Touch-and-Go Sample Acquisition Mechanism (TAGSAM)[14] (Methods).

Results

We conducted elemental analyser–isotope ratio mass spectrometry (EA-IRMS) measurements of Bennu aggregates, including a hot-water extract and solid residue (Methods), and found comparable total abundances of C (4.5–4.7 wt%) and N (0.23–0.25 wt%) as the early analyses[5] (Extended Data Table 1). The hot-water extract was enriched in ^{15}N (+180 ± 47‰) (Extended Data Table 1 and Supplementary Table 4) and had a high concentration of ammonia ~13.6 µmol g^{-1} (Fig. 1 and Extended Data Table 2). The ammonia concentration corresponded to ~40% of the estimated total N in the Bennu hot-water extract before dry-down (Extended Data Table 1 and Supplementary Table 4). The large ^{15}N indicates that the ammonia was not derived from comparatively ^{15}N-depleted spacecraft hydrazine propellant (δ^{15}N = +4.7‰; Supplementary Information).

We performed untargeted analyses of methanol extracts of Bennu aggregate using Fourier-transform ion cyclotron resonance–mass spectrometry (FTICR-MS; Methods). The mass spectra of the extracts contained tens of thousands of compounds with mass-to-charge ratios (m/z) between 100 and 700 that correspond to ~16,000 molecular formulae consisting of C, H, N, O, S and Mg (Fig. 2). We identified a continuum of molecular sizes, with a range of carbon oxidation states, from non-polar or slightly polar—including polycyclic aromatic hydrocarbons, alkylated polycyclic aromatic hydrocarbons and a homologous series of unsaturated substituted aliphatic molecules—to more polar small molecules containing only CHO, CHNO, CHOS or CHNOS (Fig. 2, Extended Data Fig. 1 and Supplementary Fig. 15). The SOM is characterized by its nitrogen-rich chemistry, with up to seven nitrogen atoms per molecule detected by means of photoionization (APPI$^+$) and electrospray ionization (ESI$^{-/+}$), respectively (Fig. 2 and Extended Data Fig. 1).

We surveyed for amino acids using pyrolysis gas chromatography–triple quadrupole–mass spectrometry (pyGC-QqQ-MS; Methods and Supplementary Fig. 14). We then determined the abundances and enantiomeric ratios of amino acids in a hot-water extract by means of liquid chromatography with ultraviolet (UV) fluorescence detection

https://doi.org/10.1038/s41550-024-02472-9

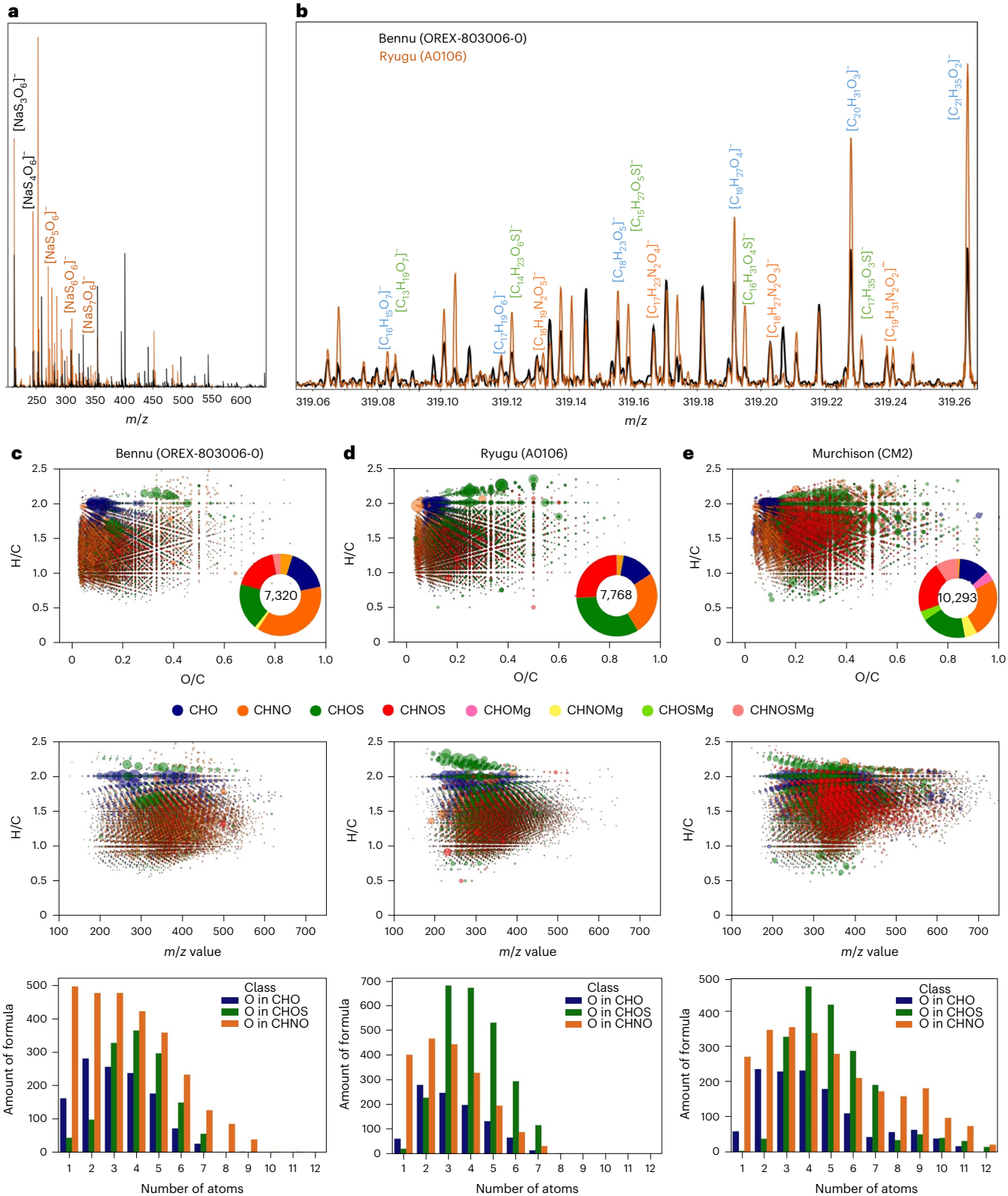

Fig. 2 | FTICR-MS data in electrospray ionization mode of the methanol extracts from Bennu (OREX-803006-0), compared with Ryugu (A0106) and Murchison. a, Mass spectra of Bennu (black) and Ryugu (orange) samples showing the relative abundance of polythionates with three to seven S atoms. **b**, Detail around $m/z = 319$ with major annotated elementary compositions (complete annotation can be found in Supplementary Fig. 3). **c**–**e**, Data visualization of the chemical compositions and number of molecules in Bennu (**c**) compared with Ryugu (**d**) and Murchison (**e**). Top, the Van Krevelen diagrams of H/C versus O/C atomic ratios of the compositional data as obtained from exact mass analysis. Coloured annuli enclose the total number of molecules assigned by mass, with colours indicating the relative abundances of the chemical families. Individual data points use the same colours to specify each family, and the size of each bubble reflects the intensity of the signal from the mass spectrum. Middle, the H/C atomic ratios as a function of m/z from 100 to 700. Bottom, the number of molecular formulae as a function of number of oxygen atoms in the CHO, CHOS and CHNO chemical families.

https://doi.org/10.1038/s41550-024-02472-9

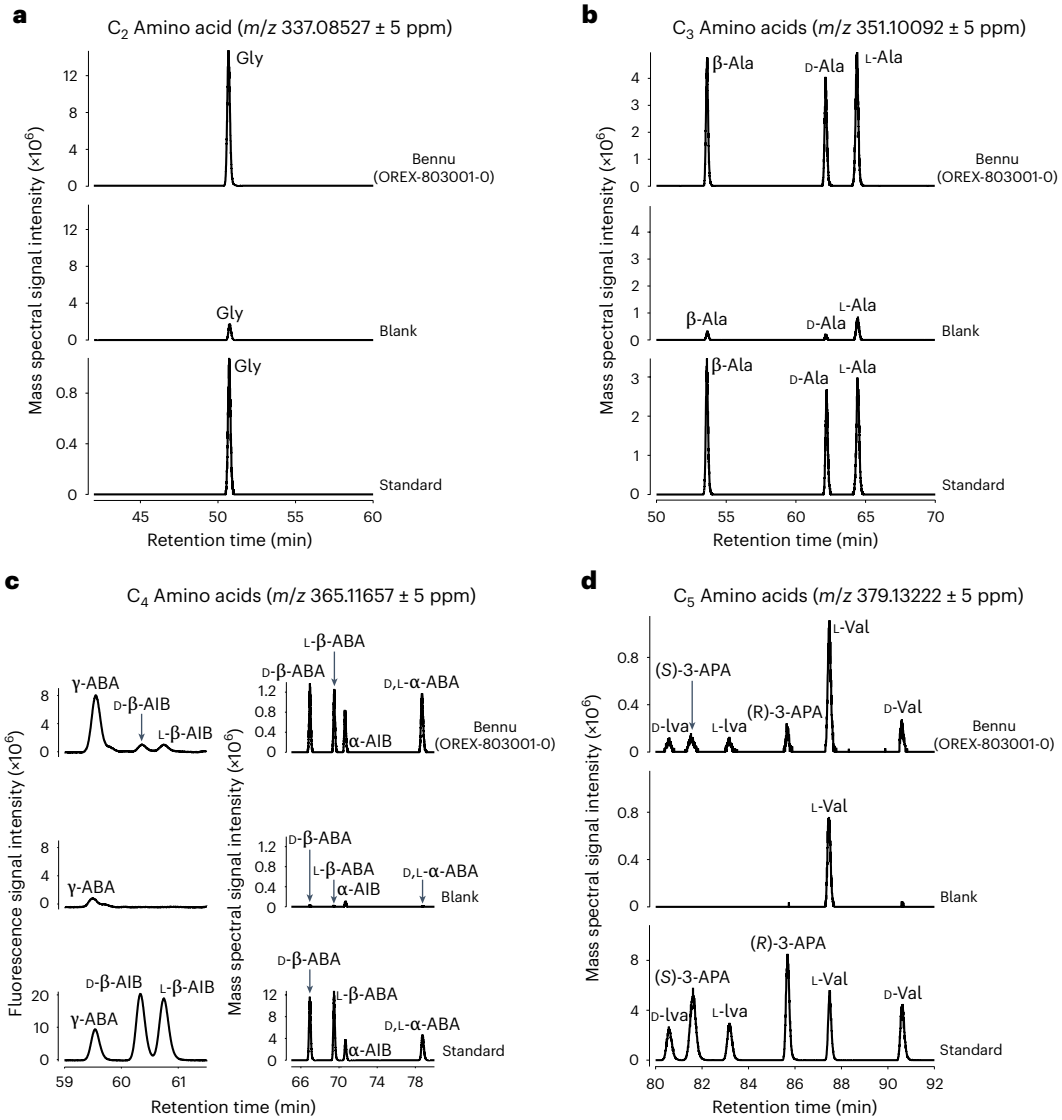

Fig. 3 | Amino acids identified by liquid chromatography mass spectrometry in the acid-hydrolysed, hot-water extract of Bennu (OREX-800031-0). **a**–**d**, Partial chromatograms obtained by LC-FD/HRMS after analysis of the standard and the 6 M HCl-hydrolysed water extracts of the FS-120 (blank) and Bennu (OREX-803001-0). **a**, Single-ion mass chromatograms at *m/z* 337.08527 corresponding to the C_2 amino acid glycine (Gly). **b**, Single-ion mass chromatograms at *m/z* 351.10092 corresponding to the C_3 amino acids β-alanine (β-Ala), D-alanine (D-Ala) and L-alanine (L-Ala). **c**, Right, single-ion mass chromatograms at *m/z* 365.11657 corresponding to the C_4 amino acids D-β-amino-*n*-butyric acid (D-β-ABA), L-β-amino-*n*-butyric acid (L-β-ABA), α-aminoisobutyric acid (α-AIB) and D,L-α-amino-*n*-butyric acid (D,L-α-ABA). Left, the UV fluorescence separation and detections of the C_4 amino acids γ-amino-*n*-butyric acid (γ-ABA) and D- and L-β-aminoisobutryic acids (D- and L-β-AIB). These C_4 amino acids were also detected in the single-ion chromatogram at *m/z* 365.11657; however, a large *o*-phthaldialdehyde/N-acetyl-L-cysteine (OPA/NAC) derivative peak eluted at a similar time as these amino acids, suppressing amino acid peak intensities. **d**, Single-ion mass chromatograms at *m/z* 379.13222 corresponding to the C_5 amino acids D-isovaline (D-Iva), L-isovaline (L-Iva), (*S*)-3-aminopentanoic acid (*S*-3-APA), (*R*)-3-aminopentanoic acid (*R*-3-APA), L-valine (L-Val) and D-valine (D-Val). The amino acids detected in the blank are likely to be derived from the solvents and derivatization reagents used for sample processing and analysis.

and mass spectrometry (LC-FD/MS; Fig. 3, Methods, Extended Data Fig. 2 and Supplementary Figs. 8 and 9).

A total of 33 amino acids were identified in the Bennu aggregates along with an uncounted suite of C_6 and C_7 aliphatic amino acids that were also detected but were not identified by name with standards (Fig. 3, Extended Data Tables 2 and 3 and Extended Data Fig. 2). These included 14 of the 20 standard protein amino acids used in terrestrial biology (Supplementary Table 12), all previously reported in meteorites[13]. Glycine was the most abundant amino acid (44 nmol g^{-1}), with the majority in a free form, that is, without acid hydrolysis (Extended Data Table 3). Methionine, tyrosine and asparagine were tentatively detected at trace levels above background near the 0.1 nmol g^{-1} detection limit (Supplementary Table 12).

In addition, 19 non-protein amino acids were identified (Extended Data Table 3 and Supplementary Figs. 6, 8 and 9). All possible isomers of the C_3 to C_5 primary aliphatic amino acids were identified in the hot-water extract, as well as leucine, isoleucine and ε-amino-*n*-caproic acid at trace levels (Fig. 3, Extended Data Table 3 and Supplementary Figs. 8 and 9).

All chiral non-protein amino acids that could be enantiomerically resolved, including isovaline, norvaline, β-amino-*n*-butyric acid, β-aminoisobutyric acid and 3-aminopentanoic acid, were present as racemic or near racemic mixtures (equal abundances of D- and L-enantiomers) within analytical uncertainties (Extended Data Table 4). The detection of racemic alanine and aspartic acid within error indicates that the sample was pristine, with negligible biological L-protein

https://doi.org/10.1038/s41550-024-02472-9

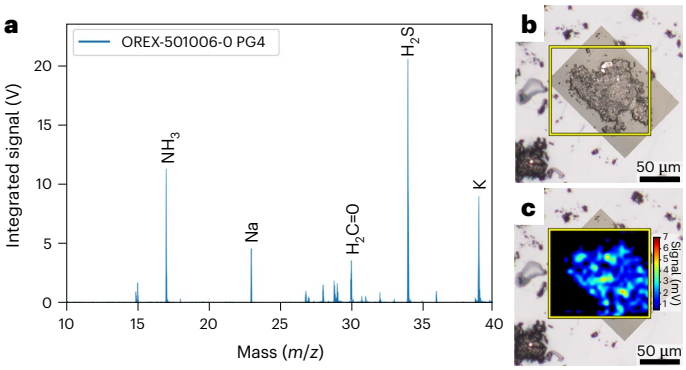

Fig. 4 | Ammonia and formaldehyde in Bennu (OREX-501006-0) identified by μ-L²MS. a, Summed mass spectrum acquired from several ~100 μm grains mounted on a KBr window with mass peaks for ammonia (NH_3), sodium (Na), formaldehyde ($H_2C{=}O$), hydrogen sulfide (H_2S) and potassium (K) indicated. Spectrum acquired by μ-L²MS using a vacuum UV photoionization at 118 nm. **b**, Optical mosaic of particle with yellow box demarking region mapped by μ-L²MS. **c**, Spatial map of ammonia distribution overlaid over optical image. The μ-L²MS laser beam spot size was 5 μm.

amino acid contamination. An L-valine excess of ~34% was measured in the same hot-water extract after acid hydrolysis (Extended Data Table 4); however, we also observed elevated levels of L-valine in the procedural blank (Fig. 3), so laboratory contamination is a possible explanation. Isotopic measurements of valine will be needed to constrain the origin of the measured L-excess in the Bennu extract.

Ammonia and formaldehyde are potential precursors for the synthesis of amino acids and other soluble organic molecules and were key targets for this investigation. Ammonia was independently identified, along with formaldehyde, in an avionics deck sample using micro two-step laser mass spectrometry (μ-L²MS) (Fig. 4 and Methods). Ammonia was also heterogeneously distributed in these particles at the ~5 μm scale (Fig. 4). Most of the ammonia in the Bennu aggregate samples was likely to have been originally retained as salts or bound to clay minerals or organic matter[15,16] because highly volatile free ammonia is prone to loss. Volatile methylamine (914 nmol g^{-1}) and ethylamine (121 nmol g^{-1}), which are derivatives of ammonia, dominated the 16 aliphatic primary amines identified in the hot-water extract (Extended Data Table 2 and Supplementary Fig. 6) and were also likely to be present as salts.

Nine C_1–C_7 monocarboxylic acids and two dicarboxylic acids were identified in the hot-water extract by GC-QqQ-MS (Extended Data Table 5 and Supplementary Fig. 10). Formic (4,106 nmol g^{-1}) and acetic (1,436 nmol g^{-1}) acids were the two most abundant carboxylic acids detected.

At least 23 different N-heterocycles, including all five canonical biological nucleobases (adenine, guanine, cytosine, thymine and uracil) (Extended Data Table 6), were identified in an acid extract by high-performance liquid chromatography with electrospray ionization and high-resolution mass spectrometry (HPLC/ESI-HRMS; Methods and Supplementary Figs. 11–13). Many of these N-heterocycles were also detected in aggregate material using wet chemistry pyGC-QqQ-MS (Supplementary Fig. 14).

Discussion

Evidence for extraterrestrial soluble organic matter

The diversity of SOM in the Bennu methanol extract (Fig. 2) is inconsistent with terrestrial biology, which has a much simpler distribution[17]. The large ^{15}N enrichment ($\delta^{15}N$ = +180‰; Extended Data Table 1) in the hot-water extract that consisted of ammonia, amines, amino acids, N-heterocycles and other N-containing molecules falls well outside the $\delta^{15}N$ terrestrial organics range of −10‰ to +20‰ (ref. 18). The complex distribution of amines, carboxylic acids and mostly racemic amino acids, including several non-protein amino acids that are rare or non-existent in biology (Extended Data Tables 2–5), strongly supports an extraterrestrial origin of these molecules. The violation of Chargaff's rules (1:1 ratio of purine and pyrimidine bases should exist in the DNA of any organism) and diversity of N-heterocycles, including biologically uncommon molecules (Extended Data Table 6), also indicate a non-terrestrial origin.

Bennu's volatile-rich nature compared with other astromaterials

The Bennu aggregate samples analysed in this study had a higher mass-weighted average abundance of total C and N than previously studied CI and CM meteorites[19] and aggregate samples from Ryugu (Supplementary Table 3). This high volatile content may be related to the formation environment and/or alteration history of Bennu's parent body. Although Bennu's mineralogy and elemental composition are similar to those of the extensively altered CI1 chondrites[5], the bulk H and N isotopic compositions (Extended Data Table 1 and Supplementary Fig. 3) suggest a closer affinity to less aqueously altered type-2 chondrites, such as Tagish Lake and Tarda.

The diversity of SOM in the Bennu aggregates is comparable with that in Ryugu samples and the CM2 meteorite Murchison[17,20], though with a lower mass range and carbon oxidation state than Murchison (Fig. 2 and Extended Data Fig. 1). The nitrogen-rich composition of the Bennu aggregates analysed so far contrasts with the sulfur-rich chemistry of the Ryugu samples[20], reflecting low-temperature aqueous processing on Bennu's parent body and a nitrogen-rich organic chemistry distinct from that of the most aqueously altered CI and CM chondrites.

The water-extracted ammonia abundance that we measured for Bennu was 12 times higher than in Murchison and 75 times higher than in Ryugu (Fig. 1 and Extended Data Table 2). It is exceeded only by that of the CR2 Graves Nunataks (GRA) 95229 (ref. 16) and the CI1 Orgueil[21,22]. A different Orgueil sample extract[16] had much lower free ammonia abundances compared with Bennu (Fig. 1). Because hydrothermal treatment at 300 °C and 100 MPa releases additional insoluble organic matter-bound ammonia from these CCs[16], the abundance of ammonia in the Bennu hot-water extract is likely to represent a lower limit (Extended Data Table 2). Ammonium salts have also been identified in comet 67P/Churyumov–Gerasimenko[23,24] and the dwarf planet Ceres[25]. Carboxylic acids are typically among the most abundant soluble organic compound classes in CCs (Fig. 5)[26], and these molecules could have served as the counterions to any ammonium salts in Bennu (for example, ammonium formate as observed in comet 67P (refs. 23,24)).

The C_1–C_6 amine distribution follows the trend of decreasing concentration with increasing size observed in CI1, CM2 and $C2_{ung}$ chondrites (Extended Data Table 2). However, the higher overall abundance and broader distribution of amines compared with Ryugu and Orgueil (Extended Data Table 2) could be explained by a lower degree of aqueous activity during organic synthesis in Bennu's parent body. Ryugu samples exhibit a much higher abundance of isopropylamine versus the less thermally stable *n*-propylamine[27], whereas the straight-chain and branched amine abundances we measured for Bennu were similar to each other (Extended Data Table 2). This observation may also be indicative of less extensive hydrothermal alteration in Bennu's parent body.

The Bennu hot-water extract displays greater structural diversity of monocarboxylic acids compared with Ryugu with nine C_1–C_7 carboxylic acids identified (Extended Data Table 5). Although the Ryugu aggregate has much higher total abundances of formic and acetic acids compared with Bennu, no other monocarboxylic acids were reported in the Ryugu extract above 0.1 nmol g^{-1} (Extended Data Table 5). This difference could be a result of a more acidic pH of the fluids on Ryugu's

https://doi.org/10.1038/s41550-024-02472-9

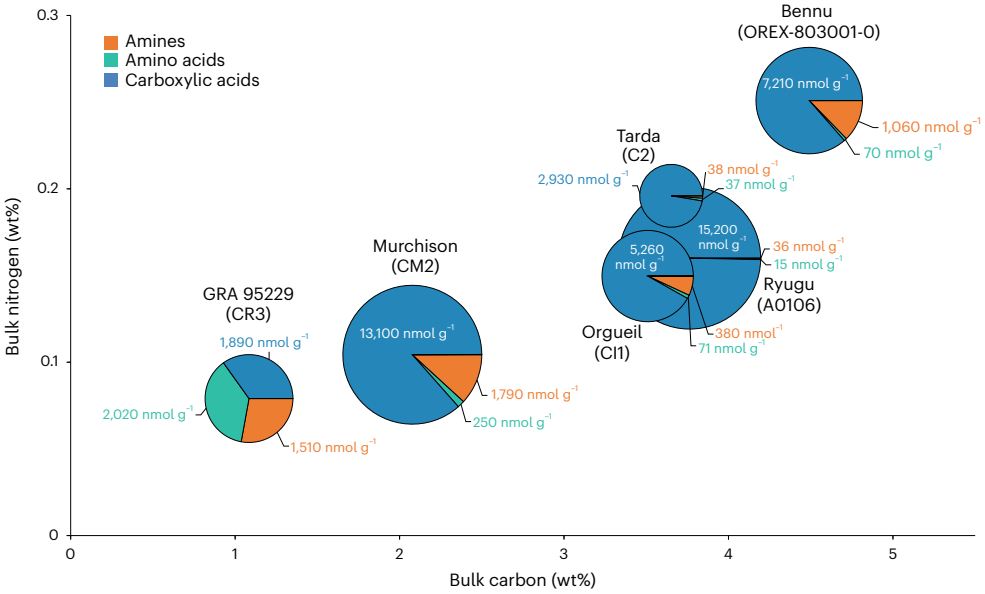

Fig. 5 | Distribution and total abundances of amines, amino acids and carboxylic acids in Bennu (OREX-803001-0) compared with Ryugu (A0106) and selected CCs. Relative percentages of amines (orange), amino acids (green) and carboxylic acids (blue) are given in the individual pie charts with their overall size proportional to the total sum of the abundances of the three soluble organic compound classes. The pie charts are plotted on a bulk N versus C diagram to illustrate the total C and N abundance differences between the samples in weight percentage. The values for the total sum of the abundances of the molecules detected in each compound class are also given in nanomoles per gram for each pie slice. Although N-heterocycles were also quantified in Bennu and Murchison, these data were excluded from this figure due to their low abundances relative to the other compound classes and incomplete data for the other samples. The N-heterocycle abundance data for Bennu, Murchison, Orgueil and Ryugu are included in Extended Data Table 6. Other water-soluble organic compounds such as aldehydes and ketones, hydroxy acids, cyanides and amides have been identified in CCs[2] but were not analysed in this study and are therefore also not included in the figure. The amine, amino acid and carboxylic acid data for Murchison and Bennu are from this investigation (Extended Data Tables 2, 3 and 5). Previously published data from Ryugu[20] and GRA 95229 (ref. 15) are also shown. For Orgueil, published amine[58] and amino acid[59] data were used, whereas the carboxylic acid data are from this study (Extended Data Table 5). The data for Tarda from Extended Data Tables 2, 3 and 5 were also measured in this study.

parent body[21] compared with Bennu's, leading to their evaporation and/or more extensive aqueous alteration, ultimately decomposing or altering carboxylic acids[28]. The structural diversity of carboxylic acids in Bennu is consistent with an origin through stochastic low-temperature free radical reactions on interstellar dust grains[26]. Isotopic analyses of carboxylic acids are needed to further constrain the abiotic origins of these molecules in Bennu.

The total abundance of identified C_2 to C_6 protein and non-protein amino acids in the Bennu hot-water extract (~70 nmol g^{-1}) was lower by a factor of 3.6 than that in Murchison but 4.7 times higher than in Ryugu extracts (Fig. 6 and Extended Data Table 3). Bennu's total amino acid abundance resembles that of CI1 and some less altered CM2 and $C2_{ung}$ chondrites (Fig. 6a). However, the amino acid distribution is dominated by glycine, with lower relative abundances of α-alanine, β-alanine, α-aminoisobutyric acid and isovaline compared with CCs (Fig. 6a). The high relative abundances of glycine and racemic mixtures of most α-amino acids suggest a formation by means of HCN polymerization and/or Strecker-cyanohydrin synthesis during aqueous alteration in Bennu's parent body[2]. However, alternate amino acid formation mechanisms[2,29] are required to explain the formation of the β-, γ- and δ-amino acids observed in the hot-water extract (Extended Data Fig. 2 and Extended Data Table 3).

The low β-alanine/glycine ratio (~0.08) that we measured for Bennu is unexpected based on trends observed in CCs (Fig. 6a) and Bennu's CI-like elemental composition and mineralogy[5]. Higher β-alanine/glycine ratios, such as those found in type-1 chondrites and Ryugu samples (>2.7; Fig. 6a), align with extensive hydrothermal alteration, whereas the lower ratio in Bennu is closer to the less aqueously altered type-2 chondrites (Fig. 6a).

Bennu's amino acid distribution indicates a distinct chemical composition and/or lower-temperature aqueous alteration history of its parent body compared with those of Ryugu and the aqueously altered CCs. Future analyses of the distribution and stable isotopic compositions of amino acids in Bennu samples, including their precursors and related structures, will provide further insight into the formation and evolution of these prebiotic molecules.

The measurement of racemic isovaline (Fig. 6b) and other amino acids, within analytical error, was also unexpected (Extended Data Table 4). Based on the evidence for extensive water activity in Bennu's parent body[5,30,31], we predicted that Bennu samples would show some L-isovaline excess, following the empirical trend of higher extraterrestrial L-isovaline excesses in more aqueously altered CCs[13]. Furthermore, substantial L excesses in aspartic and glutamic acids (up to ~60%) measured in some lithologies of the Tagish Lake meteorite and attributed to amplification by crystallization of conglomerate-forming amino acids during parent body aqueous alteration[32], were not observed in Bennu aggregate either (Extended Data Table 4). The source of the meteoritic L-amino acid enrichments remains a mystery. At least for now, the lack of any amino acid enantiomeric excesses of confirmed extraterrestrial origin in the Bennu material analysed here, as well as in samples from Ryugu[20,27] and some lithologies of Tagish Lake and Tarda (Extended Data Table 4), challenges the hypothesis that the emergence of left-handed protein-based life on Earth was influenced by an early Solar System bias toward L-amino acids[13].

The total abundance of N-heterocycles identified in Bennu samples (~5 nmol g^{-1}; Extended Data Table 6) is 5–10 times higher than reported in Ryugu[33] and Orgueil[34]. The elevated abundances and more complex distribution of N-heterocycles again may reflect a lower degree of hydrothermal alteration in Bennu's parent body during organic synthesis compared with Ryugu's, which is consistent with trends that have been observed in aqueously altered CI and CM chondrites[34]. However, the ratio of purines to pyrimidines is much lower

https://doi.org/10.1038/s41550-024-02472-9

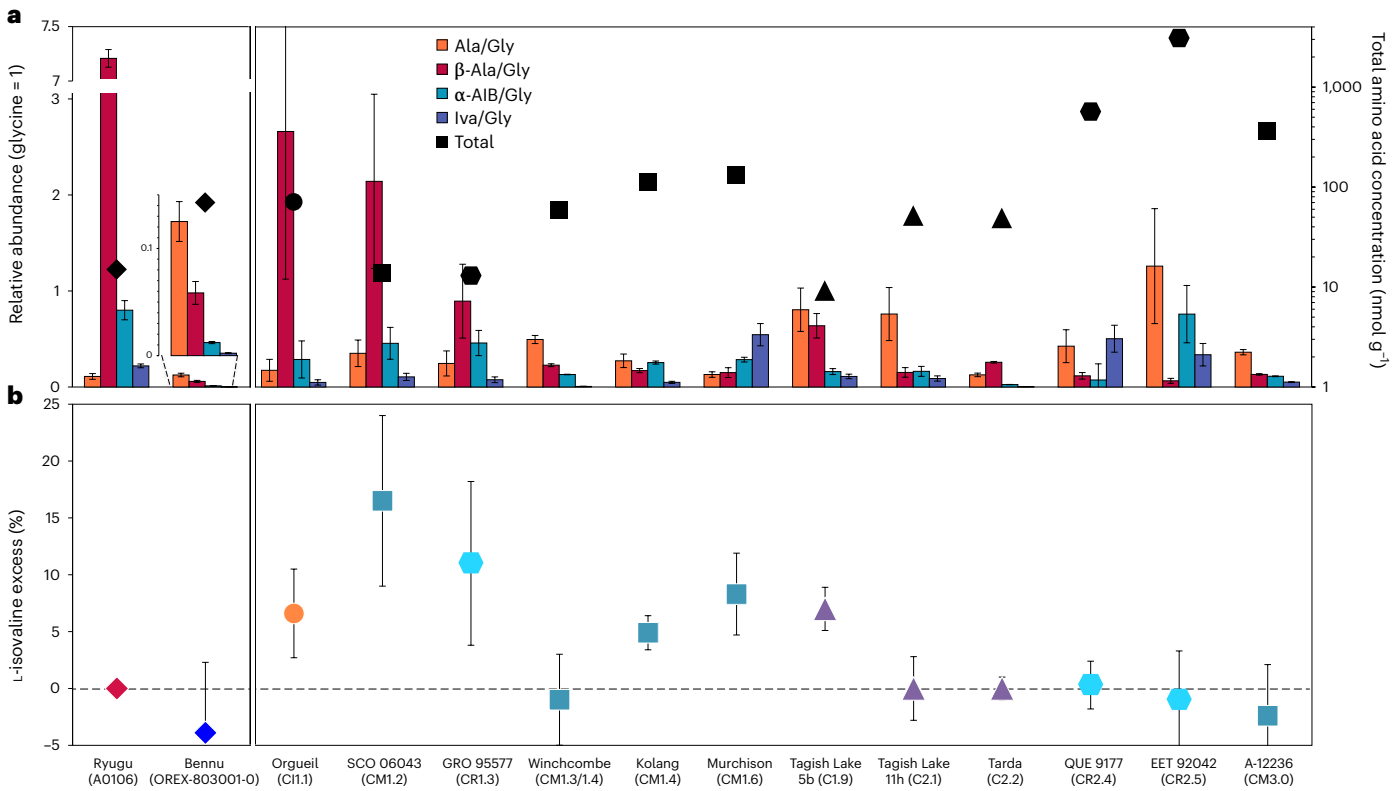

Fig. 6 | Relative abundances and total concentrations of amino acids and percentage of L-isovaline enantiomeric excesses measured by liquid chromatography mass spectrometry in Bennu (OREX-803001-0) compared with Ryugu (A0106) and selected CCs. a, The relative molar abundances (left *y* axis, glycine = 1) of alanine (Ala), β-alanine (β-Ala), α-aminoisobutyric acid (α-AIB) and isovaline (Iva) are shown as coloured bars with uncertainties determined by standard error propagation of the absolute errors. The total concentrations of identified C_2 to C_6 amino acids in the 6 M HCl-hydrolysed, hot-water extracts of the samples are designated by the black data points (right *y* axis, logarithmic scale). **b**, L-isovaline excesses ($\%L_{ee} = \%L - \%D$) and associated standard errors were calculated from the average individual abundances of D- and L-isovaline in the same extracts. The amino acid data for Bennu are the average values reported in Extended Data Tables 3 and 4. Published amino acid data from Ryugu, Orgueil, SCO 06043, GRO 95577, Murchison, Tagish Lake 5b and 11h, QUE 99177, EET 92042 and A-12236 are shown for comparison[20,27,32,59,60]. The Winchcombe, Kolang and Tarda-RV data are newly published here. The CCs are ordered from least to most aqueously altered (right to left) as inferred from their petrologic type assignments shown in parentheses based on the abundance of H in OH/H_2O (ref. 56). The colours and symbols used were selected to differentiate between asteroids Bennu and Ryugu, and the different CC groups (CI, CM, $C2_{ung}$ and CR).

in the Bennu extract (0.55; Extended Data Table 6) than in Murchison (~2.8) and Orgueil (~1.1). This elevated abundance of pyrimidines over purines may be related to differences in the parent bodies' chemical composition, formation pathways and/or aqueous alteration histories. N-heterocycles can be readily synthesized from ammonia and formaldehyde, especially under alkaline conditions[35]. Because pyrimidines are preferentially formed over purines in interstellar ice–analogue irradiation experiments[36], it is also possible that Bennu's N-heterocycles and/or their chemical precursors were inherited from a cold molecular cloud environment. The unusual richness of N-heterocycles may be of relevance for prebiotic chemistry. Further studies of nucleobase chemistry in samples returned from Bennu, from precursors to nucleic acids, are warranted.

Bennu's origin and implications for prebiotic chemistry

The elevated volatile content, the large ^{15}N enrichments of ammonia and other water-soluble N-containing molecules and the high abundance of N-rich isotopically anomalous organic matter[37] observed in the Bennu samples suggest that the parent body accreted ices from a reservoir in the outer Solar System, where ammonia ice was stable (beyond Jupiter's current orbit). Dynamical simulations predict that Bennu derived from a secondary parent body in the inner main belt (2.1–2.5 au) that broke up 730–1,550 Myr ago[38]. The parent body may have originated in the outer Solar System, perhaps emplaced into the asteroid belt during giant-planet migrations, as has previously been proposed for CI chondrites and Ryugu[39]. Alternatively, ices may have migrated inward by means of pebble drift, a process where small, icy pebbles drift inward from the outer Solar System and accrete onto forming planetesimals in the asteroid belt. This mechanism would allow material from more distant, colder regions, where ammonia and other volatile ices are stable, to be incorporated into bodies forming closer to the Sun[40].

B-type asteroids such as Bennu[41], so named for their blue spectral slopes, and other small bodies that emit particles[42] have been hypothesized[43] to be fragments of extinct comets sampling a continuum of objects, from dry planetesimals that formed close to the Sun to volatile-rich icy bodies that formed well beyond the water snow line. There is some evidence of low-temperature aqueous activity in comets, including the spectroscopic detection of hydrated minerals and carbonates in the impact ejecta of comet 9P/Temple 1 by the Spitzer Space Telescope[44] and cubanite in samples from comet 81P/Wild[45]. Nevertheless, the phyllosilicate-dominated bulk mineralogy of Bennu samples[5] and the spacecraft observations of metre-sized carbonate-rich veins[31] on Bennu both imply large-scale hydrothermal activity for millions of years that may not be consistent with a cometary parent body origin.

Alternatively, the presence of ammonium and carbonate salts, high organic carbon content and evidence of rock-fluid interactions observed in Ceres[25,46,47] suggest that Bennu may consist of fragments of a Ceres-like primitive icy body that experienced extensive low-temperature aqueous activity. Petrologic data from Bennu samples

indicate that late-stage fluid in the parent body sequentially precipitated evaporite minerals, starting with Ca and Mg carbonates, progressing to phosphates, followed by Na carbonates and concluding with halides and sulfates[48]. These minerals strongly imply alkaline pH, substantial concentrations of dissolved inorganic carbon and fluid temperatures below ~55 °C (ref. 48). This dynamically changing environment in Bennu's parent body is likely to have fostered intricate interactions among brine fluid chemistry, soluble organics and freshly exposed mineral surfaces. High concentrations of ammonium salts in Bennu's parent body could have created liquid brines at very low temperatures (NH_3–H_2O eutectic of 176 K), and thus provided an aqueous environment for organic chemistry to continue even as the abundances of short-lived radionuclides responsible for internal heating were exhausted[49]. For example, a suite of amino acids dominated by glycine and the purines adenine and guanine were produced in dilute NH_4CN kept at 195 K for 25 yr (ref. 50). Eutectic freezing, phyllosilicate catalysis, low-temperature template polymerization and Mg salts are employed in the laboratory polymerization of activated nucleotides[51].

Additional analyses of Bennu samples, coupled with laboratory analogue experiments and future sample return missions from a comet and Ceres, will be important to further understand the origin and evolution of prebiotic organic matter in Bennu and potential chemical links between volatile-rich asteroids and primitive icy bodies. Regardless of their origins, asteroids such as Bennu could have been a source of N-rich volatiles and compounds of biological importance, including ammonia, amino acids, nucleobases, phosphates and other chemical precursors that contributed to the prebiotic inventory that led to the emergence of life on Earth.

Methods

Before these investigations, validation of the analytical methods used in this study were performed on Murchison and Sutter's Mill as part of OSIRIS-REx sample analysis readiness tests[52–54].

Samples used in this investigation

The Bennu aggregates studied (Supplementary Fig. 1) consisted of a mixture of mostly fine (<100 µm) to intermediate (100–500 µm) sized particles with some coarse (>500 µm) grains dominated by hydrous silicate minerals (~80% phyllosilicates by volume) with lower abundances (≤10%) of sulfides, magnetite, carbonates, anhydrous silicates (olivine and pyroxene) and other minor phases[5]. The Bennu sample nomenclature as well as the detailed processing and analytical flow of the aggregate samples are summarized in Supplementary Table 1 and Supplementary Fig. 2.

Two aggregate samples (OREX-500002-0 and OREX-500005-0) that were included as part of the 'quick-look' (QL)[5,12] analyses were removed from the avionics deck surface, weighed and then containerized under N_2 in the curation glovebox[55] at the NASA Johnson Space Center (JSC). OREX-500002-0 (~22 mg) consisted primarily of dark fines and some intermediate-sized particles, with some bright and highly reflective particles, and numerous (>5) white fibres thought to be derived from the sample return capsule aluminized Kapton multilayer insulation filled with fibreglass. The sample was sealed under N_2 between two glass concavity slides and shipped from NASA JSC to the Carnegie Institution for Science (CIS). This sample was inspected under an optical microscope at CIS, and the fibres were physically removed from the sample with organically clean stainless-steel tweezers. A 1.1 mg subsample of the aggregate (OREX-501029-0) was then transferred from the concavity slide to a separate glass pyrolysis tube at CIS and carried by hand to the NASA Goddard Space Flight Center (GSFC) for targeted amino acid and N-heterocycle analyses using wet chemistry and pyGC-QqQ-MS (more detail about the method in the 'Coordinated analyses of organics in the aggregate samples' section below). The remaining ~20 mg were further split into multiple subsamples for elemental and stable isotopic analyses of bulk carbon, nitrogen and hydrogen, using an EA-IRMS instrument at CIS (details in the next section).

OREX-500005-0 consisted of mostly dark fines with an average grain size <100 µm, but with some particles up to ~500 µm. Some bright and highly reflective particles were also present in this aggregate sample; however, no fibres were observed. OREX-500005-0 (~88 mg) was sealed under N_2 inside a glass vial with a Viton stopper and crimped aluminium lid. It was subsampled to obtain OREX-501006-0 (<1 mg) for coordinated optical and UV fluorescence microscopy and µ-L^2MS analyses at NASA JSC (see 'Coordinated analyses of organics in the aggregate samples' section for more detail about the methods below).

Bulk material from the touch-and-go sample acquisition mechanism (TAGSAM) was subsampled to obtain TAGSAM aggregate (TA) samples OREX-800031-0 (~52 mg) and OREX-800044-0 (~109 mg). OREX-800031-0 was shipped from JSC to GSFC in a glass concavity slide (Supplementary Fig. 1) that was hermetically sealed under high purity N_2 inside an Eagle Stainless container. The container was opened inside an ISO 5 HEPA-filtered laminar flow hood housed in an ISO ~7 white room and the aggregate sample was subsampled and distributed for multiple analyses following a coordinated analysis scheme (Supplementary Fig. 2). A similar mass of a powdered sample of the CM2 Murchison from the University of Illinois, Chicago, and a powdered sample of fused silica (FS-120, HP Technical Ceramics) that had been previously ashed at 500 °C in air overnight to remove organic contaminants were also processed in parallel with the Bennu OREX-800031-0 aggregate sample. Procedural solvent blanks were also processed in parallel and analysed. OREX-800044-0 was shipped from JSC to Hokkaido University in Japan in a glass concavity slide (Supplementary Fig. 1) that was hermetically sealed under high purity N_2 inside an Eagle Stainless container. It was further subsampled in a glass concavity slide to OREX-800044-101 (17.75 mg) and shipped to Kyushu University in Japan.

Bulk C, N and H contents and their isotopic compositions

The elemental abundances of carbon (C, wt%), nitrogen (N, wt%) and hydrogen (H, wt%) and their isotopic compositions $\delta^{13}C$, in parts per thousand relative to the Vienna Peedee Belemnite, $\delta^{15}N$, in parts per thousand relative to Earth atmospheric nitrogen, and δD, in parts per thousand relative to the Vienna Standard Mean Ocean Water isotope reference, were analysed in subsamples of OREX-500002-0 and OREX-803007-0 and in a sample of the Murchison meteorite processed in parallel with OREX-803007-0 at GSFC after extraction in water at 100 °C for 24 h. These measurements were made with: (1) a Thermo Scientific Delta V^{plus} isotope ratio mass spectrometer (IRMS) connected to a Carlo Erba elemental analyser (EA) by means of a Conflo III interface for C and N analyses; and (2) a Thermo Scientific Delta Q IRMS connected to a Thermo Finnigan Thermal Conversion elemental analyser by means of a Conflo IV interface for H analyses using previously described methods[56]. The subsample masses used for H and C + N analyses were ~1–1.5 mg and 5.5 mg, respectively. Subsamples were placed in an Ar-flushed glovebox and heated to 120 °C for 48 h to reduce the amount of adsorbed atmospheric water before analysis (Supplementary Table 2). The reported uncertainties for the elemental and isotopic analyses correspond to a 1σ standard deviation, which was determined based on either replicate analyses of standards or analyses of at least two aliquots of individual samples, with the larger error reported.

Small aliquots (~2.5% of total extracted volume) of the hot-water extracts from TA OREX-803001-0 (designated split OREX-803001-112) and the parallel processed Murchison meteorite were transferred to separate tin capsules, acidified with 2 µl 6 M HCl, and then evaporated to dryness under vacuum at room temperature in a Labconco CentriVap Concentrator at GSFC. The capsules were crimped and analysed in series along with appropriate procedural blanks and standards using the nano EA-IRMS instrument at Pennsylvania State University (PSU) to determine the total C and N abundances as well as the $\delta^{13}C$ and

$\delta^{15}N$ values following published methods[57]. These analyses were performed after verification of the analytical method with the predicted concentration of ammonia in the TA water extract and corresponding volume of NH_4OH. The nano EA-IRMS system at PSU employed a Flash IRMS elemental analyser that was coupled by means of a ConFlo IV Universal Interface to a Thermo Scientific Delta V^{plus} Plus IRMS with a universal triple collector. Additional description of the nano EA-IRMS data processing methods and mass balance calculations can be found in the Supplementary Information.

Coordinated analyses of organics in the aggregate samples

OREX-800031-0 was subsampled for multiple analyses (Supplementary Fig. 2). OREX-803007-0 (23.6 mg) was allocated for bulk H, C and N measurements using EA-IRMS analyses at CIS. OREX-803006-0 (3.3 mg) was allocated for non-targeted molecular profiling of soluble organics in a methanol extract using FTICR-MS at Helmholtz-Zentrum in Munich, Germany. OREX-803004-0 (1.0 mg) was heated at 85 °C for 1.5 h in a sealed pyrolysis tube containing a 5 µl solution (4:1 v/v) of *N*-(*tert*-butyldimethylsilyl)-*N*-methyl-trifluoroacetamide and *N,N*-dimethylformamide and the sample was then analysed directly for the *N*-(*tert*-butyldimethylsilyl)-*N*-methyl-trifluoroacetamide derivatives of amino acids and N-heterocycles by pyGC-QqQ-MS at NASA GSFC. The remaining mass of OREX-803001-0 (25.6 mg) was flame-sealed in a glass ampoule with 1 ml Milli-Q ultrapure water (18.2 MΩ, <3 ppb total organic C) and heated at 100 °C for 24 h.

After water extraction, OREX-803001-0 was centrifuged (5 min at 3,000 rpm), and the water supernatant was separated from the solid residue. Some of the solid residue (OREX-803001-103, 22.9 mg) after water extraction was dried under vacuum at room temperature and sent to CIS for bulk H, C and N measurements. 17.5% of the OREX-803001-0 hot-water extract was analysed directly for free ammonia, hydrazine, aliphatic amines and protein amino acids. These analyses were performed by AccQ•Tag derivatization and liquid chromatography with UV fluorescence detection and either time-of-flight mass spectrometry (LC-FD/ToF-MS) or triple quadrupole mass spectrometry.

Approximately 2.5% of the OREX-803001-0 water extract was analysed by nano EA-IRMS for total C and N at PSU, as previously described. The remaining 80% of the OREX-803001-0 water extract was split equally, with 40% of the water extract desalted by cation exchange chromatography followed by *o*-phthaldialdehyde/*N*-acetyl-L-cysteine (OPA/NAC) derivatization and analysis using both LC-FD/ToF-MS and liquid chromatography with UV fluorescence detection and high-resolution mass spectrometry (LC-FD/HRMS) to determine the free amino acid abundances in the extract. The other 40% was dried, acid-hydrolysed under 6 M HCl vapour at 150 °C for 3 h and then desalted to determine the average total (free + bound) amino acid abundances using both LC-FD/ToF-MS and LC-FD/HRMS. We also measured the distribution and abundances of the 2-pentanol derivatives of free mono- and dicarboxylic acids in the water wash collected during desalting (cation exchange) of the non-hydrolysed water extract of Bennu (OREX-803001-0) using GC-QqQ-MS.

A separate 17.75 mg aggregate sample (OREX-800044-101), subsampled from Bennu OREX-800044-0, was extracted in HCl (Tama Chemicals Co., Ltd.) and analysed for N-heterocycles using HPLC/ESI-HRMS at Kyushu University in Japan. A 14.4 mg ashed sample of sea sand (FUJIFILM Wako Pure Chemical Corporation; 30–50 mesh) was used as a processing blank for OREX-800044-101. Procedural solvent blanks were also processed in parallel and analysed.

A small subsample (<1 mg) of the QL aggregate (OREX-501006-0) was prepared at NASA JSC for coordinated analysis by optical and UV fluorescence microscopy and µ-L^2MS. Approximately a dozen grains of the QL aggregate were transferred to an infrared grade potassium bromide (KBr) window and gently pressed into the KBr surface using an optical grade sapphire window. The sample mount was imaged optically and under UV fluorescence using an Olympus BX-60 microscope equipped with a tungsten halogen and Hg-arc illumination sources. Native fluorescence images were obtained using 330–385 nm excitation and 420 nm long-pass emission filters. After optical and UV fluorescence imaging, the sample was transferred to a µ-L^2MS instrument and in situ mass spectra were acquired at a 5 µm spatial resolution using an infrared laser (CO_2; 10.6 mm) for desorption, a vacuum ultraviolet laser (Nd:YAG 9th harmonic; 118 nm) for photoionization and a reflectron time-of-flight mass spectrometer for mass analysis. Additional details of the imaging and µ-L^2MS analyses can be found in the Supplementary Information.

Data availability

The instrument data supporting the experimental results in this study are available at https://astromat.org at the DOIs given in Supplementary Table 14 and/or within the manuscript and its Supplementary Information. Source data are provided with this paper.

References

1. Pearson, V. K. et al. Carbon and nitrogen in carbonaceous chondrites: elemental abundances and stable isotopic compositions. *Meteorit. Planet. Sci.* **41**, 1899–1918 (2006).
2. Glavin, D. P. et al. in *Primitive Meteorites and Asteroids* (ed. Abreu, N.) 205–271 (Elsevier, 2018).
3. DeMeo, F. E. & Carry, B. Solar system evolution from compositional mapping of the asteroid belt. *Nature* **505**, 629–634 (2014).
4. Lee, M. R. et al. CM carbonaceous chondrite falls and their terrestrial alteration. *Meteorit. Planet. Sci.* **56**, 34–48 (2021).
5. Lauretta, D. S. et al. Asteroid (101955) Bennu in the laboratory: properties of the sample collected by OSIRIS-REx. *Meteorit. Planet. Sci.* **59**, 2453–2486 (2024).
6. Lauretta, D. S. et al. OSIRIS-REx: sample return from asteroid (101955) Bennu. *Space Sci. Rev.* **212**, 925–984 (2017).
7. Lauretta, D. S. et al. The unexpected surface of asteroid (101955) Bennu. *Nature* **568**, 55–60 (2019).
8. Simon, A. A. et al. Widespread carbon-bearing materials on near-Earth asteroid (101955) Bennu. *Science* https://doi.org/10.1126/science.abc3522 (2020).
9. Kaplan, H. H. et al. Composition of organics on asteroid (101955) Bennu. *Astron. Astrophys.* **653**, L1 (2021).
10. Lauretta, D. S. et al. Spacecraft sample collection and subsurface excavation of asteroid (101955) Bennu. *Science* **377**, 285–291 (2022).
11. DellaGiustina, D. N. et al. Variations in color and reflectance on the surface of asteroid (101955) Bennu. *Science* **370**, eabc3660 (2020).
12. Lauretta, D. S., Connolly Jr, H. C., Grossman, J. N. & Polit, A. T. OSIRIS-REx sample analysis plan–revision 3.0. Preprint at https//arxiv.org/abs/2308.11794 (2023).
13. Glavin, D. P., Burton, A. S., Elsila, J. E., Aponte, J. C. & Dworkin, J. P. The search for chiral asymmetry as a potential biosignature in our solar system. *Chem. Rev.* **120**, 4660–4689 (2020).
14. Bierhaus, E. B. et al. The OSIRIS-REx spacecraft and the touch-and-go sample acquisition mechanism (TAGSAM). *Space Sci. Rev.* **214**, 1–46 (2018).
15. Pizzarello, S. et al. Abundant ammonia in primitive asteroids and the case for a possible exobiology. *Proc. Natl Acad. Sci. USA* **108**, 4303–4306 (2011).
16. Pizzarello, S. & Williams, L. B. Ammonia in the early Solar System: an account from carbonaceous chondrites. *Astrophys. J.* https://doi.org/10.1088/0004-637X/749/2/161 (2012).
17. Schmitt-Kopplin, P. Z. et al. High molecular diversity of extraterrestrial organic matter in Murchison meteorite revealed 40 years after its fall. *Proc. Natl Acad. Sci. USA* **107**, 2763–2768 (2010).

18. Hoefs, J. *Stable Isotope Geochemistry* 54–57 (Springer-Verlag, 2009).
19. Alexander, C. M. O'D. et al. The provenances of asteroids, and their contributions to the volatile inventories of the terrestrial planets. *Science* **337**, 721–723 (2012).
20. Naraoka, H. et al. Soluble organic molecules in samples of the carbonaceous asteroid (162173) Ryugu. *Science* **379**, eabn9033 (2023).
21. Yoshimura, T. et al. Chemical evolution of primordial salts and organic sulfur molecules in the asteroid 162173 Ryugu. *Nat. Commun.* **14**, 5284 (2023).
22. Laize-Générat, L. et al. Nitrogen in the Orgueil meteorite: abundant ammonium among other reservoirs of variable isotopic compositions. *Geochim. Cosmochim. Acta* **387**, 111–129 (2024).
23. Altwegg, K. et al. Evidence of ammonium salts in comet 67P as explanation for the nitrogen depletion in cometary comae. *Nat. Astron.* **4**, 533–540 (2020).
24. Poch, O. et al. Ammonium salts are a reservoir of nitrogen on a cometary nucleus and possibly on some asteroids. *Science* **367**, eaaw7462 (2020).
25. De Sanctis, M. C. et al. Ammoniated phyllosilicates with a likely outer Solar System origin on (1) Ceres. *Nature* **528**, 241–244 (2015).
26. Aponte, J. C., Woodward, H. K., Abreu, N. M., Elsila, J. E. & Dworkin, J. P. Molecular distribution, ^{13}C-isotope, and enantiomeric compositions of carbonaceous chondrite monocarboxylic acids. *Meteorit. Planet. Sci.* **54**, 415–430 (2019).
27. Parker, E. T. et al. Extraterrestrial amino acids and amines identified in asteroid Ryugu samples returned by the Hayabusa2 mission. *Geochim. Cosmochim. Acta* **347**, 42–57 (2023).
28. Takano, Y. et al. Primordial aqueous alteration recorded in water-soluble organic molecules from the carbonaceous asteroid (162173) Ryugu. *Nat. Commun.* **15**, 5708 (2024).
29. Koga, T. & Naraoka, H. Synthesis of amino acids from aldehydes and ammonia: implications for organic reactions in carbonaceous chondrite parent bodies. *ACS Earth Space Chem.* **6**, 1311–1320 (2022).
30. Hamilton, V. E. et al. Evidence for widespread hydrated minerals on asteroid (101955) Bennu. *Nat. Astron.* **3**, 332–340 (2019).
31. Kaplan, H. H. et al. Bright carbonate veins on asteroid (101955) Bennu: implications for aqueous alteration history. *Science* **370**, eabc3557 (2020).
32. Glavin, D. P. et al. Unusual non-terrestrial L-proteinogenic amino acid excesses in the Tagish Lake meteorite. *Meteorit. Planet. Sci.* **47**, 1347–1364 (2012).
33. Oba, Y. et al. Uracil in the carbonaceous asteroid (162173) Ryugu. *Nat. Commun.* **14**, 1292 (2023).
34. Callahan, M. P. et al. Carbonaceous meteorites contain a wide range of extraterrestrial nucleobases. *Proc. Natl Acad. Sci. USA* **108**, 13995–13998 (2011).
35. Naraoka, H. et al. Molecular evolution of N-containing cyclic compounds in the parent body of the Murchison meteorite. *ACS Earth Space Chem.* **1**, 540–550 (2017).
36. Oba, Y. et al. Identifying the wide diversity of extraterrestrial purine and pyrimidine nucleobases in carbonaceous meteorites. *Nat. Commun.* **13**, 2008 (2022).
37. Nguyen, A. N. et al. N-rich isotopically anomalous nanoglobules and organic matter in Bennu. In *86th Annual Meeting of the Meteoritical Society* https://www.hou.usra.edu/meetings/metsoc2024/pdf/6446.pdf (2024).
38. Walsh, K. J. et al. Numerical simulations suggest asteroids (101955) Bennu and (162173) Ryugu are likely second or later generation rubble piles. *Nat. Commun.* **15**, 5653 (2024).
39. Hopp, T. et al. Ryugu's nucleosynthetic heritage from the outskirts of the Solar System. *Sci. Adv.* **8**, eadd8141 (2022).
40. Booth, R. A. & Ilee, J. D. Planet-forming material in a protoplanetary disk: the interplay between chemical evolution and pebble drift. *Mon. Not. R. Astron. Soc.* **487**, 3998–4011 (2019).
41. Lauretta, D. S. et al. Episodes of particle ejection from the surface of the active asteroid (101955) Bennu. *Science* **366**, eaay3544 (2019).
42. Fernandez, Y. R., McFadden, L. A., Lisse, C. M., Helin, E. F. & Chamberlin, A. B. Analysis of POSS images of comet–asteroid transition object 107P/1949 W1 (Wilson–Harrington). *Icarus* **128**, 114–126 (1997).
43. Nuth, J. A.III et al. Volatile-rich asteroids in the inner Solar System. *Planet. Sci. J.* **1**, 82 (2020).
44. Lisse, C. M. et al. Spitzer spectral obserations of the Deep Impact ejecta. *Science* **313**, 635–640 (2006).
45. Berger, E. L., Zega, T. J., Keller, L. P. & Lauretta, D. S. Evidence for aqueous activity on comet 81P/Wild 2 from sulfide mineral assemblages in stardust samples and CI chondrites. *Geochim. Cosmochim. Acta* **75**, 3501–3513 (2011).
46. Castillo-Rogez, J. et al. Insights into Ceres's evolution from surface composition. *Meteorit. Planet. Sci.* **53**, 1820–1843 (2018).
47. Marchi, S. et al. An aqueously altered carbon-rich Ceres. *Nat. Astron.* **3**, 140–145 (2019).
48. McCoy, T. J. et al. An evaporite sequence from ancient brine recorded in Bennu samples. *Nature* https://doi.org/10.1038/s41586-024-08495-6 (2025).
49. Dyl, K. A. et al. Early solar system hydrothermal activity in chondritic asteroids on 1–10-year timescales. *Proc. Natl Acad. Sci. USA* **109**, 18306–18311 (2012).
50. Levy, M., Miller, S. L., Brinton, K. & Bada, J. L. Prebiotic synthesis of adenine and amino acids under Europa-like conditions. *Icarus* **145**, 609–613 (2000).
51. Szostak, J. W. The narrow road to the deep past: in search of the chemistry of the origin of life. *Angew. Chem. Int. Ed. Engl.* **56**, 10959–11271 (2017).
52. Cody, G. D. et al. Testing the effect of x-ray computed tomography on chondritic insoluble organic matter and exploring parent body molecular evolution. *Meteorit. Planet. Sci.* **59**, 3–22 (2024).
53. Nguyen, A. N. et al. Micro- and nanoscale studies of insoluble organic matter and C-rich presolar 2 grains in Murchison and Sutteras Mill in preparation for Bennu sample analysis. *Meteorit. Planet. Sci.* **59**, 2831–2850 (2024).
54. Glavin, D. P. et al. Investigating the impact of x-ray computed tomography imaging on soluble organic matter in the Murchison meteorite: implications for Bennu sample analyses. *Meteorit. Planet. Sci.* **59**, 105–133 (2024).
55. Righter, K. et al. Curation planning and facilities for asteroid Bennu samples returned by the OSIRIS-REx mission. *Meteorit. Planet. Sci.* **58**, 572–590 (2023).
56. Alexander, C. M. O'D., Howard, K., Bowden, R. & Fogel, M. L. The classification of CM and CR chondrites using bulk H, C and N abundances and isotopic compositions. *Geochim. Cosmochim. Acta* **123**, 244–260 (2013).
57. Baczynski, A. A., Brodie, C. R., Kracht, O. & Freeman, K. H. Sequential measurement of ^{13}C, ^{15}N, and ^{34}S isotopic composition on nanomolar quantities of carbon, nitrogen, and sulfur using nano-elemental/isotope ratio mass spectrometry. *Rapid Commun. Mass Spectrom.* **37**, e9444 (2023).
58. Aponte, J. C., Dworkin, J. P. & Elsila, J. E. Indigenous aliphatic amines in the aqueously altered Orgueil meteorite. *Meteorit. Planet. Sci.* **50**, 1733–1749 (2015).
59. Glavin, D. P. et al. The effects of parent body processes on amino acids in carbonaceous chondrites. *Meteorit. Planet. Sci.* **45**, 1948–1972 (2010).

60. Glavin, D. P. et al. Abundant extraterrestrial amino acids in the primitive CM carbonaceous chondrite Asuka 12236. *Meteorit. Planet. Sci.* **55**, 1979–2006 (2020).
61. Alexander, C. M. O'D. et al. Elemental, isotopic, and structural changes in Tagish Lake insoluble organic matter produced by parent body processes. *Meteorit. Planet. Sci.* **49**, 503–525 (2014).
62. Burton, A. S., Grunsfeld, S., Elsila, J. E., Glavin, D. P. & Dworkin, J. P. The effects of parent-body hydrothermal heating on amino acid abundances in CI-like chondrites. *Polar Sci.* **8**, 255–263 (2014).
63. Koga, T., Takano, Y., Oba, Y., Naraoka, H. & Ohkouchi, N. Abundant extraterrestrial purine nucleobases in the Murchison meteorite: implications for a unified mechanism for purine synthesis in carbonaceous chondrite parent bodies. *Geochim. Cosmochim. Acta* **365**, 253–265 (2024).
64. Stoks, P. G. & Schwartz, A. W. Uracil in carbonaceous meteorites. *Nature* **282**, 709–710 (1979).

Acknowledgements

We are grateful to the entire OSIRIS-REx team for making the return of samples from asteroid Bennu possible. We thank the Astromaterials Acquisition and Curation Office, part of the Astromaterials Research and Exploration Science Division at NASA Johnson Space Center, for their efforts in sample return capsule recovery, preliminary examination and long-term curation. We also greatly appreciate support from the OSIRIS-REx Sample Analysis Micro Information System team. We are grateful to R. Vargas (meteorite hunter) for providing a sample of the C2 ungrouped Tarda meteorite, L. Garvie (Arizona State University) for providing the CM1/2 Kolang meteorite (sample ASU 2147) and D. Hill (Lunar and Planetary Laboratory, University of Arizona) for allocating the CM2 Winchcombe meteorite (sample UA2925,12). We also thank R. Minard and the Clifford N. Matthews research group at the University of Illinois, Chicago, for providing the Murchison meteorite used in this investigation. We also appreciate the careful review of the manuscript by C.W.V. Wolner. This material is based upon work supported by NASA award no. NNH09ZDA007O and under contract no. NNM10AA11C issued through the New Frontiers Program. Z.G. and G.D. are supported by NASA OSIRIS-REx Sample Analysis Participating Scientist Program (ORSA-PSP) award. no. 80NSSC22K1692. Y.H., E.S. and B.K. are supported by NASA ORSA-PSP award no. 80NSSC22K1691. K.H.F., A.A.B., C.H.H., O.M.M. and M.M. are supported by NASA ORSA-PSP award no. 80NSSC22K1690. Work at the Molecular Foundry and Advanced Light Source was supported by the Office of Science, Office of Basic Energy Sciences, of the US Department of Energy under contract no. DE-AC02-05CH11231. P.S.-K. and M.L. were funded by the German Research Foundation—project-ID 364653263—TRR 235 (CRC 235) and project-ID 521256690—TRR 392/1 2024 (CRC 392/1 B2). Y.O. is supported by the Japan Society for the Promotion of Science under KAKENHI grant nos 21H04501 and 23H03980. D.I.F, C.M.O'D.A. and G.C. are supported by the Emerging Worlds grant nos 80NSSC20K0344 and 80NSSC21K0654, and D.I.F. is also funded through Exobiology grant no. 80NSSC21K0485. P.R.H. and Y.Z. acknowledge support by the TAWANI Foundation. A.H.C., D.N.S., F.S, H.L.M. and K.K.F. are supported by the Center for Research and Exploration in Space Science and Technology II cooperative agreement with NASA and the University of Maryland, Baltimore County, under award no. 80GSFC24M0006. A.E.H. is supported by 21-ORSAPS21_2-0009. The Jet Propulsion Laboratory is operated by the California Institute of Technology under contract with NASA (contract no. 80NM0018D0004). This research used resources of the Advanced Light Source, a U.S. DOE Office of Science User Facility under contract no. DE-AC02-05CH11231.

Author contributions

D.P.G. and J.P.D. contributed equally. D.P.G, J.P.D., J.C.A., H.L.M., A.M., E.T.P., Y.O.,T.K., D.I.F., C.M.O'D.A., P.S-K., A.B., K.H.F., Z.G., M.A.M., G.D., P.H., S.J.C., A.N.N., K.L.T.-K., S.A.S., H.C.C. and D.S.L. conceptualized the study. D.P.G, J.P.D., J.C.A., H.L.M., A.M., E.T.P., Y.O.,T.K., D.I.F., C.M.O'D.A., G.C., P.S-K., M.L., P.C., A.S., T.G., B.M.G., A.B., K.H.F., Z.G., M.A.M., G.D., P.H., S.J.C., A.N.N., P.H., F.S., D.N.S., K.L.T.-K., S.A.S., E.B. and A.S.B. were responsible for the methodology and the investigation. The original draft was written by D.P.G., J.P.D., J.C.A., H.L.M., A.M., E.T.P., Y.O., T.K., P.S.-K., D.I.F., C.M.O'D.A., A.B., K.H.F., Z.G., M.A.M., G.D., S.J.C. and A.N.N. All coauthors reviewed and edited the manuscript.

Competing interests

The authors declare no competing interests.

Additional information

Extended data is available for this paper at https://doi.org/10.1038/s41550-024-02472-9.

Supplementary information The online version contains supplementary material available at https://doi.org/10.1038/s41550-024-02472-9.

Correspondence and requests for materials should be addressed to Daniel P. Glavin.

Peer review information *Nature Astronomy* thanks Zita Martins, Larry Nittler and the other, anonymous, reviewer(s) for their contribution to the peer review of this work.

Daniel P. Glavin[1,37] ✉, Jason P. Dworkin[1,37], Conel M. O'D. Alexander[2], José C. Aponte[1], Allison A. Baczynski[3], Jessica J. Barnes[4], Hans A. Bechtel[5], Eve L. Berger[6], Aaron S. Burton[7], Paola Caselli[8], Angela H. Chung[1,9,10], Simon J. Clemett[6,11], George D. Cody[2], Gerardo Dominguez[12], Jamie E. Elsila[1], Kendra K. Farnsworth[1,10,13], Dionysis I. Foustoukos[2], Katherine H. Freeman[3], Yoshihiro Furukawa[14], Zack Gainsforth[15], Heather V. Graham[1], Tommaso Grassi[8], Barbara Michela Giuliano[8], Victoria E. Hamilton[16], Pierre Haenecour[4], Philipp R. Heck[17,18],

Amy E. Hofmann[19], Christopher H. House[3], Yongsong Huang[20], Hannah H. Kaplan[1], Lindsay P. Keller[6], Bumsoo Kim[6,20,21], Toshiki Koga[22], Michael Liss[23,24], Hannah L. McLain[1,9,10], Matthew A. Marcus[5], Mila Matney[3], Timothy J. McCoy[25], Ophélie M. McIntosh[3], Angel Mojarro[1,26], Hiroshi Naraoka[27], Ann N. Nguyen[6], Michel Nuevo[28], Joseph A. Nuth III[1], Yasuhiro Oba[29], Eric T. Parker[1], Tanya S. Peretyazhko[6,21], Scott A. Sandford[28], Ewerton Santos[20], Philippe Schmitt-Kopplin[8,23,24], Frederic Seguin[1,10], Danielle N. Simkus[1,9,10], Anique Shahid[8,30], Yoshinori Takano[22,31], Kathie L. Thomas-Keprta[6,32], Havishk Tripathi[1,33], Gabriella Weiss[1,13], Yuke Zheng[17,18], Nicole G. Lunning[6], Kevin Righter[34], Harold C. Connolly Jr.[4,35,36] & Dante S. Lauretta[4]

[1]Solar System Exploration Division, NASA Goddard Space Flight Center (GSFC), Greenbelt, MD, USA. [2]Earth and Planets Laboratory, Carnegie Institution for Science, Washington, DC, USA. [3]Department of Geosciences, Pennsylvania State University, University Park, PA, USA. [4]Lunar and Planetary Laboratory, University of Arizona, Tucson, AZ, USA. [5]Lawrence Berkeley National Laboratory, Berkeley, CA, USA. [6]Astromaterials Research and Exploration Science Division, NASA Johnson Space Center, Houston, TX, USA. [7]NASA Headquarters, Washington, DC, USA. [8]Center for Astrochemical Studies, Max Planck Institute for Extraterrestrial Physics, Garching, Germany. [9]Department of Chemistry, Catholic University of America, Washington, DC, USA. [10]Center for Research and Exploration in Space Science and Technology, NASA GSFC, Greenbelt, MD, USA. [11]ERC, Inc., JETS/Jacobs, Houston, TX, USA. [12]California State University San Marcos, San Marcos, CA, USA. [13]Center for Space Sciences and Technology, University of Maryland Baltimore County, Baltimore, MD, USA. [14]Department of Earth Science, Tohoku University, Sendai, Japan. [15]Space Science Laboratory, University of California, Berkeley, CA, USA. [16]Southwest Research Institute, Boulder, CO, USA. [17]Robert A. Pritzker Center for Meteoritics and Polar Studies, Negaunee Integrative Research Center, Field Museum of Natural History, Chicago, IL, USA. [18]Department of the Geophysical Sciences, University of Chicago, Chicago, IL, USA. [19]Jet Propulsion Laboratory, California Institute of Technology, Pasadena, CA, USA. [20]Department of Earth, Environmental, and Planetary Science, Brown University, Providence, RI, USA. [21]Amentum, JSC Engineering and Technical Support (JETSII) Contract, NASA Johnson Space Center, Houston, TX, USA. [22]Biogeochemistry Research Center, Japan Agency for Marine-Earth Science and Technology (JAMSTEC), Natsushima, Yokosuka, Japan. [23]Technical University Munich, Freising, Germany. [24]Research Unit Analytical Biogeochemistry, Helmholtz Munich, Neuherberg, Germany. [25]National Museum of Natural History, Smithsonian Institution, Washington, DC, USA. [26]Oak Ridge Associated Universities, Oak Ridge, TN, USA. [27]Department of Earth and Planetary Sciences, Kyushu University, Fukuoka, Japan. [28]NASA Ames Research Center, Moffett Field, CA, USA. [29]Institute of Low Temperature Science, Hokkaido University, N19W8 Kita-ku, Sapporo, Japan. [30]Department of Physics, Technische Universität München, Muenchen, Germany. [31]Institute for Advanced Biosciences, Keio University, Kakuganji, Tsuruoka, Yamagata, Japan. [32]Barrios, JETS/Jacobs, Houston, TX, USA. [33]Southeastern Universities Research Association, Washington, DC, USA. [34]Department of Earth and Environmental Sciences, University of Rochester, Rochester, NY, USA. [35]Department of Geology, School of Earth and Environment, Rowan University, Glassboro, NJ, USA. [36]Department of Earth and Planetary Sciences, American Museum of Natural History, New York, NY, USA. [37]These authors contributed equally: Daniel P. Glavin, Jason P. Dworkin.
✉e-mail: daniel.p.glavin@nasa.gov

https://doi.org/10.1038/s41550-024-02472-9

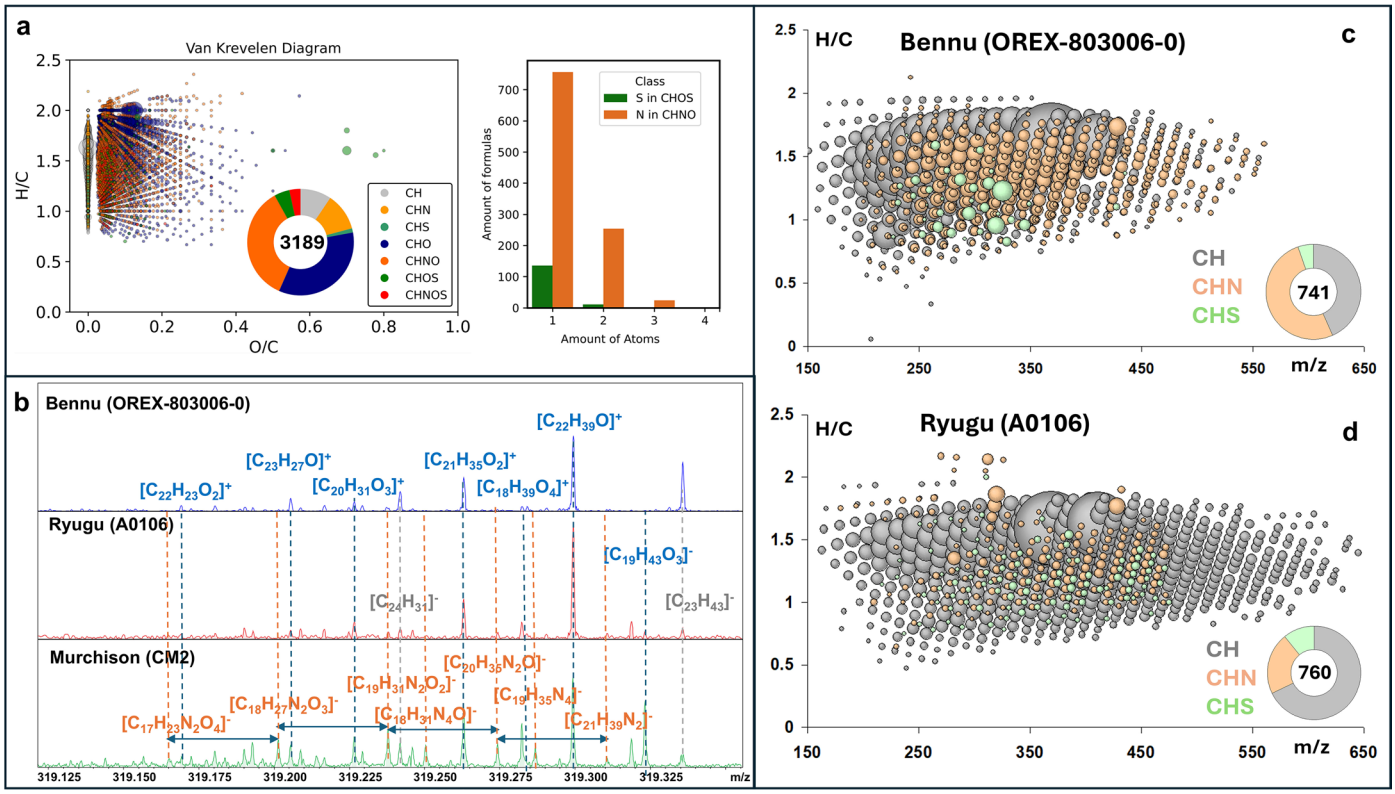

Extended Data Fig. 1 | APPI(+) ionization FTICR-MS analysis of Bennu (OREX-803006-0) compared to Murchison and Ryugu (A0106). a, The low oxygenated molecules observed in the Bennu methanol extract as illustrated in the Van Krevelen diagram. **b**, Details around nominal mass $m/z = 319$ with the annotation of some m/z signals. The H/C versus m/z diagrams of **c**, Bennu and **d**, Ryugu, showing the lower molecular mass and higher relative abundance of CHN in the Bennu sample also in oxygen poor molecules. Colored annuli enclose the total number of molecules assigned by mass, with colors indicating the relative ratios of the chemical families.

https://doi.org/10.1038/s41550-024-02472-9

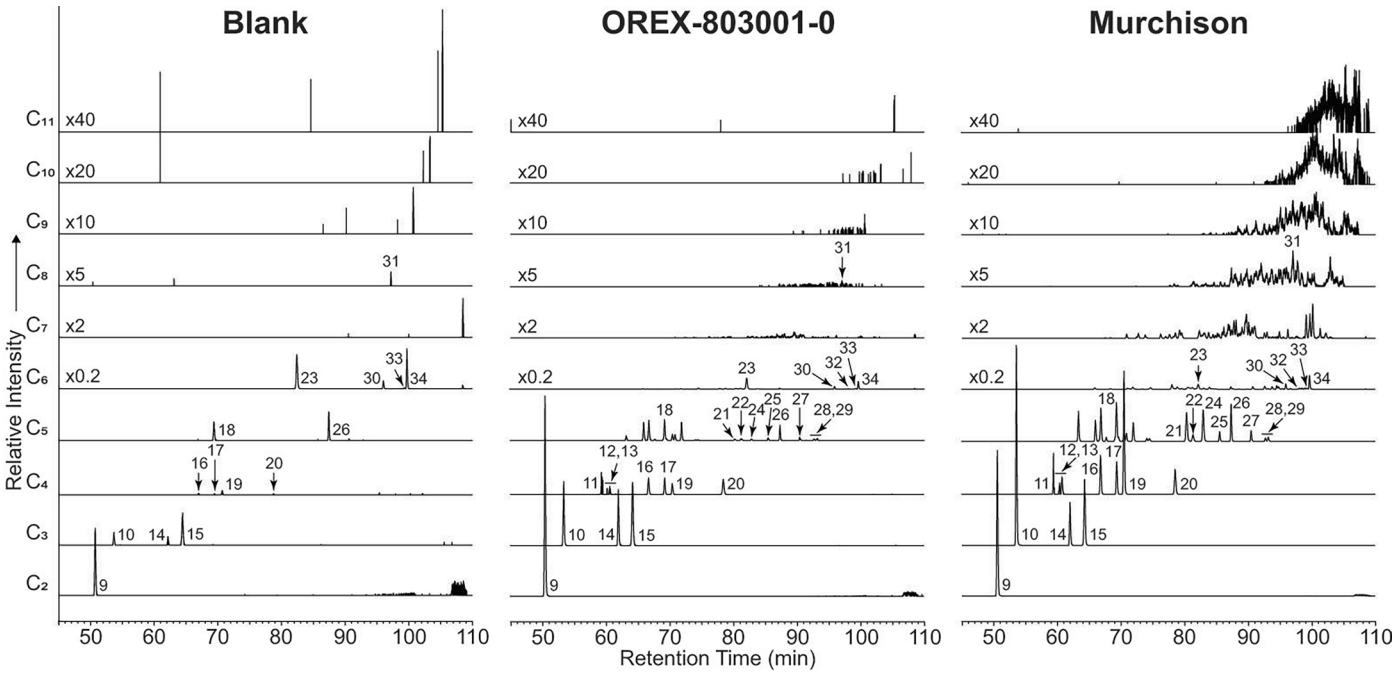

Extended Data Fig. 2 | LC-HRMS chromatograms showing the elution of C_2 to C_{11} amino acids in the acid-hydrolyzed, hot-water extracts of the procedural blank, Bennu (OREX-803001-0), and Murchison. The 45–110 min regions of the LC-HRMS single-ion mass chromatograms corresponding to the *o*-phthaldialdehyde/*N*-acetyl-L-cysteine (OPA/NAC) derivatives of C_2 to C_{11} aliphatic primary amino acids in positive ion mode via heated electrospray ionization and a 5 ppm mass accuracy with corresponding *m/z* values as follows: **C2**: *m/z* = 337.08527; **C3**: *m/z* = 351.10092; **C4**: *m/z* = 365.11657; **C5**: *m/z* = 379.13222; **C6**: *m/z* = 393.14787; **C7**: *m/z* = 407.16352; **C8**: *m/z* = 421.17917; **C9**: *m/z* = 435.19482; **C10**: *m/z* = 449.21047; and **C11**: *m/z* = 463.22612. Similar single-ion chromatograms were obtained for the non-hydrolyzed water extracts. Peaks were identified by comparisons of their retention times and exact monoisotopic masses with those in the amino acid standard analyzed on the same day, and are designated by peak number as follows: (9) glycine, (10) β-alanine, (11) γ-amino-*n*-butyric acid, (12) D-β-aminoisobutyric acid, (13) L-β-aminoisobutyric acid, (14) D-alanine, (15) L-alanine, (16) D-β-amino-*n*-butyric acid, (17) L-β-amino-*n*-butyric acid, (18) δ-aminovaleric acid, (19) α-aminoisobutyric acid, (20) D,L-α-amino-*n*-butyric acid, (21) D-isovaline, (22) (S)-3-aminopentanoic acid, (23) ε-amino-*n*-caproic acid, (24) L-isovaline, (25) (R)-3-aminopentanoic acid, (26) L-valine, (27) D-valine, (28) D-norvaline, (29) L-norvaline, (30) L-isoleucine, (31) 8-aminooctanoic acid, (32) D-isoleucine, (33) D-leucine, and (34) L-leucine. Note: the C_7–C_{11} traces for the procedural blank and Bennu analyses feature spurious signal spikes that are due to instrumental background noise and do not represent analyte peaks.

https://doi.org/10.1038/s41550-024-02472-9

Extended Data Table 1 | Total C, N, and H contents and stable isotopic compositions of Bennu aggregate samples, compared with selected CCs and Ryugu samples (A0106 and C0107)

Samples	C (wt.%)	$\delta^{13}C$ (‰)	N (wt.%)	$\delta^{15}N$ (‰)	H (wt.%)	δD (‰)	N/C (atomic)	H/C (atomic)
Bennu (OREX-500002-0, Avionics Deck)								
OREX-501034/35/38-0 (fines, <0.1 mm)[a]	4.7 ± 0.4	2.7 ± 0.1	0.24 ± 0.02	74.6 ± 0.1	0.85 ± 0.04	330 ± 4	0.044 ± 0.005	2.2 ± 0.2
OREX-501036/37/39-0[b] (fines, <0.1 mm)[c]	4.7 ± 0.4	3.2 ± 0.1	0.23 ± 0.02	75.5 ± 0.1	0.90 ± 0.04	315 ± 2	0.042 ± 0.005	2.3 ± 0.2
OREX-501040/41-0[b] (intermediate,0.2 mm)[c]	4.7 ± 0.4	–0.5 ± 0.1	0.24 ± 0.02	57.1 ± 0.1	0.93 ± 0.05	305 ± 2	0.044 ± 0.005	2.4 ± 0.2
Bennu (OREX-800031-0, TAGSAM)								
OREX-803007-0[b] (aggregate, <0.5 mm)[a]	4.5 ± 0.2	3.3 ± 0.9	0.25 ± 0.01	82 ± 15	0.93 ± 0.05	344 ± 13	0.048 ± 0.003	2.5 ± 0.2
OREX-803001-103 (residue after water extraction @ 100°C 24h)[a]	4.2 ± 0.2	–2.2 ± 0.6	0.20 ± 0.01	58.0 ± 0.8	1.02 ± 0.03	294 ± 3	0.041 ± 0.003	2.9 ± 0.2
OREX-803001-112 (hot-water extract)[d]	-	–9 ± 3	-	180 ± 47	n.d.	n.d.	-	n.d.
Murchison (CM2)								
Murchison (UIC) (powder, <0.2 mm)[a]	1.97 ± 0.08	–3.5 ± 0.2	0.12 ± 0.01	43.6 ± 0.2	0.97 ± 0.06	–19 ± 7	0.052 ± 0.005	5.9 ± 0.4
Murchison (UIC) (residue after water extraction @ 100°C 24h)[a]	1.78 ± 0.07	–10.4 ± 0.2	0.09 ± 0.01	33.1 ± 0.2	1.02 ± 0.06	–51 ± 3	0.043 ± 0.005	6.8 ± 0.5
Murchison (UIC) (hot-water extract)[d]	-	23 ± 9	-	55 ± 8	n.d.	n.d.	-	n.d.
Tarda and Tagish Lake ($C2_{ung}$)								
Tarda (EPL)[e] (powder, <0.2 mm)[a]	3.78 ± 0.09	8.4 ± 0.2	0.23 ± 0.01	55.7 ± 0.2	1.02 ± 0.05	492 ± 4	0.052 ± 0.003	3.2 ± 0.2
Tarda (RV)[f] (powder, <0.2 mm)[a]	3.65 ± 0.16	5.1 ± 0.3	0.19 ± 0.01	50.6 ± 0.1	0.67 ± 0.08	520 ± 4	0.045 ± 0.003	2.2 ± 0.3
Tagish Lake (5b)[g] (powder, <0.2 mm)	4.11 ± 0.12	10.1 ± 0.3	0.24 ± 0.01	76.2 ± 0.3	0.945 ± 0.003	508 ± 4	0.050 ± 0.003	2.7 ± 0.1
Tagish Lake (11h)[g] (powder, <0.2 mm)	4.13 ± 0.12	9.4 ± 0.3	0.19 ± 0.01	62.6 ± 0.3	0.872 ± 0.004	557 ± 6	0.039 ± 0.002	2.5 ± 0.1
Ryugu (Hayabusa2)								
Ryugu (A0106)[h] (aggregate, <1 mm)	3.76 ± 0.14	–0.6 ± 2.0	0.16 ± 0.01	43.0 ± 9.0	1.14 ± 0.09	252 ± 13	0.036 ± 0.003	3.6 ± 0.3
Ryugu (C0107)[i] (aggregate, <1 mm)	3.59 ± 0.47	1.2 ± 10.0	0.14 ± 0.01	36.8 ± 3.6	1.05 ± 0.10	269 ± 13	0.033 ± 0.005	3.5 ± 0.6

[a]Sample heated at 120°C for 48 h under Ar (<0.1 ppm H_2O and O_2) in a glovebox, and then kept there at room temperature for 66 h without exposure to atmosphere prior to EA-IRMS analysis.
[b]Data from ref. 5.
[c]Sample under Ar in glovebox at room temperature without any exposure to atmosphere prior to EA-IRMS analysis.
[d]Water extract first acidified by adding 2 μL of 6 M HCl to the extract (~71 μL) to preserve volatile ammonia and amines in a tin capsule and then dried under vacuum at room temperature for 2 h prior to Nano EA-IRMS analysis. The total C and N abundances (nmol) in the OREX-803001-112 and Murchison dried water extracts were also measured and are shown in Supplementary Table 4. Based on mass balance calculations accounting for the mass loss of C and N and change in their EA-IRMS isotopic compositions from the aggregate during extraction, the water extract should be even more isotopically enriched in ^{13}C and ^{15}N ($\delta^{13}C$ ~ +80‰ and $\delta^{15}N$ ~ +178‰; Supplementary Data Table 4). The lower $\delta^{13}C$ is likely due to the loss of carbonates and carboxylic acids from the acidification.
[e]Tarda (EPL) meteorite sample obtained by the Carnegie Earth and Planets Laboratory (EPL).
[f]Tarda (RV) meteorite sample provided by meteorite dealer Roberto Vargas (RV).
[g]Data from ref. 61. Only the errors for H reported. The precision for C and N elemental analyses was estimated to be 3% of the reported values and the precision of the C and N isotope measurements was estimated to be ±0.3‰ based on the highest variability observed in standards and replicate analyses.
[h]Data from ref. 20.
[i]Data from ref. 33.
n.d. = not determined.

https://doi.org/10.1038/s41550-024-02472-9

Extended Data Table 2 | Blank-subtracted free abundances of ammonia, amines, and amino acids, as measured by LC-FD/ToF-MS, in the hot-water extract of Bennu (OREX-803001-0), compared with selected CCs and Ryugu (A0106)[a]

Free Ammonia, Amines & Protein Amino Acids	Bennu (OREX-803001-0)	Murchison (CM2)	Tarda ($C2_{ung}$)	Orgueil (CI1)[b]	Ryugu (A0106)[b]
Ammonia (nmol g^{-1})	**13,613 ± 357**	**1,098 ± 144** **~1,600[c]**	**n.d.**	**~4,400[c]** **33,540 ± 3,080[d]** **37,777 ± 6,111[e]**	**180 ± 60[d]**
Amines					
Hydrazine	<0.1	<0.1	<0.1	n.r.	n.r.
Methylamine	914 ± 88	1,308 ± 189	30.3 ± 0.2	331.5 ± 0.5	23.8 ± 0.6
Ethylamine	121 ± 7	289 ± 31	7.1 ± 0.2	27.3 ± 2.4	11.4 ± 0.3
Isopropylamine	6.8 ± 0.3	47 ± 5	0.27 ± 0.02	5.1 ± 0.1	0.59 ± 0.03
n-Propylamine	7.0 ± 0.3	60 ± 8	0.32 ± 0.01	4.8 ± 0.1	0.05 ± 0.01
(*R,S*)-*sec*-Butylamine	0.47 ± 0.02	3.5 ± 0.4	n.d.	4.9 ± 0.4	<0.1
Isobutylamine	1.3 ± 0.2	18 ± 2	n.d.	<0.7	<0.1
n-Butylamine	1.0 ± 0.3	7.7 ± 1.4	n.d.	1.4 ± 0.1	<0.1
tert-Butylamine	3.4 ± 0.4	11 ± 1	n.d.	1.3 ± 0.2	<0.1
3-Pentylamine	0.34 ± 0.02	5.5 ± 0.4	n.d.	<0.7	<0.1
(*R,S*)-3-Methyl-2-butylamine	0.44 ± 0.02	7.8 ± 0.9	n.d.	<0.7	<0.1
(*R,S*)-*sec*-Pentylamine	0.56 ± 0.02	9.9 ± 0.8	n.d.	<0.7	<0.1
(*R,S*)-2-Methylbutylamine	0.54 ± 0.02	2.6 ± 0.1	n.d.	<0.7	<0.1
tert-Pentylamine	1.3 ± 0.1	13 ± 1	n.d.	1.1 ± 0.2	<0.1
Isopentylamine	0.53 ± 0.04	0.88 ± 0.01	n.d.	<0.7	<0.1
n-Pentylamine	0.49 ± 0.02	1.2 ± 0.1	n.d.	<0.7	<0.1
n-Hexylamine	0.54 ± 0.02	0.70 ± 0.04	n.d.	<0.7	<0.1
Sum Amines (nmol g^{-1})	**1,060 ± 89**	**1,786 ± 192**	**38.0 ± 0.3**	**377 ± 3**	**35.8 ± 0.7**
Protein Amino Acids					
D,L-Histidine	<0.1	<0.1	<0.1	n.r.	n.r.
D,L-Asparagine	tr.	tr.	<0.1	n.r.	n.r.
D,L-Glutamine	<0.1	<0.1	<0.1	n.r.	n.r.
D,L-Serine	tr.	0.14 ± 0.05	1.70 ± 0.06	0.10 ± 0.03	0.52 ± 0.03
D,L-Arginine	<0.1	<0.1	<0.1	n.r.	n.r.
Glycine	10.1 ± 0.5	11.1 ± 1.2	7.2 ± 0.8	4.0 ± 1.3	1.62 ± 0.04
D,L-Aspartic acid	tr.	tr.	0.9 ± 0.2	0.89 ± 0.48	0.25 ± 0.02
D,L-Glutamic acid	0.01 ± 0.01	0.23 ± 0.02	0.29 ± 0.02	0.12 ± 0.07	0.033 ± 0.001
D,L-Threonine	tr.	0.28 ± 0.02	0.32 ± 0.01	n.r.	<0.1
D,L-Alanine	1.60 ± 0.03	4.1 ± 0.4	0.15 ± 0.04	1.13 ± 0.25	0.17 ± 0.01
D,L-Proline	0.11 ± 0.01	0.89 ± 0.07	0.25 ± 0.03	n.r.	n.r.
D,L-Cysteine	<0.1	<0.1	<0.1	n.r.	n.r.
D,L-Tyrosine	tr.	tr.	0.14 ± 0.12	n.r.	n.r.
D,L-Lysine	<0.1	<0.1	<0.1	n.r.	n.r.
D,L-Methionine	<0.1	<0.1	<0.1	n.r.	n.r.
D,L-Valine	0.081 ± 0.004	0.81 ± 0.06	0.26 ± 0.01	0.04 ± 0.01	<0.2
D,L-Leucine	0.036 ± 0.003	0.13 ± 0.02	0.17 ± 0.01	n.r.	<0.2
D,L-Isoleucine	tr.	0.10 ± 0.01	0.14 ± 0.01	n.r.	<0.1
D,L-Phenylalanine	tr.	tr.	<0.1	n.r.	n.r.
D,L-Tryptophan	<0.1	<0.1	<0.1	n.r.	n.r.
Sum Protein Amino Acids (nmol g^{-1})	**11.9 ± 0.5**	**17.8 ± 1.3**	**11.5 ± 0.8**	**6.3 ± 1.4**	**2.59 ± 0.05**

[a]Hot-water extracts (100°C for 24 h) of the Bennu aggregate subsample (OREX-803001-0; 25.6 mg), the CM2 Murchison meteorite (University of Chicago at Illinois; 26.3 mg), the C2 ungrouped Tarda meteorite (Roberto Vargas, RV; 723 mg), and Ryugu (A0106; 13.08 mg extracted in water at 105°C for 20 h) were analyzed directly after AccQ·Tag derivatization using liquid chromatography with UV fluorescence and mass spectrometry. Compounds were identified by comparison of elution time and mass spectra to that of standards. Values are the average of three measurements (n = 3) with a standard error, $\delta x = \sigma_x \cdot (n)^{-1/2}$. The error in the total sum was determined by adding the absolute errors of the individual compounds in quadrature.

[b]Abundances of free amines and protein amino acids in Ryugu (A0106)[27]. Previously published data of the amine abundances (free and acid-labile) for the CI1 Orgueil meteorite[58] and the free protein amino acid data[62] are shown.

[c]Free ammonia concentrations in water and dichloromethane/methanol (9:1, v/v) extracts of the CI1 Orgueil and CM2 Murchison meteorites using gas chromatography mass spectrometry[16].

[d]Free ammonia concentrations with 1-sigma error calculated from the NH_4^+ abundances measured in the hot-water extracts (105ºC for 20 h) of Ryugu (A0106) and the CI1 Orgueil using ion chromatography and mass spectrometry[21].

[e]Free ammonia concentration with 1-sigma error calculated from the NH_4^+ abundance measured using ion chromatography of a cold-water leachate of the CI1 Orgueil meteorite after ten sequential extractions in ultrapure water by ultrasonication for 10 min at -2ºC to +8ºC, followed by centrifugation and filtration[22].

Abbreviations: n.r. = not reported; n.d. = not determined; tr. = amino acid was tentatively identified at trace levels but was below the limit of quantitation.

https://doi.org/10.1038/s41550-024-02472-9

Extended Data Table 3 | Free and total amino acid abundances, as measured by LC-FD/ToF-MS and LC-FD/HRMS, in the hot-water extract of Bennu (OREX-803001-0), compared with selected CCs and Ryugu (A0106)

Amino Acid	Bennu (OREX-803001-0)		Murchison (CM2)		Tarda ($C2_{ung}$)	Orgueil (CI1)[b]	Ryugu (A0106)[c]
	Free (nmol g^{-1})	*Total (nmol g^{-1})*	*Free (nmol g^{-1})*	*Total (nmol g^{-1})*	*Total (nmol g^{-1})*	*Total (nmol g^{-1})*	*Total (nmol g^{-1})*
Glycine	33 ± 1 (6)	44 ± 1 (6)	28 ± 1 (6)	80 ± 2 (6)	11.2 ± 0.5	11.5 ± 6.0	0.46 ± 0.05
D-Alanine	2.8 ± 0.4 (6)	4.0 ± 0.6 (6)	4.5 ± 0.6 (6)	8.5 ± 1.2 (6)	0.93 ± 0.04	0.90 ± 0.19	0.025 ± 0.006
L-Alanine	2.6 ± 0.4 (6)	3.9 ± 0.6 (6)	4.2 ± 0.6 (6)	11.5 ± 1.5 (6)	1.62 ± 0.06	1.1 ± 0.3	<0.44
β-Alanine	1.6 ± 0.3 (6)	3.3 ± 0.5 (6)	14.2 ± 1.6 (6)	29.2 ± 3.8 (6)	3.8 ± 0.2	30.7 ± 7.6	3.3 ± 0.1
D-Serine	0.21 ± 0.09 (6)	0.18 ± 0.03 (6)	0.38 ± 0.07 (6)	0.54 ± 0.08 (6)	0.21 ± 0.01	<0.01	0.06 ± 0.01
L-Serine	0.24 ± 0.01 (6)	≤0.7[d] (6)	0.4 ± 0.1 (6)	3.6 ± 0.6 (6)	0.78 ± 0.03	<0.01	0.18 ± 0.03
D-Isoserine	<0.01 (3)	0.027 ± 0.004 (3)	0.057 ± 0.003 (3)	0.51 ± 0.02 (3)	n.d.	n.r.	n.r.
L-Isoserine	<0.01 (3)	0.026 ± 0.004 (3)	0.065 ± 0.008 (3)	0.51 ± 0.02 (3)	n.d.	n.r.	n.r.
D-Aspartic Acid	0.94 ± 0.12 (6)	1.35 ± 0.14 (6)	0.69 ± 0.11 (6)	2.4 ± 0.3 (6)	0.42 ± 0.01	0.41 ± 0.23	<0.06
L-Aspartic Acid	0.79 ± 0.16 (6)	1.22 ± 0.12 (6)	0.73 ± 0.15 (6)	5.1 ± 0.6 (6)	0.95 ± 0.03	0.41 ± 0.21	0.02 ± 0.01
D-Threonine	<1 (6)	<0.2 (6)	<0.2 (6)	1.2 ± 0.4 (6)	n.d.	n.r.	<0.02
L-Threonine	<1 (6)	<0.2 (6)	<1 (6)	13 ± 4 (6)	n.d.	n.r.	<0.04
D,L-α-ABA	0.55 ± 0.03 (6)	0.80 ± 0.02 (6)	1.90 ± 0.04 (6)	3.23 ± 0.08 (6)	0.19 ± 0.01	0.69 ± 0.48	<0.02
D-β-ABA	0.34 ± 0.05 (6)	0.55 ± 0.08 (6)	1.9 ± 0.3 (6)	3.4 ± 0.5 (6)	0.58 ± 0.02	2.1 ± 1.1	0.32 ± 0.01
L-β-ABA	0.33 ± 0.05 (6)	0.53 ± 0.08 (6)	1.6 ± 0.2 (6)	2.8 ± 0.4 (6)	0.60 ± 0.02	1.8 ± 0.6	0.32 ± 0.01
γ-ABA	0.37 ± 0.04 (6)	3.03 ± 0.13 (6)	2.9 ± 0.4 (6)	9.2 ± 0.7 (6)	2.9 ± 0.1	2.7 ± 1.3	3.5 ± 0.2
α-AIB	0.21 ± 0.03 (6)	0.61 ± 0.05 (6)	18.6 ± 0.9 (6)	21.0 ± 1.2 (6)	0.54 ± 0.03	3.3 ± 1.4	0.38 ± 0.02
D-β-AIB	0.087 ± 0.002 (3)	0.16 ± 0.01 (3)	0.60 ± 0.01 (3)	1.25 ± 0.06 (3)	n.d.	tr.	0.20 ± 0.01
L-β-AIB	0.088 ± 0.001 (3)	0.16 ± 0.01 (3)	0.66 ± 0.01 (3)	1.30 ± 0.07 (3)	n.d.	tr.	0.17 ± 0.02
D-Glutamic Acid	0.08 ± 0.02 (6)	0.79 ± 0.06 (6)	0.64 ± 0.07 (6)	3.5 ± 0.3 (6)	0.79 ± 0.04	0.32 ± 0.11	<0.03
L-Glutamic Acid	0.07 ± 0.01 (6)	≤0.8[d] (6)	0.85 ± 0.11 (6)	10.6 ± 1.1 (6)	7.04 ± 0.14	0.56 ± 0.15	<0.03
D-Valine	0.08 ± 0.01 (6)	0.16 ± 0.01 (6)	0.93 ± 0.09 (6)	1.64 ± 0.04 (6)	0.05 ± 0.01	0.19 ± 0.05	<0.07 (0.026)[f]
L-Valine	0.09 ± 0.01 (6)	0.32 ± 0.06 (6)	1.0 ± 0.1 (6)	4.3 ± 0.2 (6)	0.81 ± 0.01	0.48 ± 0.02	<0.06 (0.056)[f]
D-Isovaline	0.015 ± 0.003 (6)	0.080 ± 0.007 (6)	5.3 ± 1.2 (6)	5.97 ± 0.70 (6)	0.04 ± 0.01	0.31 ± 0.03	<0.05 (0.053)[f]
L-Isovaline	0.016 ± 0.002 (6)	0.074 ± 0.006 (6)	5.4 ± 1.0 (6)	5.90 ± 0.80 (6)	0.04 ± 0.01	0.42 ± 0.02	<0.05 (0.047)[f]
D-Norvaline	0.024 ± 0.004 (6)	0.052 ± 0.005 (6)	0.15 ± 0.01 (6)	0.246 ± 0.006 (6)	<0.1	0.11 ± 0.01	<0.04 (0.017)[f]
L-Norvaline	0.029 ± 0.007 (6)	0.051 ± 0.004 (6)	0.14 ± 0.01 (6)	0.245 ± 0.006 (6)	<0.1	0.12 ± 0.01	<0.04 (0.017)[f]
(*R*)-3-APA	0.038 ± 0.004 (6)	0.074 ± 0.003 (6)	0.32 ± 0.04 (6)	0.68 ± 0.04 (6)	0.06 ± 0.01	1.6 ± 0.1[e]	<0.06
(*S*)-3-APA	0.038 ± 0.003 (6)	0.072 ± 0.002 (6)	0.33 ± 0.04 (6)	0.73 ± 0.03 (6)	0.06 ± 0.01		<0.08
D,L- and D,L-*allo*-3-A-2-MBA	0.09 ± 0.01 (3)	0.25 ± 0.01 (3)	0.29 ± 0.01 (3)	2.08 ± 0.03 (3)	1.10 ± 0.01	0.55 ± 0.03	tr.
3-A-3-MBA	<0.01 (3)	0.1 ± 0.1 (3)	0.25 ± 0.03 (3)	0.25 ± 0.05 (3)	0.23 ± 0.05	<0.26	tr.
3-A-2,2-DMPA	0.04 ± 0.01 (3)	0.125 ± 0.002 (3)	0.82 ± 0.03 (3)	2.50 ± 0.01 (3)	0.05 ± 0.01	0.59 ± 0.03	0.055 ± 0.002
D,L-3-A-2-EPA	0.04 ± 0.01 (3)	0.121 ± 0.001 (3)	0.25 ± 0.01 (3)	0.98 ± 0.01 (3)	<0.1	1.5 ± 0.1	tr.
D,L-4-APA	0.02 ± 0.01 (3)	0.500 ± 0.003 (3)	0.21 ± 0.01 (3)	1.37 ± 0.02 (3)	0.14 ± 0.01	2.4 ± 0.2	tr.
D,L-4-A-2-MBA	0.02 ± 0.01 (3)	0.51 ± 0.01 (3)	0.11 ± 0.01 (3)	1.62 ± 0.06 (3)	0.11 ± 0.01	1.5 ± 0.1	<0.17
D,L-4-A-3-MBA	<0.01 (3)	0.046 ± 0.001 (3)	0.02 ± 0.01 (3)	0.190 ± 0.003 (3)	0.03 ± 0.01	2.8 ± 0.1	tr.
5-APA	0.06 ± 0.01 (6)	1.01 ± 0.04 (6)	1.2 ± 0.3 (6)	6.4 ± 0.3 (6)	1.26 ± 0.02	1.2 ± 0.2	1.2 ± 0.1
D-Leucine	tr. (3)	0.09 ± 0.01 (3)	<0.1 (3)	0.9 ± 0.2 (3)	n.d.	n.r.	<0.05
L-Leucine	<0.3 (3)	<0.3 (3)	<0.1 (3)	1.3 ± 0.5 (3)	n.d.	n.r.	<0.06
D-Isoleucine	tr. (6)	0.069 ± 0.005 (6)	0.25 ± 0.05 (6)	0.4 ± 0.1 (6)	n.d.	n.r.	<0.04
L-Isoleucine	<0.1 (6)	≤0.4[d] (6)	0.24 ± 0.02 (6)	2.3 ± 0.2 (6)	n.d.	n.r.	<0.04
ε-Amino-*n*-caproic acid	<0.1 (3)	0.19 ± 0.07 (3)	0.24 ± 0.06 (3)	0.9 ± 0.1 (3)	<0.1	0.82 ± 0.79	4.5 ± 2.6
Sum C_2 to C_6 amino acids	**45 ± 1**	**70 ± 2**	**101 ± 2**	**253 ± 7**	**37 ± 1**	**71 ± 10**	**15 ± 3**

[a]Hot-water extracts (100°C for 24 h) of the Bennu aggregate subsample (OREX-803001-0; 25.6 mg), the CM2 Murchison meteorite (University of Illinois Chicago, UIC; 26.3 mg), the C2 ungrouped Tarda meteorite (Roberto Vargas, RV; 723 mg), the CI1 Orgueil meteorite (Musée National d'Histoire Naturelle de Paris; 1 g), and Ryugu (A0106; 13.08 mg extracted in water at 105°C for 20 h) were analyzed after desalting using cation exchange chromatography and *o*-phthaldialdehyde/*N*-acetyl-L-cysteine (OPA/NAC) derivatization (15 min). The OPA/NAC amino acid derivatives were identified using liquid chromatography with UV fluorescence detection/time-of-flight mass spectrometry (LC-FD/ToF-MS) and LC-FD/high-resolution mass spectrometry (HRMS). The reported uncertainties in the individual amino acid concentrations in OREX-803001-0 and Murchison are based on the averages of three or six individual measurements (n) from both instruments with a standard error, $\delta x = \sigma_x \cdot (n)^{-1/2}$. The error in the total sum was determined by adding the absolute errors of the individual compounds in quadrature.

[b]Data from ref. 59.

[c]Data from ref. 27, unless otherwise noted.

[d]Non-blank corrected value given as an upper limit for the concentration in the sample extract due to peak areas near background levels and ambiguity associated with the procedural blank contribution to the sample peak. Values included in the sum.

[e]Combined abundance of D- and L-enantiomers. Enantiomers were separated but could not be identified due to lack of optically pure standards.

[f]Single measurement made by 3D HPLC with UV fluorescence detection from ref. 20.

Abbreviations: tr. = trace, amino acid tentatively identified above background but was below the limit of quantitation; n.r. = not reported; n.d. = not determined; A = amino; ABA = amino-*n*-butyric acid; AIB = aminoisobutyric acid; APA = aminopentanoic acid; DMPA = dimethylpropanoic acid; EPA = ethylpropanoic acid; MBA= methylbutanoic acid.

https://doi.org/10.1038/s41550-024-02472-9

Extended Data Table 4 | Summary of the D/L ratios and corresponding L-enantiomeric excesses (L_{ee}) of protein and non-protein amino acids measured in Bennu (OREX-803001-0) and Murchison hot-water extracts

Amino Acid (# of analyses)	Bennu (OREX-803001-0)				Murchison (CM2)			
	Free		*Total*		*Free*		*Total*	
	D/L	L_{ee} (%)	D/L	L_{ee} (%)	D/L	L_{ee} (%)	D/L	L_{ee} (%)
Aspartic Acid (6)	1.2 ± 0.3	–9 ± 13	1.11 ± 0.16	–5.1 ± 7.5	0.95 ± 0.24	2.8 ± 12	0.47 ± 0.08	36 ± 6
Glutamic Acid (6)	1.1 ± 0.3	–7 ± 15	>0.98	<0.6	0.76 ± 0.13	14 ± 7	0.33 ± 0.05	50 ± 4
Serine (6)	0.84 ± 0.17	8 ± 9	>0.26	<59	1.06 ± 0.41	–3 ± 20	0.15 ± 0.03	74 ± 4
Isoserine (3)	n.d.	n.d.	1.04 ± 0.11	–1.9 ± 5.4	0.87 ± 0.12	6.7 ± 6.6	1.01 ± 0.06	–0.6 ± 3.0
Threonine (6)	n.d.	n.d.	n.d.	n.d.	n.d.	n.d.	0.09 ± 0.04	84 ± 5
Alanine (6)	1.07 ± 0.22	–3 ± 11	1.03 ± 0.16	–1.8 ± 8.0	1.05 ± 0.21	–2.6 ± 10	0.74 ± 0.14	15 ± 8
Valine (6)	0.89 ± 0.17	6 ± 9	0.5 ± 0.1	34 ± 7	0.90 ± 0.12	5.4 ± 6.5	0.38 ± 0.02	45 ± 2
Leucine (3)	n.d.	n.d.	>0.3	<54	n.d.	n.d.	0.72 ± 0.33	16 ± 19
Isoleucine (6)	n.d.	n.d.	>0.17	<71	1.02 ± 0.21	–1 ± 10	0.17 ± 0.05	70 ± 5
β-ABA (6)	1.0 ± 0.2	–2 ± 10	1.03 ± 0.22	–1.6 ± 10.9	1.22 ± 0.25	–10 ± 11	1.21 ± 0.25	–9 ± 12
β-AIB (3)	1.00 ± 0.03	0.05 ± 1.28	0.99 ± 0.07	0.6 ± 3.6	0.92 ± 0.02	4.3 ± 0.8	0.96 ± 0.07	1.9 ± 3.5
Isovaline (6)	0.94 ± 0.23	3 ± 12	1.08 ± 0.13	–3.9 ± 6.2	0.99 ± 0.30	0.6 ± 15	1.02 ± 0.16	–0.8 ± 6.5
Norvaline (6)	0.83 ± 0.24	9 ± 13	1.01 ± 0.09	–0.5 ± 4.9	1.06 ± 0.09	–2.9 ± 4.3	1.00 ± 0.04	–0.2 ± 1.8
3-APA (6)	0.99 ± 0.13	0.4 ± 6.5	1.03 ± 0.05	–1.6 ± 2.6	0.98 ± 0.17	1 ± 9	0.93 ± 0.07	3.6 ± 3.4

[a]The uncertainties for the D/L ratios and L-enantiomeric excesses (L_{ee}) are based on the individual amino acid abundance values and their standard errors propagated through the relevant equations with L_{ee} (%) = [(L – D)/(L + D)]×100. The large errors in some of the values are due to the relatively small mass of sample available for this study (~10 mg equivalent for the non-hydrolyzed and 6M HCl-hydrolyzed, hot-water extracts) and the relatively low amino acid concentrations in the Bennu aggregate resulting in a low signal-to-noise ratio for the measurements.

Abbreviations: n.d. = not determined due to trace amino acid abundances present at or below the detection limit or due to an interfering compound; ABA = amino-*n*-butyric acid; AIB = aminoisobutyric acid; APA = aminopentanoic acid.

https://doi.org/10.1038/s41550-024-02472-9

Extended Data Table 5 | Blank-subtracted free abundances of carboxylic acids identified by GC-QqQ-MS analyses of the hot-water extract of Bennu (OREX-803001-0), compared with selected CCs and Ryugu (A0106)[a]

Free Carboxylic Acids	Bennu (OREX-803001-0) nmol g^{-1}	Murchison (CM2) nmol g^{-1}	Tarda ($C2_{ung}$) nmol g^{-1}	Orgueil (CI1)[b] nmol g^{-1}	Ryugu (A0106)[c] nmol g^{-1}
Monocarboxylic acids					
Formic acid	4,106 ± 91	3,814 ± 86	416 ± 79	1,404 ± 67	9,466 ± 103
Acetic acid	1,436 ± 72	4,507 ± 43	865 ± 67	2,018 ± 89	5,708 ± 1,536
Propanoic acid	156 ± 8	251 ± 4	94 ± 7	153 ± 6	<0.1
Isobutyric acid	42 ± 2	49 ± 1	23 ± 1	25 ± 1	<0.1
2,2-Dimethylpropanoic acid	40 ± 3	36 ± 1	<0.1	38 ± 2	<0.1
Butyric acid	85 ± 9	120 ± 4	33 ± 3	43 ± 2	<0.1
2-Methylbutyric acid	<0.1	43 ± 2	19 ± 1	17 ± 1	<0.1
Isopentanoic acid	95 ± 7	115 ± 4	22 ± 1	19 ± 1	<0.1
2,2-Dimethylbutyric acid	<0.1	<0.1	<0.1	<0.1	<0.1
3,3-Dimethylbutyric acid	<0.1	<0.1	<0.1	<0.1	<0.1
Pentanoic acid	35 ± 1	44 ± 1	28 ± 1	26 ± 1	<0.1
2-Ethylbutyric/2-Methylpentanoic acid	<0.1	<0.1	<0.1	<0.1	<0.1
3-Methylpentanoic acid	<0.1	<0.1	<0.1	17 ± 1	<0.1
4-Methylpentanoic acid	<0.1	<0.1	<0.1	13 ± 1	<0.1
Hexanoic acid	<0.1	<0.1	33 ± 7	38 ± 1	<0.1
Benzoic acid	346 ± 10	257 ± 3	<0.1	37 ± 1	<0.1
Dicarboxylic acids					
Oxalic acid	844 ± 44	3,603 ± 14	533 ± 53	1,079 ± 38	<0.1 (14)[d]
Malonic acid	<0.1	<0.1	780 ± 169	253 ± 9	<0.1 (0.6)[d]
Succinic acid	<0.1	196 ± 7	52 ± 2	34 ± 1	<0.1 (9.3)[d]
Fumaric/Maleic acid	<0.1	<0.1	<0.1	28 ± 1	<0.1 (1.7)[d]
Glutaric acid	25 ± 1	37 ± 2	31 ± 1	23 ± 1	<0.1 (3.5)[d]
Sum Carboxylic Acids (nmol g^{-1})	**7,210 ± 125**	**13,072 ± 98**	**2,929 ± 205**	**5,263 ± 118**	**15,203 ± 1,539[e]**

[a]Hot-water extracts (100°C for 24 h) of the Bennu aggregate subsample (OREX-803001-0; 25.6 mg), the CM2 Murchison meteorite (University of Chicago at Illinois; 26.3 mg), the C2 ungrouped Tarda meteorite (Roberto Vargas, RV; 723 mg), and Ryugu (A0106; 13.08 mg extracted in water at 105°C for 20 h) were desalted by cation exchange chromatography and then analyzed after 2-pentanol derivatization using gas chromatography with triple quadrupole mass spectrometry. Compounds identified by comparison of elution time and mass spectra to that of standards. Values are the average of three measurements (n = 3) with a standard error, $\delta x = \sigma_x \cdot (n)^{-1/2}$. The error in the total sum was determined by adding the absolute errors of the individual compounds in quadrature.

[b]Data first reported in this study for CI1 Orgueil using the same extraction and derivatization methods as OREX-800031-0 and Murchison.

[c]Values measured in a hot-water extract (105°C for 20 h) by gas chromatography mass spectrometry[20], unless otherwise noted.

[d]Values for dicarboxylic acids in a hot-water extract (105°C for 20 h) measured by capillary electrophoresis high-resolution mass spectrometry[27]. No errors were reported[27].

[e]Note that several other mono-, di-, and tricarboxylic acids were identified in the Ryugu (A0106) hot-water extract[27] and are not included in this Table, therefore this value is a lower limit for the total abundance of carboxylic acids.

https://doi.org/10.1038/s41550-024-02472-9

Extended Data Table 6 | Blank-subtracted abundances of N-heterocycles identified by HPLC/HRMS analyses of a 6 M HCl extract of Bennu (OREX-800044-101), compared with selected CCs and Ryugu (A0106)[a]

N-Heterocycles	Bennu (OREX-800044-101) nmol g^{-1}	Murchison (CM2)[b] nmol g^{-1}	Orgueil (CI1)[c] nmol g^{-1}	Ryugu (A0106)[d] nmol g^{-1}
Canonical Nucleobases				
Uracil	0.90 ± 0.06	1.90 ± 0.04	0.24	0.10 ± 0.05
Thymine	0.57 ± 0.04	0.59 ± 0.04	n.r.	n.r.
Cytosine	0.31 ± 0.07	0.26 ± 0.01	n.r.	n.r.
Adenine	0.26 ± 0.12[e]	0.90 ± 0.03	0.05	n.r.
Guanine	0.12 ± 0.07	4.3 ± 0.7	0.13	n.r.
Other Purines and Pyrimidines				
Purine	0.004 ± 0.002	0.033 ± 0.001	0.04	n.r.
Hypoxanthine	0.12 ± 0.05	1.12 ± 0.02	0.04	n.r.
Xanthine	0.40 ± 0.17	1.49 ± 0.09	<0.07	n.r.
Isoguanine	0.13 ± 0.04[e]	0.62 ± 0.01	n.r.	n.r.
2-Aminopurine	n.d.	0.004 ± 0.001	n.r.	n.r.
8-Aminopurine	n.d.	0.23 ± 0.01	n.r.	n.r.
2,6-Diaminopurine (DAP) + 6,8-DAP[f]	0.17 ± 0.04	0.18 ± 0.01	<0.01	n.r.
1-Methyluracil	0.03 ± 0.01	0.06	n.r.	n.r.
6-Methyluracil	0.39 ± 0.04	0.36	n.r.	n.r.
Other N-Heterocycles				
Imidazole	*tentative*	16	n.r.	n.r.
2-Imidazole carboxylic acid	0.05 ± 0.01	0.21	n.r.	0.054
4-Imidazole carboxylic acid	0.13 ± 0.01	3.1	n.r.	0.15 ± 0.03
2-Methyl-1H-imidazole carboxylic acid	0.41 ± 0.05	n.r.	n.r.	n.r.
Picolinic acid	*tentative*	*tentative*	n.r.	n.r.
Nicotinic acid (vitamin B3)	0.43 ± 0.07	2.5	n.r.	0.40 ± 0.01
Isonicotinic acid	0.17 ± 0.04	1.2	n.r.	0.40 ± 0.16
2-Methylnicotinic acid	0.04 ± 0.01	n.r.	n.r.	n.r.
5-Methylnicotinic acid	0.12 ± 0.03	n.r.	n.r.	n.r.
6-Methylnicotinic acid	0.14 ± 0.03	n.r.	n.r.	n.r.
Sum all Purines (nmol g^{-1})	1.2 ± 0.2	8.9 ± 0.7	~0.26	-
Sum all Pyrimidines (nmol g^{-1})	2.2 ± 0.1	3.2 ± 0.1	~0.24	0.10 ± 0.05
Sum all N-Heterocycles (nmol g^{-1})	4.9 ± 0.3	35 ± 1	~0.48	1.1 ± 0.2
Ratio (Purines/Pyrimidines)	**0.55 ± 0.09**	**2.8 ± 0.2**	**~1.08**	**-**

[a]Compounds identified by comparison of elution time and mass spectra to standards. Values are the average of two measurements (n = 2) with a standard error, $\delta x = \sigma_x \cdot (n)^{-1/2}$. The error in the sum was determined by adding the errors of the individual compounds in quadrature.
[b]Values represent the combined extractable total abundances in hot-water and 6 M HCl extracts[63].
[c]Values for purines from a formic acid extract[34], and the uracil abundance from water, formic acid, and HCl extracts[64].
[d]Values represent the total abundances in the 6 M HCl hydrolyzed, hot-water extract[33].
[e]Upper limit.
[f]2,6-DAP and 2,8-DAP co-eluted under the chromatographic conditions used, therefore the sum of abundances is reported assuming both compounds have similar ionization responses and detection efficiencies.
Abbreviations: n.r. = not reported; n.d. = not determined.

nature astronomy

Supplementary information

https://doi.org/10.1038/s41550-024-02472-9

Abundant ammonia and nitrogen-rich soluble organic matter in samples from asteroid (101955) Bennu

In the format provided by the authors and unedited

Supplementary information

Materials and analytical methods

Brief overview of the composition of the Bennu aggregates. The Bennu aggregate samples studied consisted of a mixture of mostly fine (<100 μm) to intermediate (100–500 μm) sized particles with some coarse (>500 μm) grains dominated by hydrous silicate minerals (~80% phyllosilicates by volume) with lower abundances (≤ 10%) of sulfides, magnetite, carbonates, anhydrous silicates (olivine and pyroxene), and minor phases including phosphates and phosphides consistent with extensive aqueous alteration on the Bennu parent body[5]. The bulk elemental compositions of the Bennu aggregate samples are similar to the Ryugu aggregate materials and CI carbonaceous chondrites. However, enrichments of some fluid mobile elements in the "quick-look" (QL) samples that are distinct from solar composition may indicate a unique chemical component in the avionics deck material whose source has yet to be identified[5]. The insoluble organic matter in the Bennu aggregate is present in the form of plates and veins, carbonaceous–mineral aggregates, and discrete micrometer-scale nanoglobules that are abundant and widespread throughout the Bennu mineral matrix[5].

Bennu samples and controls. Images of two of the Bennu aggregate samples analyzed as part of this investigation are shown in Supplementary Fig. 1. The sample nomenclature and details of the processing and analytical flow of the Bennu aggregate samples are summarized in Supplementary Table 1 and Supplementary Fig. 2. Two aggregate samples (OREX-500002-0 and OREX-500005-0) that were studied as part of the QL analyses were removed from the avionics deck surface, weighed, and then containerized under N_2 in the curation glovebox. OREX-500002-0 (22 mg) consisted primarily of dark fines (<100 μm) and some intermediate-sized particles (100–500 μm), with some bright and highly reflective particles, and numerous (>5) fibers thought to be derived from spacecraft blanketing material. The sample was sealed under N_2 between two glass concavity slides and shipped from the NASA Johnson Space Center (JSC) to the Carnegie Institution for Science (CIS). This sample was inspected under an optical microscope at CIS, and the fibers were physically removed from the sample with ashed tweezers. A 1.1 mg subsample (OREX-501029-0) of the aggregate was then transferred from the concavity slide to an ashed glass pyrolysis tube and then hand carried to the NASA Goddard Space Flight Center (GSFC) for wet chemistry and analysis by pyrolysis gas chromatography coupled to triple quadrupole mass spectrometry (*py*-GC-QqQ-MS). The remaining ~20 mg were further split into multiple subsamples for elemental and isotopic analyses of total carbon, nitrogen, and hydrogen using an elemental analyzer–isotope ratio mass spectrometer (EA-IRMS). A second aggregate sample collected from the avionics deck (OREX-500005-0) consisted of mostly dark fines with an average grain size <100 μm, but with some particles up to ~500 μm. Some bright and highly reflective particles were also present in the aggregate sample. OREX-500005-0 was sealed under N_2 inside a glass vial with a Viton stopper and crimped aluminum lid. Although the initial mass of the sample was 88 mg, only ~1 mg of the sample was used as part of a coordinated analysis of organic matter at NASA Johnson Space Center (JSC).

A ~52 mg aggregate sample (OREX-800031-0) removed from the OSIRIS-REx TAGSAM sample collector consisting of a mixture of fine- to intermediate-sized particles was shipped under N_2 to GSFC in between two glass concavity slides (Supplementary Fig. 1) where it was subsampled for multiple analyses per the analytical scheme shown in Supplementary Fig. 2. A similar mass of a crushed sample of the Murchison CM2 (Mighei-type) carbonaceous chondrite from the University of Illinois Chicago (UIC) and a powdered sample of fused silica (FS-120, HP Technical Ceramics, Sheffield, UK) that had been previously ashed at 500°C in air overnight to remove organic contaminants were processed in parallel with the Bennu aggregate. A 23 mg aliquot of the Bennu sample (OREX-803007-0) was allocated for bulk H, C, and N analyses at CIS; 3.3 mg was dedicated for nontargeted molecular profiling of soluble organics using Fourier-transform ion cyclotron resonance mass spectrometry (OREX-803006-0) at Helmholtz Zentrum in Munich, Germany; and 1 mg (OREX-803004-0) was allocated for wet-chemistry *py*-GC-QqQ-MS analysis at NASA GSFC for additional characterization of the SOM composition. Most of the remaining mass of each sample was extracted in hot water at 100°C for 24 h, and aliquots of the water supernatant were split and analyzed for amino acids, aliphatic amines, and ammonia using liquid chromatography with UV fluorescence detection and time-of-flight mass spectrometry (LC-FD/ToF-MS) and carboxylic acids using GC-QqQ-MS. A 25.6 mg subsample (OREX-803001-0) of the Bennu aggregate OREX-800031-0 was used for the hot-water extraction, and in parallel, a 26.3 mg sample of Murchison and a 27.4 mg sample of the FS-120 were also processed. The solid residues of both Murchison and the Bennu aggregate (OREX-803001-103) after hot-water extraction were dried under vacuum and analyzed for bulk H, C, and N by EA-IRMS at CIS. The total C and N abundance and isotopic composition of a portion of the Bennu water extract (OREX-803001-112) and Murchison that was acidified with HCl and dried under vacuum was determined using the nano EA-IRMS instrument at Penn State University (PSU). The details of the hot-water extraction and analytical procedures used in this investigation are described in the section that follows.

A separate 17.75 mg sample of Bennu (OREX-800044-101), subsampled from Bennu aggregate OREX-800044-0 from the TAGSAM sample collector head (Supplementary Fig. 1), was extracted in HCl and analyzed for N-heterocycles using high performance liquid chromatography with high-resolution mass spectrometry (HPLC-HRMS) at Kyushu university in Japan. A 14.4 mg ashed sample of sea sand (FUJIFILM Wako Pure Chemical Corporation, Japan; 30–50 mesh) was used as a processing blank for OREX-800044-101. Procedural solvent blanks were also processed in parallel and analyzed.

Samples of the carbonaceous chondrites Winchcombe (CM1.3/1.4, UA 2925,12, mass 171.5 mg), Kolang (CM1.4, ASU 2147, mass 450.6 mg) and the C2 ungrouped Tarda (C2.2, mass 723.0 mg) that had been crushed using ashed ceramic mortar and pestles were also extracted in hot water and analyzed separately for amino acids using the same extraction and LC-FD/ToF-MS analytical procedures as the Bennu TA subsample OREX-803001-0 previously described. Separate aliquots (~15–20 mg) of each meteorite powder were sent to the Carnegie Institution for Science for bulk H, C, and N analyses using the same methods described in the following section.

Analytical measurements and discussion

EA-IRMS analysis of the bulk C, N, and H abundances and isotopic compositions in the solid samples

Sample preparation and analytical details. The elemental and isotopic analyses of the bulk H, C, and N were carried out at the Earth and Planets Laboratory, following previously established protocols[19,56,65]. Three samples were analyzed: (i) one recovered from the avionics deck (OREX-500002-0, 19 mg) as part of the quick-look phase of the Sample Analysis Plan[12], and (ii) (one retrieved from inside the OSIRIS-REx TAGSAM sample collector (OREX-803007-0, 23 mg; parent sample OREX-800031-0), and (iii) the dried solid residue of Bennu aggregate from the sample collector after extraction in water at 100°C for 24 h (OREX-803001-103, 23 mg). The samples consisted of a mixture of fine- to intermediate-sized particles, and subsampling commenced without any further particle size homogenization. However, a subsample of intermediates (~200 μm) was hand-picked from the fines and analyzed separately in the case of OREX-500002-0. The bulk H, C, and N elemental and isotopic compositions of these samples were determined within four days of sample delivery.

Subsamples of each aggregate were weighted into Ag capsules for H (0.877–2.161 mg), or into Sn capsules for C and N analyses (2.281–5.553 mg). Afterwards, they were put in an Ar-flushed glovebox and subjected to 120°C heating for 48 hours in order to decrease the quantity of adsorbed atmospheric H_2O[66,67]. By evaluating the δD composition of bulk Murchison pretreated at 50°C to 200°C in a series of control experiments, the adopted protocol was established. The samples were reweighed and loaded into a Zero-Blank Costech autosampler (for H analysis) while in the glovebox prior to analysis. While Ar was continuously flushing, the autosampler was transferred to the elemental analyzer–isotope ratio mass spectrometer. The samples were exposed to an Ar atmosphere for a duration exceeding 66 hours before being analyzed. A set of subsamples from the OREX-500002-0 were not exposed to the heat treatment. Blank measurements in every analytical run always included Ag and Sn capsules.

The C and N elemental abundances and isotopic compositions of the Bennu bulk aggregate samples were measured with a Thermo Scientific Delta V^{Plus} mass spectrometer interfaced with a Carlo Erba (NA 2500) elemental analyzer. As shown in Supplementary Fig. 3 and Supplementary Table 2, the Bennu aggregate samples are enriched in total C (4.5 to 4.7 wt.%)[5] and total N (0.23 to 0.25 wt.%)[5] compared to the mass weighted average values of all bulk abundances published to date on aggregate samples collected from asteroid Ryugu by the Hayabusa2 mission shown in Supplementary Table 3 (C = 3.81 wt.%, N = 0.13 wt.%)[20,33,68-71] and most unheated petrologic type 1 and 2 carbonaceous chondrites[2,3]. The combination of H and N isotopic enrichments in these Bennu aggregate samples (δD = +305 to 365 ‰, $\delta^{15}N$ = +57 to 106 ‰: Supplementary Table 2) is also distinct from the mass weighted averages for Ryugu shown in Supplementary Table 3 (δD = +200 ‰, $\delta^{15}N$ = +33 ‰)[20,33,68-71] and most unheated petrologic type 1 and 2 carbonaceous chondrites[19,56].

For the Bennu aggregate bulk H analyses, we used a Thermo Scientific Delta Q mass spectrometer connected to a Thermo Finnigan Thermal Conversion elemental analyzer (TC/EA) operating at 1400°C. N_2, CO_2 and H_2 reference gases were introduced via a Conflo III and Conflo IV interface, respectively. Reference gases and in-house standards (acetanilide, stearic acid) have been calibrated against international standard gases and

solids of known isotopic composition (Oztech Trading Company, Isoanalytical Laboratory, National Bureau of Standards-22, IAEA-60, Standard Mean Ocean Water). By analyzing internal working gas standards during analysis, the internal precision of the measured isotopic ratios and elemental compositions throughout the run was monitored regularly. To calibrate and correct the data, in-house standards, including both liquid and solid materials, were analyzed at regular intervals between samples. An H_3^+ correction determined by H-linearity tests was applied to the H measurements[14]. The reported uncertainties for the elemental and isotopic analyses correspond to a 1σ deviation, which is determined based on either replicate analyses of standards or analyses of at least two aliquots of individual samples, whichever is the larger. The replicate samples were analyzed sequentially to check for sample heterogeneity, and in the case of H, to evaluate small memory effects on δD measurements known to occur with D-enriched samples[19,73]. Blanks were run between different samples to reduce the memory effects. Memory effects were also monitored by in-house standards within the course of an analytical run. There is no memory effect for the C and N analyses[19].

Bulk elemental ratios. The bulk elemental ratios (atomic) for OREX-500002-0 and OREX-803007-0 ranged from N/C ~ 0.04 to 0.05 and H/C ~ 2.2 to 2.5 (Extended Data Table 1). The $\delta^{13}C$ and N/C values suggest that up to ~10% of the total carbon in these Bennu aggregates (~0.45 to 0.47 wt.% C) could be in carbonate[74]. The estimated abundance of carbonate C in these aggregate samples from the EA-IRMS data is in good agreement with an XRD measurement of another Bennu aggregate sample (OREX-500005-0)[5] that contained 3 ± 1 wt.% carbonate (predominately dolomite, $CaMg(CO_3)_2$), which is equivalent to 0.39 ± 0.13 wt.% C from dolomite. The composition of a ~0.2 mm intermediate-sized particle was depleted in ^{13}C ($\delta^{13}C$ = –0.5‰, Extended Data Table 1, Supplementary Table 2) compared to finer grained material from the same sample, revealing some degree of heterogeneity which may be due to a difference in the abundance of carbonate phases between the finer and coarser grained fractions. The significant contributions of H from hydrated minerals in the samples can explain the elevated bulk H/C values in these Bennu samples compared to the predicted H/C values of ~0.3 to 0.6 of the IOM based on the average 3.42 μm band depth from organic rich IR spectra of Bennu[9].

C and N mass balance estimates. The bulk C and N measurements of a Bennu aggregate sample (OREX-803001-103), after extraction in hot water, indicated that the abundances of C and N in the residue were both lower and more isotopically depleted (Extended Data Table 1, Supplementary Table 2) compared to the aggregate sample prior to water extraction. Based on mass balance calculations accounting for the mass loss of bulk C and N and change in the isotopic composition ($\delta^{13}C$ and $\delta^{15}N$ values) of the solid residue after water extraction (Extended Data Table 1), the water extract from the Bennu aggregate should be isotopically enriched in both ^{13}C and ^{15}N, with average $\delta^{13}C$ and $\delta^{15}N$ values of +80 ± 77‰ and +178 ± 86‰, respectively. The same calculations also suggested a heavy average C and N isotopic composition of the Murchison water extract ($\delta^{13}C$ ~ +61‰ and $\delta^{15}N$ ~ +80‰), but they were not as enriched as Bennu. To confirm the predicted C and N isotopic composition of the water extracts based on the mass balance

calculations, we measured the $\delta^{13}C$ and $\delta^{15}N$ values of the water extracts using the nano EA-IRMS instrument at PSU (Supplementary Table 4).

Nano EA-IRMS analysis of C and N abundances and isotopic compositions in the water extracts

Analytical details and data processing methods. Nano EA-IRMS analyses were conducted at PSU following previous methods[57]. Briefly, the nano EA-IRMS system employed a Flash™ IRMS elemental analyzer that was coupled via a ConFlo IV Universal Interface to a DELTA V Plus isotope ratio mass spectrometer with a universal triple collector. The Flash IRMS EA consisted of a Costech zero blank autosampler, a custom-made narrow-bore combination combustion–reduction reactor (18 mm O.D., 10 mm I.D., and 45.4 cm long) filled with WO3 and reduced copper grains and operated at 1,020°C, a custom-made water trap (glass tube, 15 cm long, 3.81 mm I.D.) containing magnesium perchlorate, and a carbonPLOT capillary GC column (15 m, 0.32 mm I.D., and 1.5 μm film thickness).

For any given isotope measurement, the measured value reflects a weighted average of the sample isotope value and the procedural blank:

$$A_{meas}\delta_{meas} = A_S\delta_S + A_B\delta_B\,, \qquad \text{(Equation 1)}$$

where δ_{meas} and A_{meas} are the measured isotope value and peak area, δ_S and A_S are the sample isotope value and peak area, and δ_B and A_B are the isotope value and peak area of the procedural blank. If the size, composition, and variability of the procedural blank can be measured directly, results of individual analyses (δ_{meas}) can be corrected (δ_C) for the blank contribution using experimentally determined values for δ_B and A_B ($\bar{\delta}_B$ and $\bar{A}_B$):

$$\delta_C = \frac{A_{meas}\delta_{meas} - \bar{A}_B\bar{\delta}_B}{A_{meas} - \bar{A}_B}. \qquad \text{(Equation 2)}$$

The blank-corrected isotope value uncertainty depends on the uncertainty in $\bar{A}_B$ and $\bar{\delta}_B$:

$$\sigma^2_{\delta_S} = \frac{1}{N^2}\left(\left(\frac{E^2}{N^2}\right)\left(A_B^2\sigma^2_{A_{meas}} + A^2_{meas}\sigma^2_{A_B}\right) + A^2_{meas}\sigma^2_{\delta_{meas}} + A_B^2\sigma^2_{\delta_B}\right), \qquad \text{(Equation 3)}$$

where $N = A_{meas} - A_B$ and $E = \delta_{meas} - \delta_B$.

For direct measurement of the blank, with A_B and δ_B calculated as the mean of *n* measurements of $\bar{A}_B$ and $\bar{\delta}_B$, uncertainty in the area (σA_B) and isotope measurement ($\sigma\delta_B$) is calculated as:

$$\sigma = stdev / n^{1/2} \qquad \text{(Equation 4)}$$

The uncorrected carbon and nitrogen isotope data from the Bennu (OREX-803001-112) and Murchison meteorite extracts and blanks are shown in Supplementary Table 5 and Supplementary Fig. 4. Four different types of blanks were analyzed: (a) empty tin capsules (n = 2), (b) tin capsules exposed to 75 µL Millipore water and 2 µL 6 M hydrochloric acid (HCl) dried under vacuum at room temperature in a centrivap (n = 10), (c) one 73.5 µL procedural blank water extract, and (d) one 68.9 µL fused silica (FS-120) procedural blank water extract (both c and d water extracts were processed in parallel with the Bennu (OREX-803001-112) and Murchison water extracts and were also treated with 2 µL 6 M HCl and dried at room temperature using a centrivap). 71.7 µL of the Bennu water extract and 71.1 µL of the Murchison water extract, each volume representing ~2.6% of the total extracted sample, were pipetted into individual tin capsules along with 2 µL 6 M HCl and then dried under vacuum at room temperature for 2 hours in a centrivap.

Nano EA-IRMS isotope data were corrected for blank contribution by mass balance (Equation 2) using the statistical means of the peak areas and isotope values for tin capsules treated with Millipore water and HCl (capsules + water + acid). The carbon and nitrogen peak areas and isotope values varied among the 10 blanks (Supplementary Table 5). Blanks with peak areas larger than the measured sample overestimate possible background contributions to the sample. Therefore, only the blank analyses with peak areas smaller than the samples were used for the blank correction (Supplementary Table 5 and Supplementary Fig. 4). The uncertainty in blank-corrected isotope values was calculated using Equation 3, where the uncertainty in the blank area and isotope measurements were calculated using Equation 4. For carbon, A_B = 27.8, δ_B = –26.2, σA_B = 1.5, and $\sigma\delta_B$ = 0.2 for OREX-803001-112, and A_B = 30.4, δ_B = –26.2, σA_B = 2.0, and $\sigma\delta_B$ = 0.1 for CM2 Murchison. For nitrogen, A_B = 1.5, δ_B = 3.6, σA_B = 0.2, and $\sigma\delta_B$ = 1.1 for OREX-803001-112, and A_B = 0.8, δ_B = 6.8, σA_B = 0.1, and $\sigma\delta_B$ = 1.8 for CM2 Murchison for nitrogen.

US Geological Survey (USGS, Reston, VA, USA) reference standards 63 (caffeine) and 40 (L-glutamic acid), Urea #1 (Indiana University, Bloomington, IN, USA), and PSU in-house standard Peru mud were used as calibration standards to evaluate the carbon data. Measured $\delta^{13}C$ values were normalized to the VPDB scale with a two-point calibration using USGS 40 and Urea #1. International Atomic Energy Agency (IAEA, Vienna, Austria) standards N-2 and 305B (ammonium sulfate), USGS 40, 63, and 25 (ammonium sulfate), and Urea #1 were used to evaluate the nitrogen data, with IAEA-305B and USGS 25 serving as calibration standards. The detection limit of the nano EA-IRMS system is approximately 30 nmol of nitrogen (~2Vs) and 22 nmol of carbon (~34Vs). CM2 Murchison (UIC) nitrogen was below detection limit (<2Vs).

Nitrogen abundances and isotopes. The abundance of free ammonia (13,613 nmol g^{-1}) in the hot-water extract of Bennu (OREX-803001-0) was more than 12× higher than the ammonia abundance measured in the Murchison hot-water extract (Fig. 1, Extended Data Table 2). The elevated ammonia abundance in the Bennu extract is similar to the free ammonia abundances reported for Orgueil[16,21,22] and a bulk sample of the CR3 meteorite GRA 95229[16]. An elevated amount of ammonia in the Bennu extract was also inferred from the nitrogen loss from the sample following water extraction (100°C for 24 h) calculated from the difference in measured quantities of total nitrogen in the Bennu aggregate before and after hot-water extraction (i.e., before extraction: OREX-803007-0,

0.25 ± 0.01 wt.% N; after extraction: OREX-803001-103, 0.20 ± 0.01 wt.% N, Extended Data Table 1).

The predicted and measured amounts of nitrogen recovered from the dried Bennu water extract (OREX-803001-112) were similar. The mass balance estimate (24 ± 5 nmol N) and the measured amount (6 ± 35 nmol N) were indistinguishable given the range of analytical uncertainties (Supplementary Table 4). Similarly, the calculated estimate of the nitrogen isotope abundance of the water extract ($\delta^{15}N_{AIR}$ = +178 ± 86‰) was similar to the measured value ($\delta^{15}N_{AIR}$ = +180 ± 47‰), within uncertainties (Supplementary Table 4). The Bennu water extract is significantly ^{15}N enriched relative to the hydrazine used for the propulsion system on the OSIRIS-REx spacecraft ($\delta^{15}N_{AIR}$ = 4.7 ± 1.5‰)[75]. Additional information about ammonia as a byproduct of the hydrazine thrusters used on the OSIRIS-REx spacecraft and the potential for sample contamination is discussed later.

Our measured nitrogen isotope value for Bennu (OREX-803001-112) is consistent with pristine meteorites and an outer solar system origin. Ammonia in CR2 (GRA 95229), CM2 (Murchison, Murray), CI1 (Orgueil, Ivuna), and ungrouped C2 chondrites (Tagish Lake, Bells) meteorites all exhibit ^{15}N enrichment over a notable range in ammonia released after hydrothermal treatment of the IOM in the meteorite samples ($\delta^{15}N_{NH4,AIR}$ = +50 to +455‰)[16,65]. The range in $\delta^{15}N$ values for carbonaceous meteorites likely indicates heterogeneity in process associated with the earliest history of the solar system. In contrast, the nitrogen isotope signature of hydrogen cyanide from the CM2 Murchison is more typical of Earth-like values ($\delta^{15}N_{HCN,AIR}$ = +1 to + 11‰)[16,76], indicating HCN had a source distinct from ammonia associated planetary processes[76]. For Bennu (OREX-800031-112), the elevated ^{15}N signature is in the range of carbonaceous meteorites, indicates an outer solar system source, and is inconsistent with a planetary (or spacecraft) source. The elevated amount of ammonia in samples returned from Bennu is important because of its chemical reactivity in prebiotic chemistry and potential for delivery of a reactive source of nitrogen by carbonaceous asteroids to the early Earth[15].

***Carbon abundances and isotopes*.** The measured amount of carbon in the dried extraction water (OREX-803001-112) was significantly lower than predicted by mass balance calculations (Supplementary Table 4). The mass balance estimate for carbon in the water (166 ± 155 nmol C) is nearly an order of magnitude more than was measured in the aliquot (25 ± 53 nmol C). Similarly, carbon isotope abundances did not match between the isotope mass balance estimate ($\delta^{13}C_{VPDB}$ = +80 ± 77‰) and the measured value ($\delta^{13}C_{VPDB}$ = –9 ± 3‰). The low abundance of carbon likely reflects the evolution and loss of CO_2 when the water aliquot was acidified with HCl in order to retain ammonia as ammonium chloride salt as it dried. By mass balance, we estimate the carbon lost (141 nmol C) was ^{13}C-enriched ($\delta^{13}C_{VPDB}$ = +96‰).

The elevated isotopic signature inferred for the lost carbon is similar to carbonate carbon isotope data from the carbonaceous meteorite, Tagish Lake[77], and the range of elevated values observed for CM carbonaceous chondrites[66,78]. The ^{13}C-depleted signature measured in the water extract most likely reflects soluble forms of organic carbon. The value is consistent with average NanoSIMS measurements of carbon in Bennu aggregate insoluble organic matter ($\delta^{13}C$ ~ –11‰). We note the amount of carbon lost as CO_2 indicates that most of the difference in wt.% C observed between OREX-803007-0 and OREX-803001-103 (i.e., before and after hot-water extraction) can be

attributed to carbonate dissolution. This implies just slightly less than 0.3 wt.% C, about 7% of the carbon, measured by EA-IRMS in Bennu OREX-803007-0, was originally present in water-soluble carbonate phases.

Isotopic composition of the hydrazine used in the OSIRIS-REx spacecraft thrusters and ammonia as a byproduct

The OSIRIS-REx spacecraft uses high-purity hydrazine monopropellant thrusters. At sample collection the spacecraft performed a 25.7 s burn with four 4.5 N thrusters[79] canted away from the TAG site to depart the surface of Bennu. OSIRIS-REx was required to impinge less than 180 ng/cm^2 of hydrazine on the TAGSAM surface; a calculation was made under worst case with 0.05% residual hydrazine and an 80.25 s back-away burn[75]. Since monopropellant exhaust is approximately 25% N_2, 25% H_2, and 50% NH_3, the ammonia abundance should be about 1,000 times the molar value for hydrazine from previous plume modeling. Then adjusting for the shorter duration yields 2 μmol/cm^2 (33 μg/cm^2) NH_3 impinging on TAGSAM. This value could be higher or lower depending on the complex dynamics of the plume with regolith lofted by the TAG and back-away[10]. The TAGSAM head was observed to have externally adhering particles, covering a small fraction of the TAGSAM head exterior[10]. It is possible that these particles could have adsorbed 2 μmol/cm^2 NH_3. TAGSAM 6061 aluminum and 304L stainless steel is expected to have lost any NH_3 adsorbed on the metal. Ammonia on 304L stainless steel in vacuum[80] only has a 4% sticking coefficient at 0°C. If the aluminum and stainless steel behave similarly, there would be virtually no NH_3 remaining on TAGSAM metal surfaces when the sample was stowed 8 days after sampling. Thus, any residual NH_3 would not have an opportunity to react with the bulk sample. The N- and H-isotope compositions of the hydrazine as loaded into the OSIRIS-REx spacecraft propellant tanks was measured to be $\delta^{15}N_{AIR}$ = +4.7 ± 1.5‰ and δD_{VSMOW} = +154 ± 23‰[75]. The NH_3 produced by the thruster at high temperature should have similar isotopic values. Future analyses should investigate if the NH_3 in the bulk sample as well as any NH_3-mediated reactions retain the isotopic signature of this monopropellant. We did not detect any hydrazine in the Bennu aggregate water extract OREX-803001-0 using LC-FD/MS (Supplementary Fig. 5, Supplementary Table 6) above the 0.1 nmol g^{-1} level (Extended Data Table 2).

LC-FD/QqQ-MS analysis of the AccQ•Tag derivatives of ammonia, hydrazine, aliphatic amines, and protein amino acids

Standards and reagents. All commercially purchased reagents used were acquired from Sigma-Aldrich, Fisher Scientific, Acros Organics, Combi-Blocks, Bachem, Tokyo Chemical Industry, and Waters Corporation. Amino Acid Hydrolysate H from Waters was utilized along with stock amino acids prepared by dissolving individual analyte crystals (purities ranged from 96 to 100%) in ultrapure water. Stock amino acid standard solutions were made with concentrations ranging from 0.01 to 1 M. Once the individual standard solutions of each species were made, they were combined to facilitate the analysis of all target analytes in a single run. The stock solution for the amines was made to be between 0.01 and 2 M. This solution was then diluted to make 9 standards to facilitate the analysis of all target analytes in a single run.

Sample extraction and AccQ·Tag derivatization method. The OREX-800031-0, Murchison, FS-120, and procedural blank samples were flame-sealed in glass ampoules in 1 mL of Milli-Q ultrapure water and then heated at 100°C for 24 h. The samples were centrifuged, and the water supernatants removed and transferred to separate vials with the following total volumes based on mass: 2,776.5 µL for OREX-800031-0, 2,764.7 µL for Murchison, 2,773.6 µL for the FS-120 fused silica, and 2,950.0 µL for the procedural blank. Approximately 0.35% of the water supernatants was then removed with volumes corresponding to 10.4 µL of the procedural blank, 9.8 µL of OREX-803001-0, 9.8 µL of Murchison, and 9.8 µL of the FS-120 sample. Then sodium borate was added directly to the water extracts to bring the total amount up to 80 µL, 20 µL of the AccQ·Tag derivatization agent was added, and the sample was heated to 55°C for 10 minutes as previously described[81].

As previously reported[32], laboratory experiments designed to study the impact of the 100°C for 24 h water extraction procedure on pure amino acid mixtures have shown that most amino acids do not thermally decompose or racemize during hot water extraction. However, unsurprisingly we have observed in testing with standards that some more fragile protein amino acids, such as asparagine, are not stable in hot water. Asparagine can undergo deamidation to succinimide followed by hydrolysis to aspartic acid and isoaspartic acid with rates that are dependent on the temperature and pH[54]. Glutamine and cysteine are also unstable in hot water and these protein amino acids could have also decomposed during the hot water extraction procedure as noted in a footnote in Supplementary Table 12. The previous experiments with standards to test for amino acid decomposition during hot water extraction were not done in the presence of an inorganic matrix, therefore we are unable to rule out the possibility that additional modification of the amino acid content in the Bennu aggregate and meteorite samples could have occurred due to the presence of minerals. However, previous studies have been performed with pure aliphatic amine standards mixed with serpentine (a hydrated magnesium silicate used as a meteorite analog) to test the impact of the 100°C for 24 h water extraction procedure on amines and no measurable effects on their molecular distributions or isotopic compositions were reported[82].

LC-FD/QqQ-MS analyses. The AccQ·Tag derivatized free ammonia, amino acids and amines in the water extracts were then analyzed via the commercial Waters AccQ·Tag protocol on a Xevo TQS-Micro triple quadrupole mass spectrometer equipped with an electrospray ionization source (positive ion mode) using multiple reaction monitoring (MRM) mode. The Xevo TQ-S Micro capillary voltage was set to 1.0 keV, the sampling cone was set to 40°C, the source temperature was set to 150°C, the cone gas flow was set to 50 L/h, the desolvation temperature was set to 500°C, and the desolvation gas flow was set to 1000 L/h. Samples were introduced via a Waters Acquity H-Class plus UHPLC with a fluorescence detector.

For the UHPLC analyses of amines and amino acids, a 250 µL syringe, 50 µL loop, and 15 µL needle were used. UHPLC separations were performed using two AccQ·Tag Ultra C18, 1.7 µm. 2.1 × 150 mm columns in series. Amino acid target analytes were eluted using the following gradient: 0–15min: 99.9% eluent A, 15–20 min: 99.9–95% eluent A, 20–22 min: 5% eluent A, 22–29 min: 95–90% eluent A, 29–35 min: 90–78.8% eluent A, 35–38 min: 78.8% eluent A, 38–45 min: 78.8–40.4% eluent A, 45–55 min: 40.4%

eluent A, 55–57 min: 40.4–99.9% eluent A, 57–60 min: 99.9% eluent A. The autosampler temperature was maintained at 25°C, the injection volume was 10 µL, the eluent flow rate was held at a constant 0.15 mL min^{-1}, and the column was maintained at 55°C. Amine target analytes were eluted using the following gradient: 0–2.49 min: 0–10% eluent B, 2.49–7 min: 10–20% eluent B, 7–7.99 min: 20–50% eluent B, 8–8.99 min: 100% eluent B, 8.99–9 min: 100–0% eluent B, 9–10 min: 0% eluent B. The autosampler temperature was maintained at 25°C, the injection volume was 1 µL, the eluent flow rate was held at a constant 0.7 mL min^{-1}, and the column was maintained at 55°C. The fluorescence detector was operated with an excitation wavelength of 266 nm and an emission wavelength of 473 nm. For the UHPLC analysis of ammonia and hydrazine, a 250-µL syringe, 50-µL loop, and 15-µL needle were used. UHPLC separations were performed using one AccQ·Tag Ultra C18, 1.7 µm × 2.1 × 150 mm column. Ammonia and the protein amino acids were eluted using the following gradient: 0–0.54 min: 0.1% eluent B, 0.54–5.74 min: 0.1–10% eluent B, 5.74–7.74 min: 10–21.2% eluent B, 8.04–8.64 min: 59.6% eluent B, 8.64–8.73 min: 59.6–0.1% eluent B, 8.73–10.00 min: 0.1% eluent B.

Typical LC-FD chromatograms of the AccQ·Tag derivatives of the free amino acids and amines in the standards and the hot-water extracts of Bennu (OREX-803001-0), Murchison, and the procedural blank are shown in Supplementary Fig. 6. Similarly, the LC-FD/QqQ-MS chromatograms showing the identification of the AccQ·Tag derivative of ammonia in the Bennu and Murchison water extracts are shown in Supplementary Fig. 7. Selected MRM transitions were used for the abundance quantifications for ammonia, amines, and amino acids in these analyses (Supplementary Tables 7 and 8). A linear least-square model was fitted to ammonia and each protein amino acid and amine in the standard calibration set, and these calibration curves were used to quantify the analytes in the samples. A sample of pure water that was carried through the same preparation and analytical procedures as the meteorites was used as a blank to determine the procedural and laboratory backgrounds. All derivatized extracts were analyzed in triplicate, and the average blank-corrected ammonia, protein amino acid, and amine concentrations of the samples were determined from the standard calibration set and the extracted sample mass.

LC-FD/ToF-MS analysis of the OPA/NAC derivatives of amino acids and their enantiomeric ratios

Standards and reagents. All glassware, ceramics, and sample handling tools used in sample processing were rinsed with Milli-Q ultrapure water (18.2 MΩ·cm, <3 ppb total organic carbon), wrapped in aluminum foil, and then heated in a furnace at 500°C in air overnight. Most of the chemicals and reagents were purchased from Sigma-Aldrich. A stock amino acid solution (1×10^{-6} M) was prepared by mixing individual amino acid standards (97–99% purity) in Milli-Q ultrapure water. All chiral amino acid standards were purchased as racemic mixtures (D = L), except for D- and L-threonine (Sigma-Aldrich, >98% purity, *allo*-free) and D- and L-isovaline (Acros Organics, >99% purity) which were prepared as racemic mixtures by mixing the appropriate masses of each compound in Milli-Q ultrapure water to the standard mixture. Acid vapor hydrolysis used Tamapure-AA-10-HCl 20% (metallic impurity level < 10 pg/mL). Cation-exchange resin (AG50W-X8, 100–200 mesh, hydrogen form, BIO-RAD) was used for removal of salts and interfering

ions from samples. During the desalting protocol, 1.5 N HCl, 2 M sodium hydroxide (NaOH), and 2 M ammonium hydroxide (NH_4OH) were used. The 2 M NaOH was produced by dissolution of 32 g of NaOH pellets (Sigma-Aldrich, anhydrous, ≥97%) in 400 mL Milli-Q ultrapure water, and the 2 M NH_4OH was prepared from Milli-Q ultrapure water and ammonia gas (Air Products) in vacuo. Pre-column derivatization of samples prior to LC-FD/ToF-MS analyses involved the use of 0.1 M sodium borate, *o*-phthaldialdehyde/*N*-acetyl-L-cysteine (OPA/NAC), and 0.1 M hydrazine hydrate. Sodium borate was generated by heating solid sodium borate decahydrate at 500°C, in air, for 3 h, prior to dissolution in Milli-Q ultrapure water. The OPA/NAC derivatization reagent was prepared by first generating 0.1 M OPA via dissolving 0.1 g OPA in 7.5 mL methanol (Optima Grade), then generating 0.5 M NAC via dissolving 0.408 g NAC in 5 mL Milli-Q ultrapure water, and then mixing 300 µL of 0.1 M OPA with 30 µL of 0.5 M NAC and 670 µL of 0.1 M sodium borate. The 0.1 M hydrazine (NH_2NH_2) solution was prepared by vacuum distillation of concentrated anhydrous hydrazine (98% purity) and subsequent dilution in Milli-Q ultrapure water.

Extraction and derivatization methods for amino acid analyses. The OREX-800031-0, Murchison, FS-120, and procedural blank (empty glass ampoule) were flame-sealed in pre-scored glass ampoules each containing 1 mL of Milli-Q ultrapure water, and the sealed ampoules were placed in a heating block inside an oven set at 100°C for 24 h. After heating, the glass ampoules were removed from the oven, allowed to cool to room temperature, centrifuged inside polypropylene Falcon tubes at 3,000 rpm for 5 min to separate solid particles from the liquid. The ampoules were opened, and the water supernatants were transferred from the ampoules by pipetting into pre-weighed amber glass vials. Another 1 mL of Milli-Q ultrapure water was added to each glass ampoule, the ampoules were re-centrifuged, and the supernatant was transferred to the sample amber glass vials (this process was repeated one final time to maximize the recovery of the water extracts). The total masses of the combined water supernatants transferred from each sample in the amber vials were determined using a balance with masses as follows: 2,776.5 mg for OREX-800031-0, 2,764.7 mg for Murchison, 2,773.6 mg for the FS-120, and 2,950.0 mg for the procedural blank. After extraction, 40% of the supernatant was dried under vacuum and subsequently subjected to a 6 M HCl vapor hydrolysis at 150°C for 3 h to determine total hydrolysable amino acid content. The sample was divided by volume. Since we were using water as the carrier, and water has a density of 1 g/cc, we used 1,110 µL of OREX-80031-0, 1,106 µL of Murchison, 1,110 µL of FS-120 fused silica, and 1,180 µL of the procedural blank. The HCl acid-hydrolyzed, hot-water extracts were then desalted by using cation-exchange resin (AG50W-X8, 100–200 mesh, hydrogen form, BIO-RAD), and the amino acids recovered by elution with 2 M NH_4OH (prepared from Millipore ultrapure water and NH_3(g) (AirProducts) *in vacuo*). An additional 40% of the remaining non-hydrolyzed water extracts of the samples were dried down under vacuum and taken through the identical desalting procedure in parallel with the acid-hydrolyzed extracts to determine the abundances of the free amino acids. After desalting, the samples were dried under vacuum and brought up in 100 µL of water, and 30 µL were taken and dried down with 20 µL of pH = 9 sodium borate buffer. After drying down, the samples were brought up in 20 µL of water and 5 µL of 0.1 M OPA/NAC

derivatization agent and allowed to react for 15 minutes at room temperature before being quenched with 75 µL of 0.1 M hydrazine.

LC-FD/ToF-MS analyses. Amino acid abundances, distribution, and enantiomeric ratios were determined by LC-FD/ToF-MS. The amino acids in the NH_4OH eluates were derivatized with OPA/NAC for 15 minutes at room temperature followed by their separation and analysis using a Waters ACQUITY UPLC and Waters Xevo G2-XS Q-ToF-MS operating in positive ion mode. C_2 to C_6 amino acids were chromatographically resolved using a Waters BEH C18 column (2.1 × 50 mm, 1.7 µm bead) and a Waters BEH phenyl column (2.1 × 150 mm, 1.7 µm bead) in series. Both columns were maintained at 30.0°C. The mobile phase conditions for amino acid separations were as follows: flow rate, 150 µL/min; gradient, time in minutes (%B): 0 (0), 35 (55), 45 (100). C_5 amino acid isomers and enantiomers were chromatographically separated using the same chromatography conditions as for the C_2 to C_6 amino acids but required the implementation of a different gradient. The gradient used for C_5 amino acid isomers and enantiomers was structured via time in minutes (%B): 0 (15), 25 (20), 25.06 (35), 44.5 (40), 45 (100).

During the Xevo G2-XS analysis, a dual electrospray ionization (ESI) system was used for the purpose of implementing lock mass corrections. The primary ESI source was operated using the following parameters: capillary voltage, 3.0 kV; sampling cone voltage, 40 V; source temperature, 120°C; desolvation gas (N_2) temperature, 350°C; cone gas (N_2) flow, 50 L h^{-1}, desolvation gas flow rate, 750 L h^{-1}. Due to the possibility that minor variations in the mass-to-charge (*m*/*z*) scale may occur during the course of executing experimental runs after instrument calibration is performed, a reference ESI source was implemented to supply an independent leucine enkephalin standard signal. The reference ESI source was operated using a sample infusion rate of 20 µL min^{-1}, a sample fill volume of 250 µL, a lockspray infusion rate of 10 µL min^{-1}, a capillary voltage of 3.0 kV, a reference cone voltage of 30 V, and a collision energy of 6.0 V. The ToF analyzer was operated in "Sensitivity mode," which used a reflectron to provide a full width at half maximum resolution of <22,000 based on the $[M+H]^+$ of leucine enkephalin, *m*/*z* 556.2771.

The amino acid abundances and their enantiomeric ratios in the meteorite extracts and controls were determined by comparison of the peak areas generated from the sample and control UV fluorescence chromatograms (LC-FD, λ_{ex} = 340 nm, λ_{em} = 450 nm) of their OPA/NAC derivatives to the corresponding peak areas of amino acid standards run under the same chromatographic conditions and included peak identification confirmation by accurate mass using a match tolerance of 10 ppm (ToF-MS, see Supplementary Tables 9 and 10). Typical LC-FD chromatograms of the OPA/NAC derivatives of amino acids in the Bennu (OREX-803001-0), Murchison, and procedural blank acid-hydrolyzed, hot-water extracts is shown in Supplementary Fig. 8. The LC-ToF-MS chromatograms showing separation of the C_5 amino acids in the same extracts is also shown in Supplementary Fig. 9.

LC-FD/HRMS analysis of the OPA/NAC derivatives of amino acids and their enantiomeric ratios

Standards and reagents. Chemical reagents used for these analyses were either procured from Mann Research Laboratories, Sigma-Aldrich, Fisher Chemical, Acros Organics, or Honeywell Research Chemicals. Amino acid crystals that were used to produce individual stock analytical standards had purities ≥96.8%. All other chemicals used for these analyses had purities of ≥95%, unless otherwise stated. Individual amino acid standard solutions were made at concentrations of 10^{-3} M to 10^{-1} M by separately dissolving crystals from each amino acid into Milli-Q ultrapure water. These individual amino acid standards were then combined to create a mixed amino acid standard that facilitated the analysis of all targeted amino acids in a single run. All chiral amino acids included in this mixed standard were prepared as racemic mixtures.

Preparation of OPA/NAC derivatization reagents was conducted as detailed in the LC-FD/ToF-MS analytical section, with the exception that the 0.1 M sodium borate used during derivatization was prepared using sodium tetraborate, as opposed to sodium borate decahydrate. The sodium tetraborate used during the analyses described here was first baked out overnight at 500°C, in air. Next, 2.03 g of baked-out sodium tetraborate was dissolved in 100 mL of Milli-Q ultrapure water to reach a final concentration of 0.1 M.

Liquid chromatography analyses of C_2–C_{11} amino acids relied on the use of two mobile phases: A) 35 mM ammonium formate with 7% methanol, pH adjusted to 9.0 and B) LC-MS grade methanol. Mobile phase A) was prepared by combining 780 mL of LC-MS grade water with 1.51 mL of LC-MS grade formic acid, followed by titrating this solution to pH 9.0 using 2 M aqueous ammonium hydroxide, and lastly adding 64 mL of LC-MS grade methanol. The 2 M aqueous ammonium hydroxide solution was prepared by diluting a 7.5 M stock solution of aqueous ammonium hydroxide (assay = 29.3%, ammonia in water) with LC-MS grade water to obtain a 2 M concentration. Mass calibrations of the high-resolution mass spectrometer were performed using the Thermo Scientific Pierce LTQ Velos ESI positive ion calibration mix. This calibration mix was an aqueous solution that included methanol, acetic acid, and acetonitrile. The calibration analytes in this mix were Ultramark 1621, MRFA (Met-Arg-Phe-Ala), and caffeine.

Sample preparation. Samples, blanks, and standards were derivatized as detailed in the LC-FD/ToF-MS analytical section, with the exception that standards were derivatized by first drying down 10 µL aliquots of the standard with 20 µL aliquots of 0.1 M sodium borate, as opposed to samples and blanks in which 30 µL aliquots of each blank and sample were dried down with separate 20 µL aliquots of 0.1 M sodium borate. Prior to analysis, blanks, samples, and standards were each derivatized once. Following analysis, all derivatization vials were stored at –80°C and reused for subsequent injections to perform replicate analyses. This cold storage approach was used to mitigate derivative degradation between replicate injections.

LC-FD/HRMS analyses. Amino acids were analyzed using a Thermo Fisher Scientific Vanquish Horizon liquid chromatograph coupled to a Thermo Fischer Scientific Vanquish fluorescence detector, and a Thermo Fisher Scientific Q Exactive hybrid quadrupole-Orbitrap mass spectrometer. Amino acid identifications were made by the observation of the following three measurable properties in comparison to a mixed amino acid standard: 1) chromatographic retention time, 2) optical fluorescence, and 3) accurate mass. The analyses implemented a mass tolerance of 3 ppm (Supplementary Tables 9 and 10). The

LC-HRMS chromatograms showing the elution of the C_2 to C_{11} amino acids in the acid hydrolyzed, hot-water extracts of the procedural blank, Bennu (OREX-803001-0), and the CM2 Murchison meteorite are shown in Extended Data Fig. 2. After LC-HRMS identification, amino acid quantitation was executed via manual integration of analyte peak areas using the Thermo FreeStyle software program.

Chromatographic separation was achieved using a 2.1 × 5 mm, 1.7-µm particle size Waters ACQUITY UPLC Peptide BEH C18 VanGuard Pre-column, followed by the following three stationary phases in series: 1) 2.1 × 150 mm, 1.7-µm particle size Waters ACQUITY UPLC CSH Phenyl-Hexyl, 2) 2.1 × 150 mm, 1.7-µm particle size Waters ACQUITY UPLC CSH C18, and 3) 2.1 × 150 mm, 1.7-µm particle size Waters ACQUITY UPLC CSH Phenyl-Hexyl. The C_2–C_8 amino acids were eluted using the following gradient: 0–60 min, 0–33% eluent B, 60–70 min, isocratic at 33% eluent B, 70–75 min, 33–45% eluent B, 75–80 min, isocratic at 45% eluent B, 80–100 min, 45–83% eluent B, 100–100.1 min, 83–100% eluent B, 100.1–105 min, isocratic at 100% eluent B, 105–105.1 min, 100–0% eluent B, 105.1–120 min, isocratic at 0% eluent B. The eluent flow rate was 0.11 mL min^{-1}. The stationary phases were maintained at 34°C. A pre-column heater was used, which was also kept at 34°C. The injection volume was 10 µL, and the autosampler was held at a temperature of 5°C. The fluorescence detector utilized an excitation wavelength of 340 nm and an emission wavelength of 450 nm. The fluorescence detector was kept at a constant temperature of 34°C.

The HRMS system was configured with a heated electrospray ionization (HESI) source and was operated using the following parameters: spray voltage = 3.50 kV, sheath gas (N_2) flow rate = 36 arb. unit, auxiliary gas (N_2) flow rate = 10 arb. unit, sweep gas (N_2) flow rate = 1 arb. unit, capillary temperature = 250°C, auxiliary gas heater temperature = 220°C, and S-lens RF level = 50.0%. The HRMS system was operated in Full MS–SIM scan mode according to the following parameters: polarity = positive, scan range = 100–1,500 *m/z*, mass resolution setting = 70,000 (at full-width-half-maximum for *m/z* 200), automatic gain control target = 1×10^6 ions, and maximum injection time = 200 ms. The HRMS system was calibrated daily over the 50–2,000 *m/z* range, which facilitated a mass accuracy of <2 ppm.

GC-QqQ-MS analysis of carboxylic acids

The portions of the hot-water extract allocated for analysis of carboxylic acids were basified with 20 µL of 2 M NaOH, dried under vacuum, and then derivatized with 2-pentanol using previously described methods[26,83]. The dry residues were suspended in 20 µL of 6 M HCl, 30 µL of 2-pentanol, 200 µL of DCM, and heated at 100°C for 16 h in sealed PFTE-lined screw cap vials in a heating block. After cooling to room temperature, the derivatized samples were passed through a short plug of aminopropyl silica gel (25 mm length × 5 mm I.D.), rinsed using ~3 mL of dichloromethane (DCM), dried with flowing N_2, and dissolved in 150 µL of DCM for analysis. We quantified the concentrations of carboxylic acids in the samples and procedural blank by gas chromatography coupled to triple-quadrupole mass spectrometry detection (GC-QqQ-MS). The abundances of carboxylic acids were quantified from the peak areas generated using the average value of three separate GC-QqQ-MS measurements on the same sample.

The derivatized carboxylic acids were analyzed using a Thermo Trace 13100 GC equipped with a 5 m base-deactivated fused silica guard column (Restek, 0.25 mm I.D.), two Rxi-5ms (30 m length × 0.25 mm I.D. × 0.5 μm film thickness; capillary columns connected in series using SilTite μ-union connectors, Restek), and coupled to a Thermo TSQ electron-impact triple-quadrupole mass spectrometer (ion source set at 220°C and 70 eV). The oven program used started with the temperature held at 40°C for 1 min, then ramped at 15°C min^{-1} to 110°C, ramped at 10°C min^{-1} to 140°C and held for 2 min, ramped at 10°C min^{-1} to 145°C, and finally ramped at 30°C min^{-1} to 300°C with a final hold time of 5 min. The carrier gas used was ultrahigh purity grade helium (5.0 grade) at 4.2 mL min^{-1} for carboxylic acids. Triplicate injections of derivatives were made in split mode (split flow: 5 mL min^{-1}, held for 1 min) in aliquots of 1 μL. The GC-QqQ-MS mass chromatograms of carboxylic acids identified in the Bennu and Murchison hot-water extracts and in the procedural blank and standards is shown in Supplementary Fig. 10. The mass spectra were used to identify and quantify the carboxylic acid derivatives by comparison to reference standards and application of calibration curves as described elsewhere[83].

As previously noted for amino acids, we cannot exclude the possibility that some carboxylic acids could have degraded during the hot water extraction procedure as has been shown for malonic acid[20,28]. However, previous studies have been performed with pure standards mixed with serpentine (a hydrated magnesium silicate used as a meteorite or asteroid analog) to test the impact of the 100°C 24 h water extraction procedure on monocarboxylic acids and no measurable effects on their molecular distributions or isotopic compositions were reported[26].

HPLC-HRMS analysis of N-heterocycles

Standards and reagents. Authentic standards for the nucleobases and other N-heterocyclic compounds were purchased from Tokyo Chemical Industry, Sigma-Aldrich, FUJIFILM Wako Pure Chemical, Combi-Blocks, Toronto Research Chemicals, and BLD Pharmatech Ltd. Stock standard solutions of N-heterocyclic compounds were prepared by dissolving individual analyte crystals (purities ranged from 96 to 100%) in MilliQ-water (Millipore Milli-Q grade, 18.2 MΩ·cm). Ultrapure water and 6 M hydrochloric acid (HCl) (Tama Chemicals Co., Ltd., Japan; Tama pure AA-10 grade), 3 M NaOH solution (Kanto Chemical Industry Co., Ltd., Japan; ultrapur™ grade), and ammonia solution (Kanto Chemical Industry Co., Ltd., Japan; ultrapur™ grade, 28.0%~30.0% in water) were obtained for the extraction and purification procedures. Solutions of 1 M and 0.1 M HCl, 1 M NaOH, and 10% ammonia in water (NH_4OH) were prepared and diluted from the above-mentioned solvents using ultrapure water. Ultrapure water, acetonitrile (ToF-MS grade), and formic acid (LC-MS grade; >99.5% purity) were sourced from FUJIFILM Wako Pure Chemical for HPLC/ESI-HRMS analyses. All the glassware and sea sand (FUJIFILM Wako Pure Chemical Corporation, Japan; 30–50 mesh) used for procedural blanks were rinsed with MilliQ-water, wrapped in aluminum foil, and subsequently heated at 450°C for 5 h in air prior to use.

Extraction and purification of N-heterocycles. 17.75 mg of fine- to intermediate-sized particles of the Bennu sample OREX-800044-101 were soaked in 300 μL of 6 M

HCl in a glass vial. After purging with dry N_2 gas to remove O_2 in the headspace, the glass vial was flame-sealed and heated at 110°C for 12 h. After heating, the supernatant and the Bennu sample particles were transferred to a 1.5 mL polytetrafluoroethylene (PTFE, Teflon) vial followed by centrifugation for 1 min at 10,000 rpm. The supernatant was transferred to the sample extract vial. The residue was washed twice with 300 μL of ultrapure water, and the rinse was mixed with the supernatant. The mixed supernatant was freeze-dried under reduced pressure.

The dried extract was dissolved in 0.5 mL of 0.1 M HCl for performing a desalting procedure using an improved method of cation-exchange chromatography[62,84]. In brief, 0.5 mL of AG 50W-X8 cation-exchange resin (Bio-Rad Laboratories, Inc.; analytical grade, 200–400 mesh, hydrogen form) was placed in a Pasteur glass pipet and rinsed with solvents in the following order: 1.5 mL of 1 M HCl, ultrapure water, 1 M NaOH, ultrapure water, 1 M HCl, and ultrapure water. The extract was loaded onto the cation-exchange chromatography column. The cation-exchange resins were washed with 2.5 mL of ultrapure water to recover acidic, neutral, and weakly basic compounds referred to as "H_2O fraction". Subsequently, 2.5 mL of 10% NH_4OH was loaded onto the H_2O-washed cation-exchange resins to elute basic compounds, including most nucleobases referred to as "NH_4OH fraction". The H_2O and NH_4OH fractions were freeze-dried and reconstituted into 50 μL of ultrapure water. Simultaneously, we prepared a procedural blank with baked sea sand powder using the same protocol as that applied to the Bennu samples; we analyzed the blank to validate the background signal during the procedures.

HPLC/ESI-HRMS analyses. The H_2O and NH_4OH fractions from the Bennu sample and the procedural blank, and the authentic standards of the targeted molecules were analyzed using an online HPLC/ESI-HRMS system comprising an UltiMate 3000 and Q Exactive™ Plus Hybrid Quadrupole-Orbitrap™ mass spectrometer (Thermo Fischer Scientific Inc., Waltham, MA, USA) with a mass resolution of 140,000 at a mass-to-charge ratio m/z = 200[36,62,85]. The HPLC instrument was outfitted with a reversed-phase separation column maintained at 40°C. For the detection and quantification of most purine nucleobases, we employed the following isocratic HPLC eluent program with an InertSustain PFP column (1.0 mm × 250 mm, particle size = 3 μm, GL Sciences Inc., Tokyo, Japan): solvent A (water) and solvent B (acetonitrile with 0.1% formic acid) = 90:10, held for 20 min with a flow rate of 0.05 mL min^{-1}. For pyrimidine nucleobase analyses, we used the following gradient HPLC eluent program with the HyperCarb™ column (2.1 mm × 150 mm, particle size = 3 μm, Thermo Fischer Scientific Inc., Waltham, MA, USA): solvent A (water + 0.1% formic acid) and solvent B (acetonitrile + 0.1% formic acid) = 99:1 at t = 0 min, followed by a linear gradient of A:B = 70:30 at 20 min with a flow rate of 0.2 mL min^{-1}.

We then introduced the compound solution separated using either the PFP or HyperCarb™ column into a HESI-II probe (Thermo Fischer Scientific Inc., Waltham, MA, USA) and heated it at 280°C for desolvation. The spray voltage and capillary temperature of the ion-transfer system were 3.5 kV and 295°C, respectively. To detect various organic molecules in the hot-water (HW) and HCl extracts, we recorded the mass spectra of the vaporized compounds in the positive ions over an m/z range of 111–155 or 50–500 (Supplementary Figs, 11–13), with the mass determined to an accuracy better than 5 ppm, as defined by [(measured m/z) – (calculated m/z)]/(calculated m/z) × 10^6 (ppm). The

mass accuracy was occasionally calibrated using the exact masses of protonated tyrosine (*m*/*z* = 182.0812), *tert*-butylamine (*m*/*z* = 74.0964), and a fragment ion of *tert*-butylamine (*m*/*z* = 57.0699). A positive ion with *m*/*z* = 83.0604, corresponding to an acetonitrile dimer, was used as the lock mass. For robust identification and quantification of the nucleobases, we performed the tandem mass spectrometry (MS/MS) experiments using the same ionization conditions as those used for the full-scan analyses. We subjected the targeted positive ions isolated by the quadrupole (using an isolation window of 0.4 *m*/*z*) to high-energy collisions with N_2 gas to produce fragmented ions and monitored specific mass ranges using an Orbitrap MS with a mass resolution of 140,000 at *m*/*z* = 200. Furthermore, we identified guanine in the Bennu extract based on their chromatographic retention times, exact masses, and mass-fragmentation patterns in the MS/MS measurements (Supplementary Fig. 13).

Wet-chemistry pyrolysis GC-QqQ-MS analyses of amino acids and N-heterocycles

Sample preparation and reagents. All glassware used to handle the samples and the pyrolysis tubes themselves were previously ashed at 550°C for ~16 h in air. Prior to pyrolysis, two ~1 mg Bennu aggregate samples (OREX-501029-0 and OREX-803004-0) and equivalent sample masses of Murchison used for the wet-chemistry pyrolysis experiments were prepared inside a chemical fume hood by adding 5 µL *N*-(*tert*-butyldimethylsilyl)-*N*-methyltrifluoroacetamide (MTBSTFA):*N,N*-dimethylformamide (4:1 v/v) solution (MTBSFTA from Sigma Aldrich, >97% purity; DMF from Sigma Aldrich, anhydrous, 99.8% purity) to the sample inside the pyrolysis tubes. The pyrolysis tubes containing sample and reagent were then placed inside a secondary 2 mL vial and capped with special attention to create a seal between the pyrolysis tube and polytetrafluoroethylene (PTFE) liner. Samples were then placed inside a stainless-steel heating block at 85°C for 1.5 h and vortexed every 15 min. Once complete, samples were passively cooled at room temperature for 10 min and immediately transferred to the pyroprobe chamber for pyrolysis.

Pyrolysis gas chromatography–triple quadrupole mass spectrometry (PyGC-QqQ-MS). Experiments were conducted using a CDS Analytical 6200 pyroprobe configured for manual loading with flash (10°C ms^{-1}) pyrolysis ramps of the solid samples with the MTBSTFA and DMF reagents. These derivatized samples were heated rapidly from 50 to 250°C to volatilize and thermally desorb derivatized (silylated) amino acids and N-heterocycles. The pyroprobe housing and valves were held at 300°C, and volatiles were transferred via a heated transfer line (300°C) directly into a Thermo Scientific TRACE 1600 gas chromatograph (GC) coupled to an Thermo Scientific 9610 triple quadrupole mass spectrometer (TSQ) system. The inlet temperature was held at 300°C and operated with a 2:1 split for wet-chemistry pyrolysis. The GC was fitted with an Rtx-5MS fused silica capillary column (30 m × 0.25 mm × 0.25 µm), He carrier flow at 1.5 mL min^{-1}, and MS transfer line set to 300°C. The GC oven was programmed with the following method: 40°C hold for 5 min, followed by a 3.5°C min^{-1} ramp to 300°C, then a final isothermal hold at 300°C for 8.5 min (~88 min total).

The MS source was held at 300°C and was operated in electron impact (EI) mode at 70 eV in simultaneous multiple reaction monitoring (MRM) and full scan in the *m/z* 50–

550 range. The wet-chemistry pyrolysis GC-QqQ-MS runs included MRM transitions targeting silylated protein amino acids and N-heterocycles previously identified in meteorites and interstellar ice analogs as determined by the pyrolysis of standards. Pyrolysis blanks preceded all standard pyrolysis experiments to control the cleanliness of the analytical set-up and prevent potential cross-contamination. Pyrolysis of reagent blanks (only 5 µL MTBSTFA:DMF) preceded wet-chemistry pyrolysis experiments to characterize persisting background contamination of standards. Results were analyzed using Chromeleon 7.3.1 software. Compound identification was conducted via comparison with retention time and three MRM transitions of standards (Supplementary Table 11). The total-ion chromatograms (full scan & multiple reaction monitoring, MRM) showing the detection of amino acids and N-heterocycles after wet-chemistry pyrolysis GC-QqQ-MS analyses of OREX-501029-0, OREX-803004-0, the Murchison meteorite, and the standards are shown in Supplementary Fig. 14. Comparisons of the protein amino acids and N-heterocycles detected by GC-QqQ-MS after wet chemistry and pyrolysis compared to those identified in the hot water and HCl extracts by LC-MS are shown in Supplementary Tables 12 and 13, respectively.

Nontargeted molecular profiling of soluble organic matter using FTICR-MS

Sample preparation. The 3.3 mg sample used for FTICR-MS analysis was OREX-803006-0. A subsample from OREX 803006-0 (OREX-803141-0) was analyzed with SEM-EDS and laser Raman spectroscopy. For FTICR-MS, we gently washed the sample rapidly with methanol and crushed the grains in a mortar with 400 µL methanol. The slurry was sonicated for 30 s and centrifuged. The supernatant was used for direct injection analysis.

FTICR-MS. FTICR/MS equipped with a 12-Tesla superconducting magnet in negative and positive mode ESI(–), ESI(+), and positive atmospheric pressure photoionization (APPI(+)) in direct sample injection was used at the Helmholtz Munich. The same conditions were used for the Ryugu sample to enable direct comparison, and a detailed description of the analysis and data evaluation was described earlier[86]. The FTICR-MS mass spectrum at nominal mass *m/z* 319 with annotated mass signals of the Bennu (OREX-803006-0) and Murchison (CM2) methanol extracts compared to similar analyses of a methanol extract of Ryugu (A0106) is shown in Supplementary Fig. 15.

Optical microscopy and micro two-step laser mass spectrometry (µ-L^{2}MS) imaging

Sample preparation. A subsample of the QL aggregate (OREX-501006-0) was prepared, under a laminar flow bench, by dispersing approximately a dozen grains (~ 100 µm diameter) onto a 1-inch diameter potassium bromide (KBr) window. These particles were then gently compacted into the KBr surface using an optically flat sapphire window. No further processing of the sample was required for any of the subsequent measurements.

Optical and UV fluorescence imaging. Optical and UV fluorescence imaging were performed using an Olympus BX-60 microscope equipped with a BX-FLA reflected light

fluorescence source (high-pressure 100W Hg-arc lamp). High resolution (*i.e.*, pixel resolution < Abbe diffraction limit) through focus image stacks of individual grains were acquired using a 50×/0.80 or 100×/0.95 UMPanF objective in combination with a 5.9 megapixel (2880 × 2048 pixel) Nikon DS-Fi3 CMOS image sensor and Nikon NIS Elements software. Image stacks were subsequently post-processed[87] to render composite extended depth-*of*-field images. For native fluorescence imaging acquisition times were typically 300 ms using a 330–385 nm excitation, 420 nm long-pass emission filter cube.

μ-L²MS analyses. The general operation of two-step laser mass spectrometry and its application to analysis of aromatic moieties in astromaterials has been previously described[88-92]. In the first step, laser desorption is used to release neutral organic molecules from the surface of the sample into vacuum while in the second step, a separate laser is used to photoionize the desorbed organics which are injected into a reflectron time-of-flight mass spectrometer. For the analyses performed herein two modifications to the basic instrument setup were employed: (1) a pulse shaping plasma shutter was used[93] to clip the duration of the infra-red (IR) CO_2 laser (Laser Science Inc., PRF-150) desorption pulse to ~ 100 ns and improve the spatial beam profile to ensure a 5 μm analysis spot size when focused onto the sample using a Cassegrain microscope objective; and, (2) a coherent vacuum ultraviolet (VUV) radiation source was used for non-resonant single photon ionization (SPI). This was achieved by the non-linear frequency tripling of the 3rd harmonic (λ 355 nm) of a mode-locked Q-switched picosecond Nd:YAG laser (EKSPLA PL2250) in a Xe-Ar gas cell (Xe:Ar 1:10; 80 Torr) to produce 118.2 nm (λ 10.5 eV) radiation[94,95]. Since the first ionization potentials for nearly all organic molecules lie in the range of 5–10 eV[96], single photon ionization with VUV radiation is capable of soft ionization of virtually all organic compound classes[94,95,97-100].

Prior to analysis of the Bennu aggregate, a reference / calibration sample was used to establish a consistent, comparable set of operating conditions. This was composed of finely powdered and homogenized Allende (CV3) matrix that was pressed in Au foil that provides a congruous reproducible well documented spectrum. The VUV photoionization step was first optimized by gas-phase ionization of a 1:1:1 mixture of acetone (CH_3COCH_3), cyclohexane (C_6H_{12}) and toluene ($C_6H_5CH_3$) introduced into the vacuum chamber via a manual SS sapphire-sealed variable leak valve. After which the IR laser desorption was maximized, subject to no concomitant ionization, through control of the cavity discharge voltage in combination with a wire grid polarizer / attenuator. These conditions were subsequently maintained through continuous monitoring of laser powers and shot-to-shot stability.

For the Bennu aggregate analysis the KBr mounted sample was attached to a 1-inch stainless steel (ss) sample platter using two thin strips of vacuum compatible adhesive tape (PELCO Tabs™ Carbon Conductive Tabs); the sample platter was previously cleaned by ultrasonication in isopropanol and acetone, and then vacuum dried. After loading the sample platter into the μ-L²MS main vacuum chamber, it was allowed to degas during which time the gas phase background was periodically monitored by taking μ-L²MS spectra with the infrared desorption laser blocked. Direct sample analysis began only after the vacuum chamber pressure had returned to its normal operating range ($<10^{-7}$ Torr; 1.3×10^{-5} Pa) and there was no gas phase background interference. Spatial mapping of a

sample was then performed by rastering the sample platter under the focus of the IR desorption laser in 5 μm steps and acquiring mass spectra at each location. The signal intensity of a given molecular species is a product of its photoionization cross-section and abundance.

References

65. Foustoukos, D. I., Alexander, C. M. O'D. & Cody, G. D. H and N systematics in thermally altered chondritic insoluble organic matter: An experimental study. *Geochim. Cosmochim. Acta* **300**, 44–64 (2021).

66. Vacher, L. G., Marrocchi, Y., Verdier-Paoletti, M. J., Villeneuve, J. & Gounelle, M. Inward radial mixing of interstellar water ices in the solar protoplanetary disk. *Astrophys. J. Lett.* **827**, L1 (2016).

67. Marrocchi, Y., Villeneuve, J., Batanova, V., Piani, L. & Jacquet, E. Oxygen isotopic diversity of chondrule precursors and the nebular origin of chondrules. *Earth Planet. Sci. Lett.* **496**, 132–141(2018).

68. Nakamura E., et al. On the origin and evolution of the asteroid Ryugu: A comprehensive geochemical perspective. *Proceedings of the Japan Academy, Series B* **98**, 227-282 (2022).

69. Grady M. M., et al. Comparison between carbon and nitrogen in surface and sub-surface materials from asteroid (162173) Ryugu. *Meteorit. Planet. Sci*. **58**, A6194 (2023).

70. Okazaki R., et al. Noble gases and nitrogen in samples of asteroid Ryugu record its volatile sources and recent surface evolution. *Science* **379**, eabo0431 (2023).

71. Yokoyama T., et al. Samples returned from the asteroid Ryugu are similar to Ivuna-type carbonaceous meteorites. *Science* **379**, eabn7850 (2023).

72. Sessions, A. L., Burgoyne, T. W. & Hayes, J. M. Correction of H_3^+ contributions in hydrogen isotope-ratio-monitoring mass spectrometry. *Anal. Chem.* **73**, 192–199 (2001).

73. Alexander, C. M. O'D., Fogel, M., Yabuta, H. & Cody, G. D. The origin and evolution of chondrites recorded in the elemental and isotopic compositions of their macromolecular organic matter. *Geochim. Cosmochim. Acta* **71**, 4380–4403 (2007).

74. Alexander, C. M. O'D., Bowden, R., Fogel, M. L. & Howard, K. T. Carbonate abundances and isotopic compositions in carbonaceous chondrites. *Meteorit. Planet. Sci.* **50**, 810–833 (2015).

75. Dworkin, J. P. et al. OSIRIS-REx Contamination control strategy and implementation. *Space Sci. Rev.* **214**, 19 (2018).

76. Pizzarello, S. The nitrogen isotopic composition of meteoritic HCN. *Astrophys. J.* **796**(2), L25 (2014).

77. Fujiya W. et al. Migration of D-type asteroids from the outer Solar System inferred from carbonate in meteorites. *Nat. Astron.* **3***,* 910–915 (2019).

78. Fujiya, W. et al. Comprehensive study of carbon and oxygen isotopic compositions, trace element abundances, and cathodoluminescence intensities of calcite in the Murchison CM chondrite. *Geochim. Cosmochim. Acta* **161**, 101–117 (2015).

79. Bierhaus, E. B. et al. The OSIRIS-REx spacecraft and the touch-and-go sample acquisition mechanism (TAGSAM). *Space Sci. Rev.* **214**, 1–46 (2018).

80. de Castro, A., Alegre, D. & Tabarés, F. L. Physisorption of ammonia on AISI 304 L stainless steel at different surface temperature under high vacuum conditions. *Nucl. Mater. Energy* **9**, 1–5 (2016).

81. Vinogradoff, S. et al. Influence of phyllosilicates on the hydrothermal alteration of organic matter in asteroids: Experimental perspectives. *Geochim. Cosmochim. Acta* **269**, 150–166 (2020).

82. Aponte J. C., Dworkin, J. P., & Elsila, J. E. Assessing the origins of aliphatic amines in the Murchison meteorite from their compound-specific carbon isotopic ratios and enantiomeric composition. *Geochim. Cosmochim. Acta* **141**, 331–345 (2014).

83. Aponte, J. C. et al. Extraterrestrial organic compounds and cyanide in the CM2 carbonaceous chondrites Aguas Zarcas and Murchison. *Meteorit. Planet. Sci.* **55**, 1509–1524 (2020).

84. Takano, Y., Kashiyama, Y., Ogawa, N. O., Chikaraishi, Y. & Ohkouchi, N. Isolation and desalting with cation-exchange chromatography for compound-specific nitrogen isotope analysis of amino acids: Application to biogeochemical samples. *Rapid Commun. Mass Spectrom.* **24**, 2317–2323 (2010).

85. Oba Y., Takano Y., Dworkin J. P. and Naraoka H. Ryugu asteroid sample return provides a natural laboratory for primordial chemical evolution. *Nat. Commun.* **14**, 3107 (2023).

86. Schmitt-Kopplin, P. et al. Soluble organic matter Molecular atlas of Ryugu reveals cold hydrothermalism on C-type asteroid parent body. *Nat. Commun.* **14**, 6525 (2023).

87. Forster, B., Van De Ville, D., Berent, J., Sage, D. and Unser, M. Complex wavelets for extended depth-of-field: A new method for the fusion of multichannel microscopy images. *Microsc. Res. Tech.* **65**, 33–43 (2004).

88. Hahn, J. H., Zenobi, R., Bada, J. L. and Zare, R. N. Application of two-step laser mass spectrometry to cosmogeochemistry: Direct analysis of meteorites. *Science* **239**, 1523–1525 (1988).

89. Clemett, S. J., Maechling, C. R., Zare, R. N., Swan, P. D. and Walker, R. M. Identification of complex aromatic molecules in individual interplanetary dust particles. *Science* **262,** 721-725 (1993).

90. Clemett, S. J., Sandford, S. A., Nakamura-Messenger, K., Hörz, F. and McKay, D. S. Complex aromatic hydrocarbons in Stardust samples collected from comet 81P/Wild 2. *Meteorit. Planet. Sci.* **45,** 701-722 (2010).

91. Clemett, S. J. and Zare, R. N. Microprobe two-step laser mass spectrometry as an analytical tool for meteoritic samples. In *IAU Symp. 178: Molecules in Astrophysics: Probes & Processes,* p. 305 (1996).

92. Bernstein, M. P., Sandford, S. A., Allamandola, L. J., Gillette, J. S., Clemett, S. J. and Zare, R. N. UV irradiation of polycyclic aromatic hydrocarbons in ices: Production of alcohols, quinones, and ethers. *Science* **283,** 1135-1138 (1999).

93. Hurst, N. and Harilal, S. S. Pulse shaping a transversely excited CO_2 laser using a simple plasma shutter. *Rev. Sci. Instrum.* **80**, 035101 (2009).

94. Lockyer, N. P. and Vickerman, J. C. Single photon ionization mass spectrometry using laser-generated vacuum ultraviolet photons. *Laser Chem.* **17**, 139–159 (1997).

95. Shi, Y. J. and Lipson, R. H. An overview of organic molecule soft ionization using vacuum ultraviolet laser radiation. *Can. J. Chem.* **83**, 1891–1902 (2005).

96. King, B. V., Pellin, M. J., Moore, J. F., Veryovkin, I. V., and Tripa, C. E. Estimation of useful yield in surface analysis using single photon ionization. *Appl. Surf. Sci.* **203-204**, 244–247 (2003).

97. Ferge, T., Mühlberger, F. and Zimmermann, R. Application of infrared laser desorption vacuum-UV single-photon ionization mass spectrometry for analysis of organic compounds from particulate matter filter samples. *Anal. Chem.* **77**, 4528–4538 (2005).

98. Kanno, N. and Tonokura, K. Vacuum ultraviolet photoionization mass spectra and cross-sections for volatile organic compounds at 10.5 eV. *Appl. Spectrosc.*

8, 896–902 (2007).

99. Zimmermann, R., Welthagen, W. and Gröger, T. Photo-ionisation mass spectrometry as detection method for gas chromatography: Optical selectivity and multidimensional comprehensive separations. *J. Chromatogr. A* **1184**, 296–308 (2008).

100. Hanley, L. and Zimmermann, R. Light and molecular ions: The emergence of vacuum UV single-photon ionization in mass spectrometry. *Anal. Chem.* **81**, 4174–4182 (2009).

101. Alexander, C. M. O'D., Bowden, R., Fogel, M. L. & Howard, K., Carbonate abundances and isotopic compositions in chondrites *Meteorit. Planet. Sci.* 50, 810–833 (2014).

102. Kotra, R. K. et al. Amino acids in a carbonaceous chondrite from Antarctica. *J. Mol. Evol.* **13**, 179–183 (1979).

Supplementary Figures

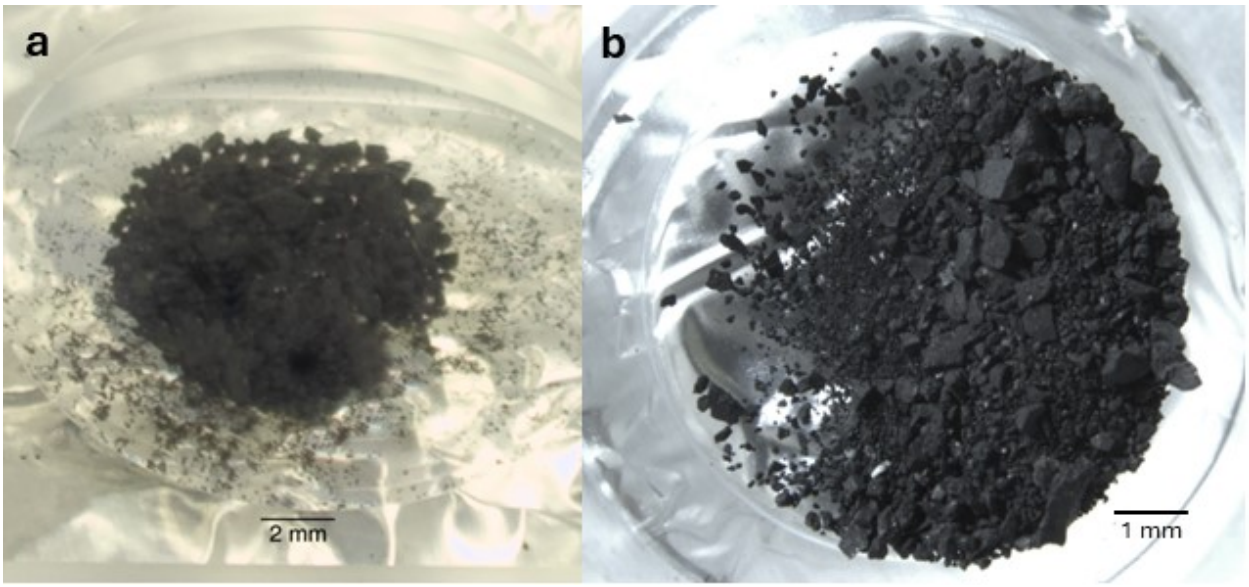

Supplementary Figure 1. Optical images of the Bennu aggregate samples from the TAGSAM head that were placed in sample tray A4 and then allocated for this study. a, Photo of OREX-800031-0 while sealed under nitrogen in between two glass concavity slides before subdivision at GSFC. At the bottom of the image a 2-mm bar is shown for scale. Reflected light from the glass slide in the original photo was digitally removed. Image taken by J. Dworkin at GSFC. **b,** Photo of OREX-800044-101 on a glass slide before extraction. The scale bar corresponds to 1 mm. Image taken by H. Naraoka at KU.

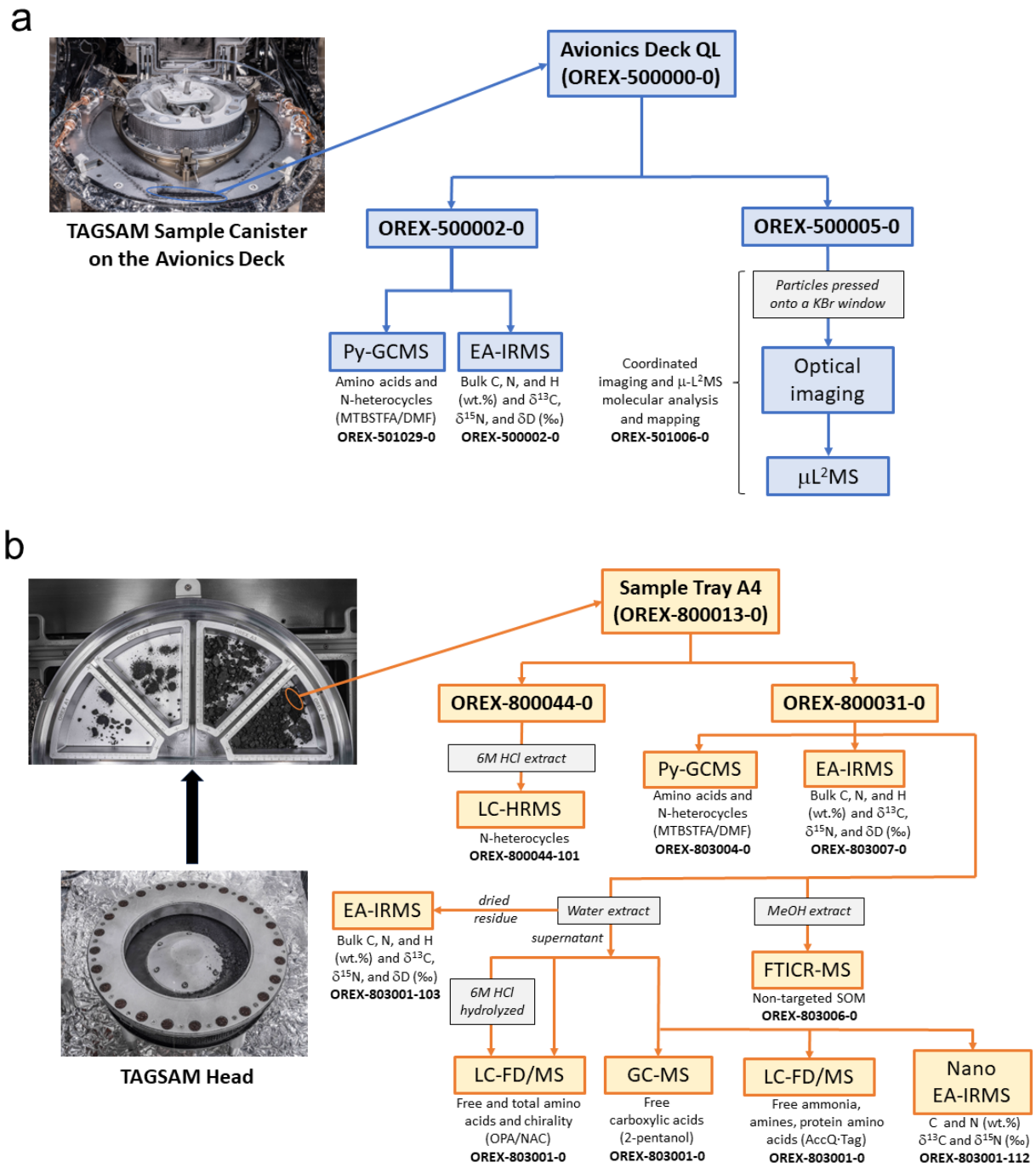

Supplementary Figure 2. Diagram of the processing and analytical scheme for the Bennu aggregate samples used in this investigation. a, Summary of the measurements described in this study that were made on the OREX-500002-0 and OREX-500005-0 aggregate samples that were collected from the surface of the avionics deck outside of the TAGSAM sample collector head and used for "Quick-Look" (QL) analyses and subsample numbers. **b,** Diagram of the analytical flow and measurements made in this study for aggregate samples OREX-800044-0 and OREX-800031-0 that were removed from underneath the Mylar flap of the TAGSAM head and placed in Tray "OREX A4" as OREX-800013-0. Image credits: NASA/Erika Blumenfeld and Joseph Aebersold.

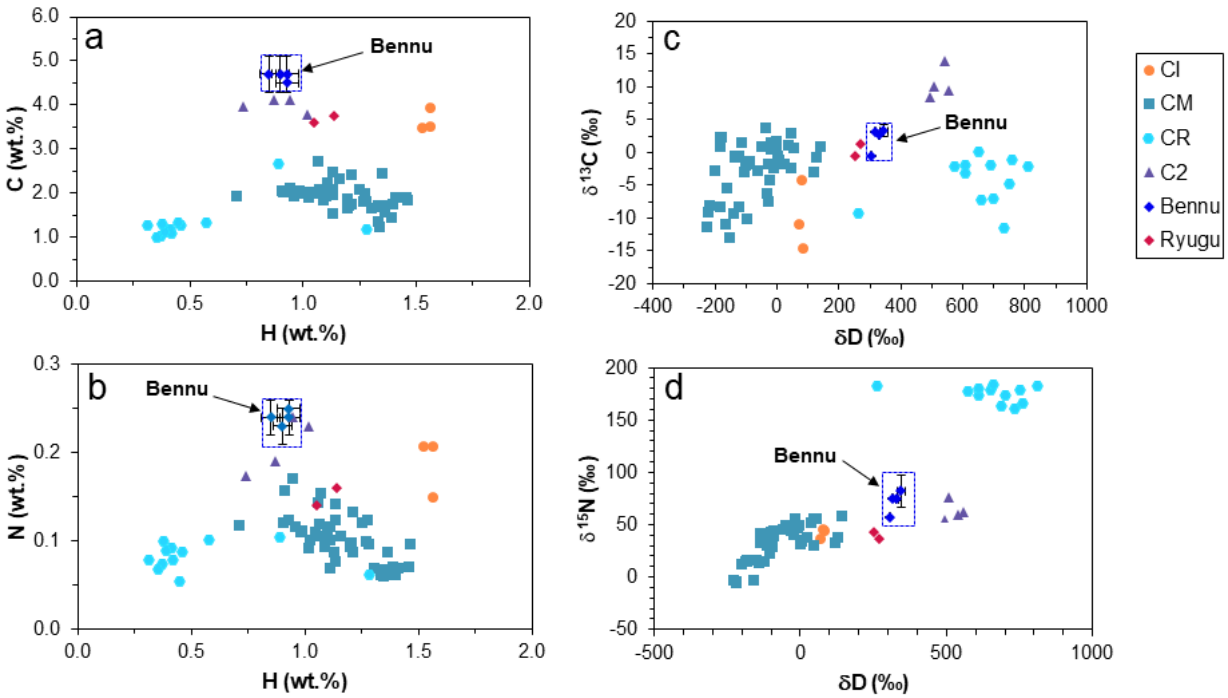

Supplementary Figure 3. Bulk C, N, and H contents and their stable isotopic compositions for the Bennu aggregate samples compared with carbonaceous chondrites and Ryugu. All elemental abundances in wt.% and stable isotopic compositions in ‰ (δ^{13}C, VPDB; δ^{15}N, AIR; δD, VSMOW). **a,** C vs. H (wt.%), **b,** N vs. H (wt.%), **c,** δ^{13}C vs. δD (‰), **d,** δ^{15}N vs. δD (‰). The average values for the four Bennu aggregate samples (OREX-500034/35/38-0, OREX-500036/37/39-0, OREX-500040/41-0, and OREX-803007-0)[1], and data for the carbonaceous chondrites[56,74,101] are based on replicate measurements made using EA-IRMS at CIS (Extended Data Table 1). The data from individual measurements made on subsamples of the Bennu aggregates are given in Supplementary Table 2. Two of the Bennu aggregate samples were heated at 120°C for 48 h under Ar prior to EA-IRMS analysis, and two were not heated, but the differences in C, N and H abundance and isotope values were small (Extended Data Table 1, Supplementary Table 2). Since OREX-803001-103 was extracted in water at 100°C for 24 h and therefore processed differently than the other samples prior to EA-IRMS analyses, the data from this Bennu sample are not included in the plots but are shown in Extended Data Table 1. The average bulk values for Ryugu are from samples A0106 and C0107[20,33]. Standard deviation error bars are shown only for the Bennu data, and the dashed blue box bounds the uncertainty in the measurements. Symbols shown in the legend correspond to different carbonaceous chondrite groups: Ivuna-type (CI), Mighei-type (CM), Renazzo-type (CR), and the ungrouped carbonaceous chondrites ($C2_{ung}$) Tagish Lake and Tarda. Data for the CI, CM, CR, and $C2_{ung}$ chondrites from Alexander et al.[19,56,61] and data first reported in this study from the $C2_{ung}$ Tarda meteorite are also included. The bulk H, C, and N data for these carbonaceous chondrites were obtained from unheated samples.

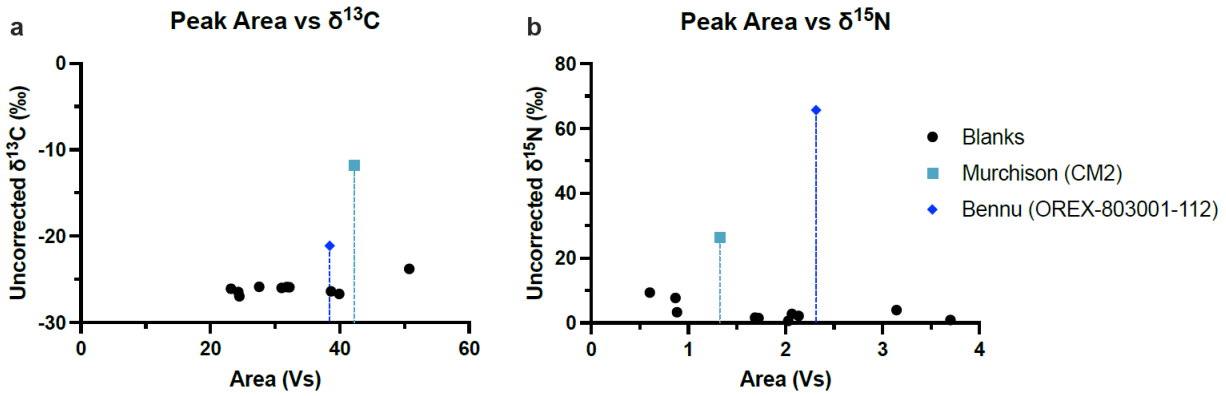

Supplementary Figure 4. Carbon and nitrogen isotope data from the nano EA-IRMS analysis of the Bennu and Murchison water extracts and the blanks. a, Carbon and **b,** nitrogen peak area and δ^{13}C and δ^{15}N values isotope results for the nano EA-IRMS system. The uncorrected isotope values are plotted against peak area for the blanks (black circles), CM2 Murchison UIC (aquamarine blue squares), and OREX-803001-112 (blue diamonds). Blanks plotting to the left of the dashed lines (those smaller than the sample) were used for the blank correction.

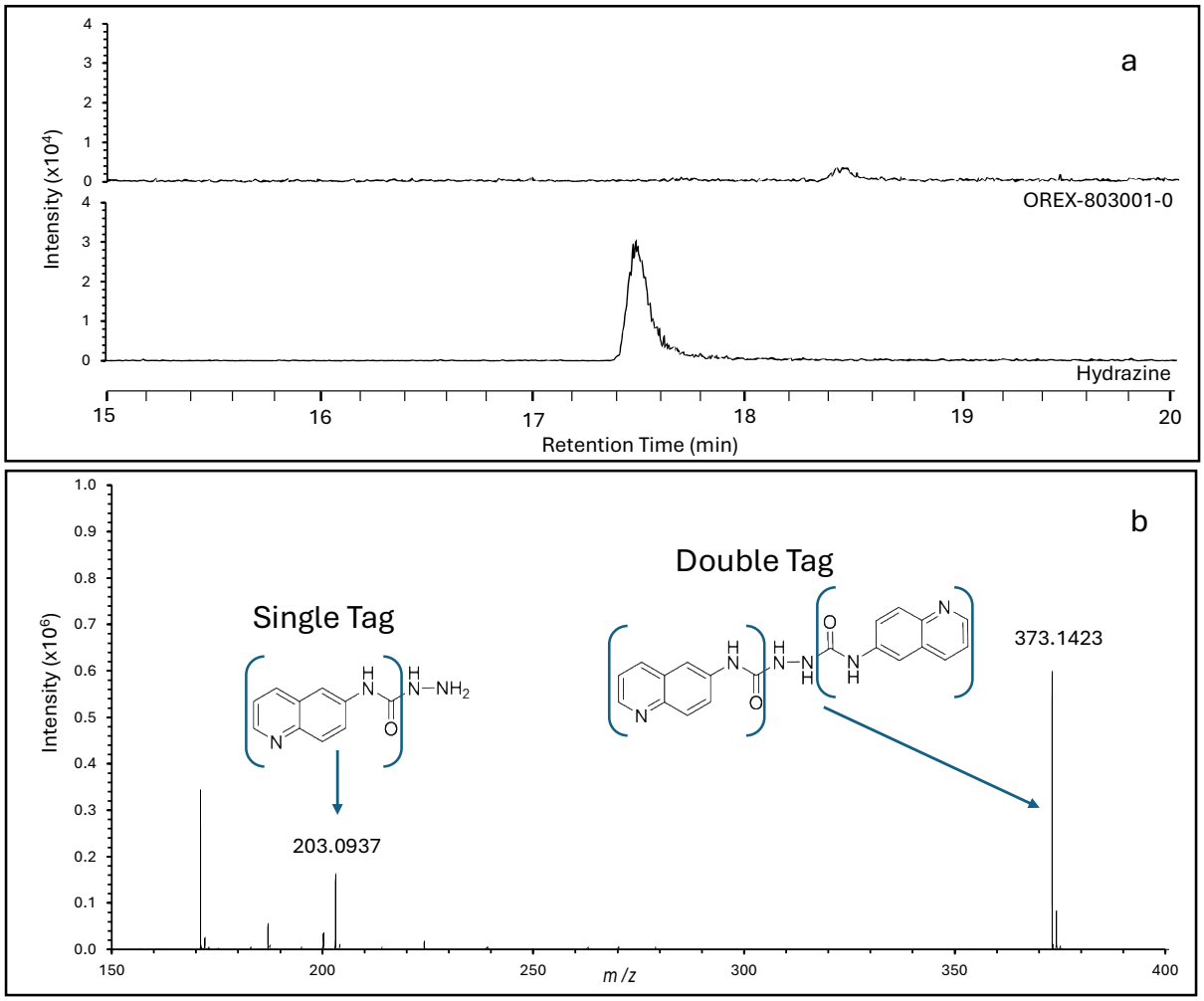

Supplementary Figure 5. LC-MS chromatograms of the 15- to 20-min region of the Bennu (OREX-803001-0) hot-water extract and a hydrazine standard after AccQ·Tag derivatization (10 min). Peaks were not identified by fluorescence since this analyte does not fluoresce with the predetermined excitation and emission wavelengths for AccQ·Tag. Peaks were identified by both single and double "AccQ·tagged" hydrazine. **a,** Mass chromatograms at *m/z* = 373.1423 with a 5-ppm exact mass window at the monoisotopic mass corresponding to the AccQ·Tag derivative of hydrazine for the OREX-803001-0 water extract and the 0.25-μM standard, and **b,** the mass spectrum at 17.45 min for the hydrazine standard with the single AccQ·Tag derivative of hydrazine at *m/z* 203.0937 and the double AccQ·Tag derivative of hydrazine at *m/z* 373.1423. No hydrazine was detected in the Bennu (OREX-803001-0) water extract above the 0.1 nmol/g level (Extended Data Table 2).

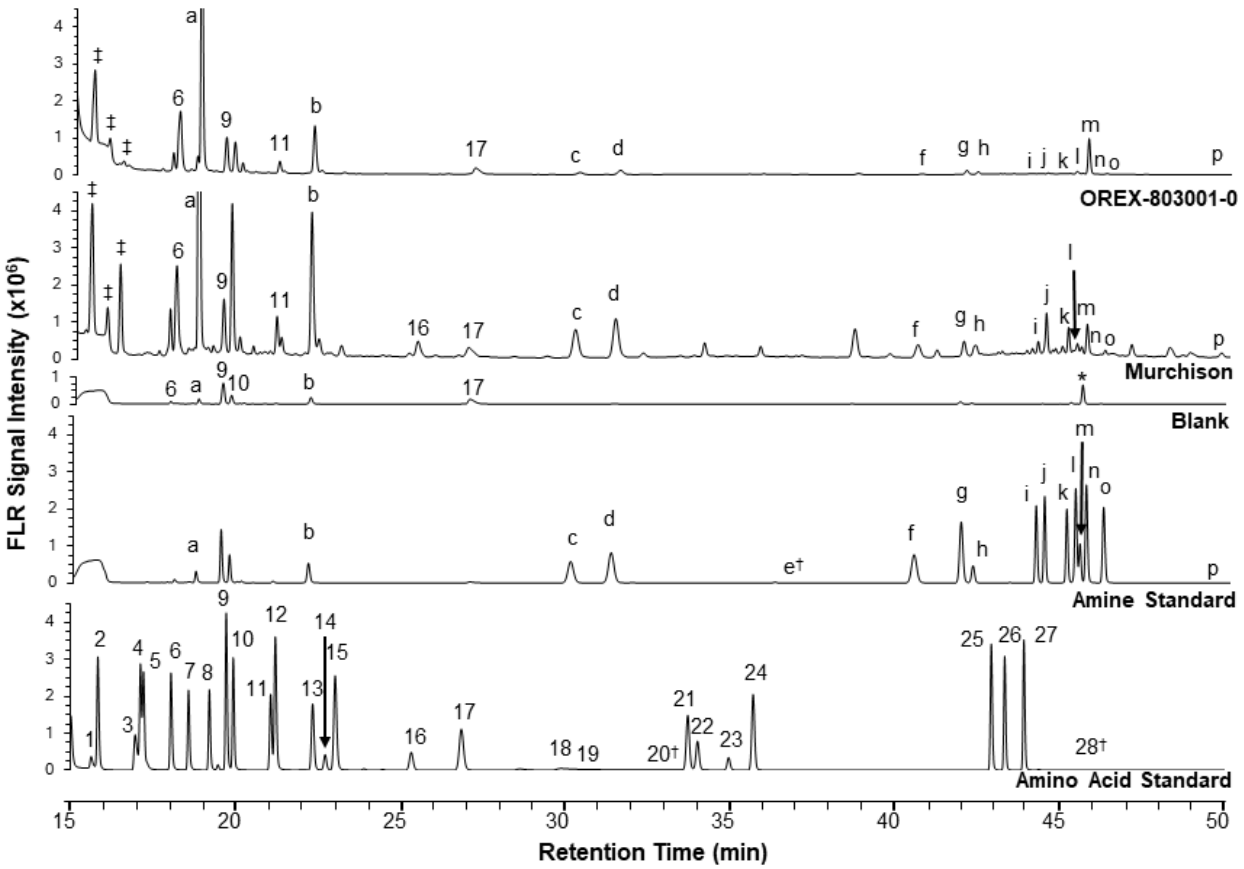

Supplementary Figure 6. Liquid chromatography with UV fluorescence detection chromatograms of free amino acids and amines in the standards and the hot-water extracts of OREX-803001-0, Murchison, and the procedural blank after derivatization (10 min) with AccQ·Tag. Chromatograms of the 15–50 min region from the LC-FD/QqQ-MS analyses. Peaks were identified by comparison to UV fluorescence retention time and molecular mass to those in the standards analyzed on the same day designated by number for amino acids and by letter for the amines. Amino acid peak identifications as follows: (1) histidine, (2) asparagine, (3) arginine, (4) glutamine, (5) serine, (6) glycine, (7) aspartic acid, (8) glutamic acid, (9) β-alanine, (10) threonine, (11) alanine, (12) γ-amino-*n*-butyric acid, (13) β-amino-*n*-butyric acid, (14) proline, (15) β-aminoisobutyric acid, (16) α-aminoisobutyric acid, (17) α-aminobutyric acid, (18) cysteine, (19) lysine, (20) tyrosine, (21) ε-amino-*n*-caproic acid, (22) isovaline, (23) methionine, (24) valine, (25) leucine, (26) isoleucine, (27) phenylalanine, and (28) tryptophan. Amine peak identifications as follows: (a) methylamine, (b) ethylamine, (c) isopropylamine, (d) propylamine, (e) *sec*-butylamine, (f) isobutylamine, (g) *n*-butylamine, (h) *tert*-butylamine, (i) 3-aminopentane, (j) 2-amino-3-methylbutylamine, (k) *sec*-pentylamine, (l) 2-methylbutylamine, (m) *tert*-pentylamine, (n) isopentylamine, (o) *n*-pentylamine, and (p) *n*-hexylamine. †Indicates that the compound does not fluoresce at the excitation and emission wavelengths used for this analysis, however the peak could still be identified and quantified by mass. ‡AccQ·Tag derivatives that were not identified.

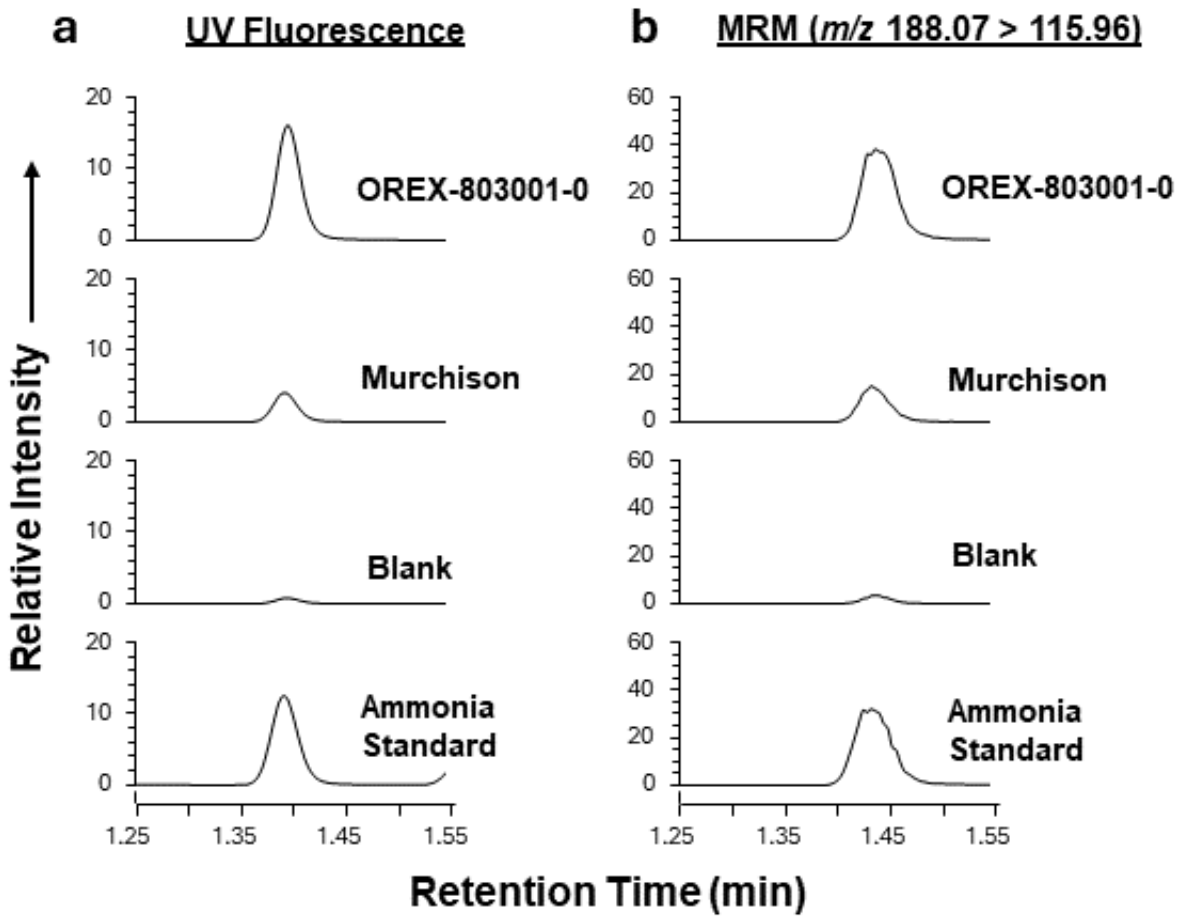

Supplementary Figure 7. LC-FD/QqQ-MS chromatograms showing the identification of the AccQ·Tag derivative of ammonia in the standard and in the hot-water extracts of the procedural blank, the CM2 meteorite Murchison, and Bennu (OREX-803001-0). **a,** UV fluorescence (λ_{ex} = 266 and λ_{em} = 473) traces with a peak at a retention time of ~1.4 min corresponding to ammonia. **b,** Multiple reaction monitoring (MRM) transition (*m/z* 188.07 to 115.96) peak also corresponding to ammonia. Chromatograms only show the 1.25 to 1.55 min region from the 10 min run (other peaks corresponding to AccQ·Tag amine derivatives were detected outside of this range and are discussed elsewhere). The ammonia derivative peaks in the water extracts were identified by comparison of the UV fluorescence retention time and parent to daughter mass transitions of the standard. The MRM data was used for ammonia abundance quantifications.

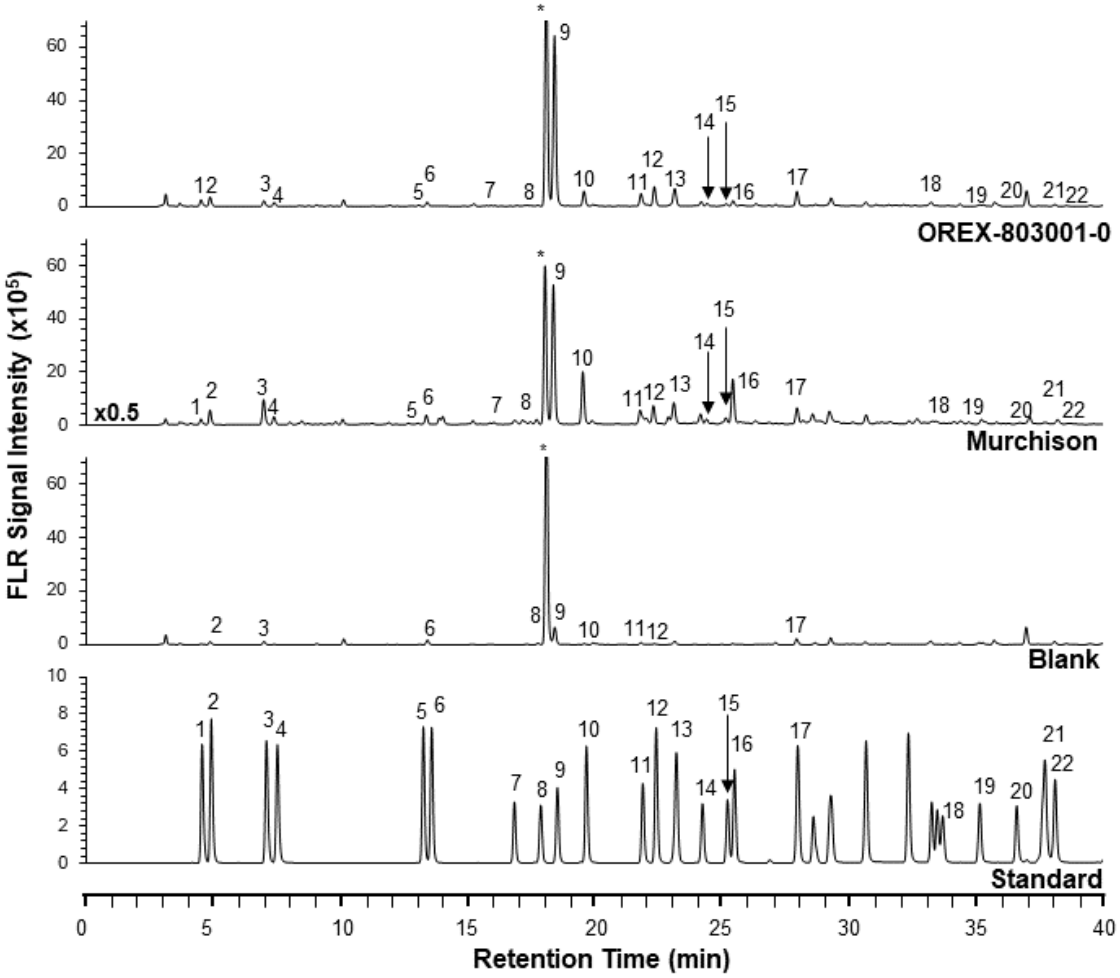

Supplementary Figure 8. Liquid chromatography with UV fluorescence detection chromatograms of amino acids in the standard and the 6 M HCl-hydrolyzed, hot-water extracts of OREX-803001-0, Murchison, and the procedural blank after derivatization (15 min) with *o*-phthaldialdehyde/*N*-acetyl-L-cysteine (OPA/NAC). No peaks were observed beyond a retention time of 40 min. The relative intensity of the Murchison trace was divided by half. Similar chromatograms were also obtained for the non-hydrolyzed water extracts. Peaks were identified by comparison to the fluorescence retention time to those in the amino acid standard analyzed on the same day and are designated by peak number as follows: (1) D-aspartic acid, (2) L-aspartic acid, (3) L-glutamic acid, (4) D-glutamic acid, (5) D-serine, (6) L-serine, (7) D-threonine, (8) L-threonine, (9) glycine, (10) β-alanine, (11) γ-aminobutyric acid, (12) D-alanine, (13) L-alanine, (14) D-β-amino-*n*-butyric acid, (15) L-β-amino-*n*-butyric acid, (16) α-aminoisobutyric acid, (17) D,L-α-amino-*n*-butyric acid, (18) ε-amino-*n*-caproic acid, (19) L-isoleucine, (20) D-isoleucine, (21) D-leucine, and (22) L-leucine. *Analytical artifact peak from the cation exchange desalting resin which did not interfere with the separation and quantification of glycine.

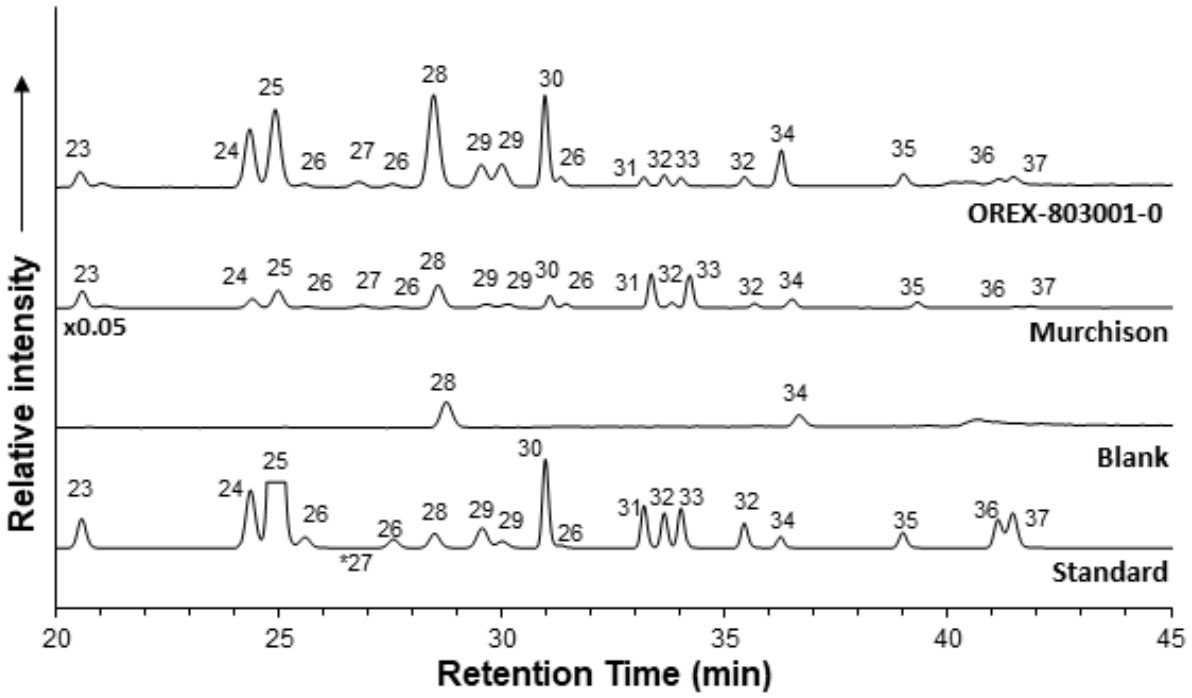

Supplementary Figure 9. LC-ToF-MS chromatograms showing separation of the C_5 amino acids identified in the procedural blank, Bennu (OREX-803001-0), and Murchison meteorite acid-hydrolyzed, hot-water extracts. The 15–40 min region of the LC-ToF-MS single ion mass chromatograms of the C_5 amino acids (*m/z* = 379.1328) with a mass tolerance of 10 ppm. *o*-phthaldialdehyde/*N*-acetyl-L-cysteine (OPA/NAC) derivatization (15 min) of amino acids in the standard and of the 6 M HCl-hydrolyzed, hot-water extracts of the procedural blank, Murchison (intensity divided by 20), and OREX-803001-0. Similar chromatograms were obtained for the non-hydrolyzed water extracts. Peaks were identified by comparison of the single ion mass chromatogram retention time to those in the amino acid standard analyzed on the same day and are designated by peak number as follows: (23) 3-amino-2,2-dimethylpropanoic acid, (24) D,L-4-aminopentanoic acid, (25) D,L-4-amino-3-methylbutanoic acid, (26) D,L- and D,L-*allo*-3-amino-2-methylbutanoic acid, (27) D,L-3-amino-2-ethylpropanoic acid, (28) 5-aminopentanoic acid, (29) D,L-4-amino-2-methylbutanoic acid, (30) 3-amino-3-methylbutanoic acid, (31) D-isovaline, (32) (R)-3-aminopentanoic acid, (33) L-isovaline, (34) (S)-3-aminopentanoic acid, (35) L-valine, (36) D-valine, (37) D-norvaline, and (38) L-norvaline.

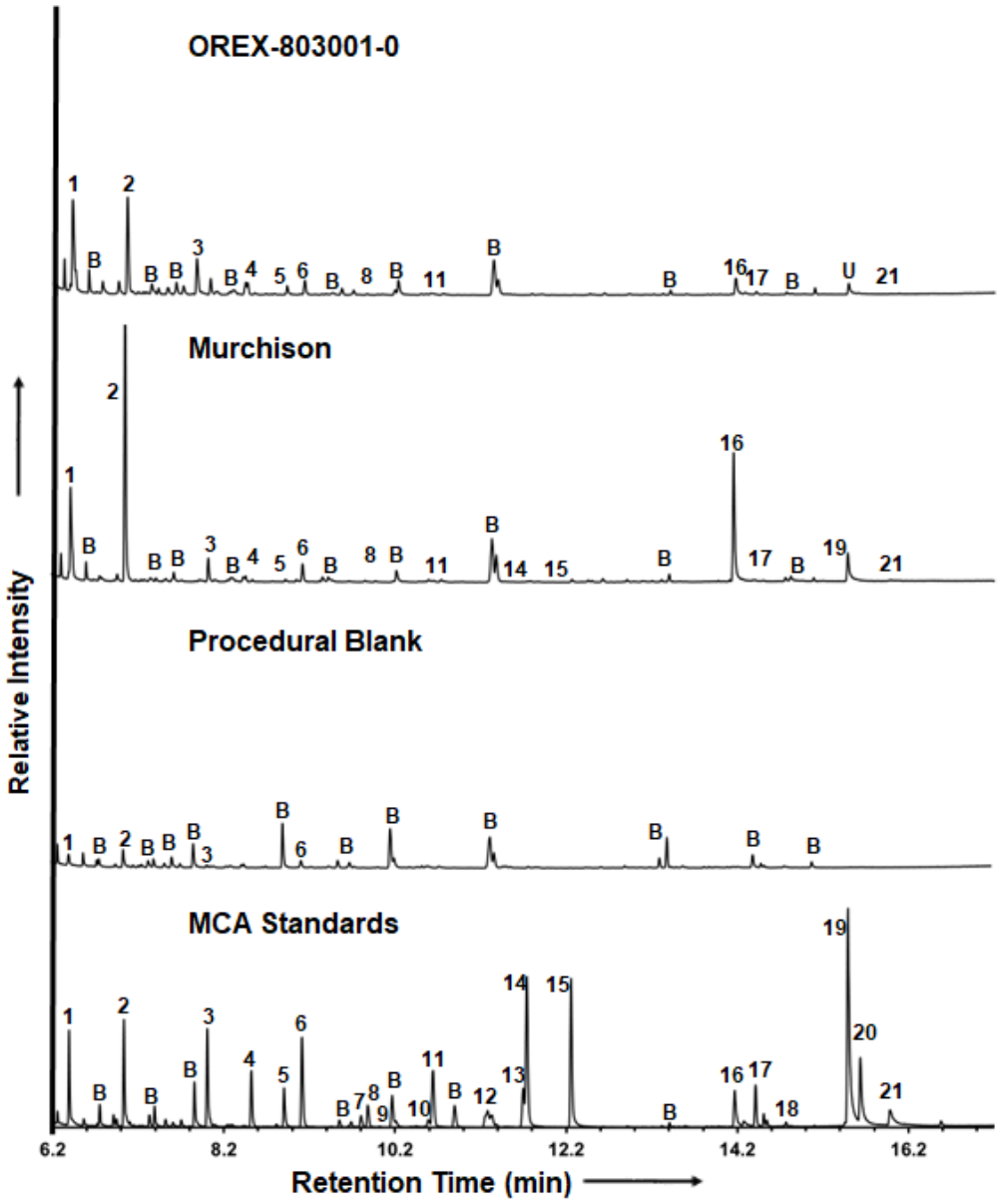

Supplementary Figure 10. GC-QqQ-MS mass chromatograms of carboxylic acids identified in the Bennu and Murchison hot-water extracts. Positive electron-impact GC-QqQ-MS chromatogram (6.2 –17.2 min region, *m/z* = 55 + 60 + 70 + 81 + 89 + 99 + 101 + 105 + 169) of 2-pentanol derivatized carboxylic acids from the hot-water extract of OREX-803001-0, the CM2 Murchison meteorite, a procedural blank, and commercially available standards (all traces excepting standards are on the same intensity scale). Peak identifications as follows: (1) formic acid, (2) acetic acid, (3) propanoic acid, (4) isobutyric acid, (5) 2,2-dimethylpropanoic acid, (6) butyric acid, (7) 2-methylbutyric acid, (8) isopentanoic acid, (9) 2,2-dimethylbutyric acid, (20) 3,3-dimethylbutyric acid, (11) pentanoic acid, (12) 2-ethylbutyric and 2-methylpentanoic acids, (13) 3-methylpentanoic acid, (14) 4-methylpentanoic acid, (15) hexanoic acid, (16) oxalic acid, (17) benzoic acid, (18) malonic acid, (19) succinic acid, (20) fumaric/maleic acid, (21) glutaric acid, (B) reaction byproduct (ethers formed from the excess alcohol used for esterification), and (U) unknown compound.

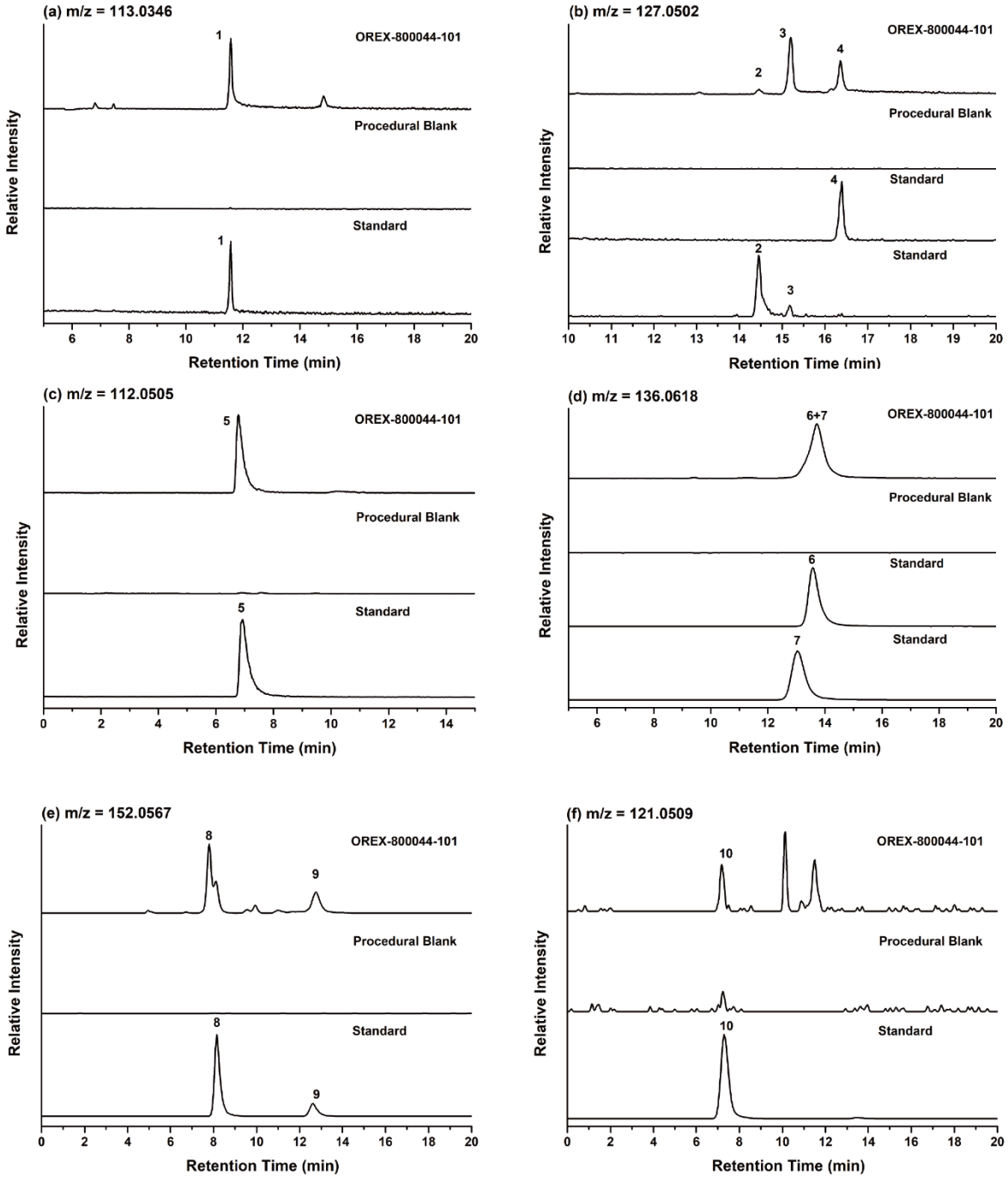

Supplementary Figure 11. High-resolution mass chromatograms of nitrogen heterocycles in the Bennu sample OREX-800044-101 and blank compared to standards. The mass-to-charge (*m*/*z*) ratios correspond to: (a) uracil, (b) thymine, (c) cytosine, (d) adenine, (e) guanine, and (f) purine. Peaks were identified in the samples by comparison of the retention time and molecular mass to those in standards analyzed on the same day and are designated by peak number as follows: (1) uracil, (2) 1-methyluracil, (3) 6-methyluracil, (4) thymine, (5) cytosine, (6) adenine, (7) 8-aminpurine, (8) guanine, (9) isoguanine, and (10) purine. The presence of guanine was also confirmed by the MS/MS measurement (Supplementary Fig. 13).

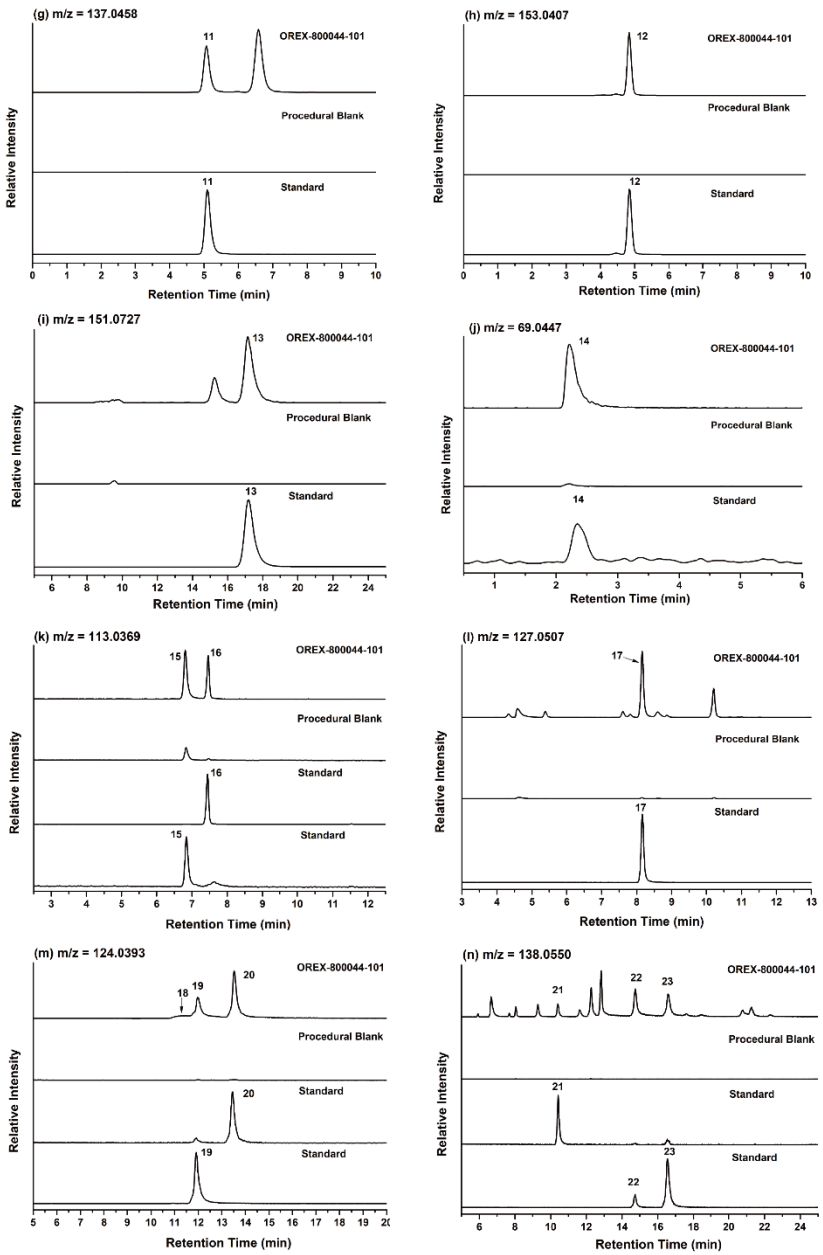

Supplementary Figure 12. High-resolution mass chromatograms of nitrogen heterocycles in the Bennu sample OREX-800044-101, the blanks, and standards. The mass-to-charge (*m/z*) ratios shown correspond to: (g) hypoxanthine, (h) xanthine, (i) diaminopurines, (j) imidazole, (k) imidazole carboxylic acids, (l) methylimidazole carboxylic acids, (m) nicotinic acid, and (n) methylnicotinic acid. Most peaks were identified in the samples by comparison of the retention time and molecular mass to those in standards analyzed on the same day and are designated by peak number as follows: (11) hypoxanthine, (12) xanthine, (13) 2,6-diaminopurine, (14) imidazole, (15) 4-imidazolecarboxylic acid, (16) 2-imidazolecarboxylic acid, (17) 2-methyl-1H-imidazole-4-carboxylic acid, (18) picolinic acid, (19) isonicotinic acid, (20) nicotinic acid, (21) 2-methylnicotinic acid, (22) 6-methylnicotinic acid, and (23) 5-methylnicotinic acid. The imidazole and picolinic acid standards were not analyzed on the same day as the Bennu samples, but the retention times were consistent with those measured previously under the same analytical conditions[63]. The 2,6-diaminopurine peak (13) may co-elute with 6,8-diaminopurine[63].

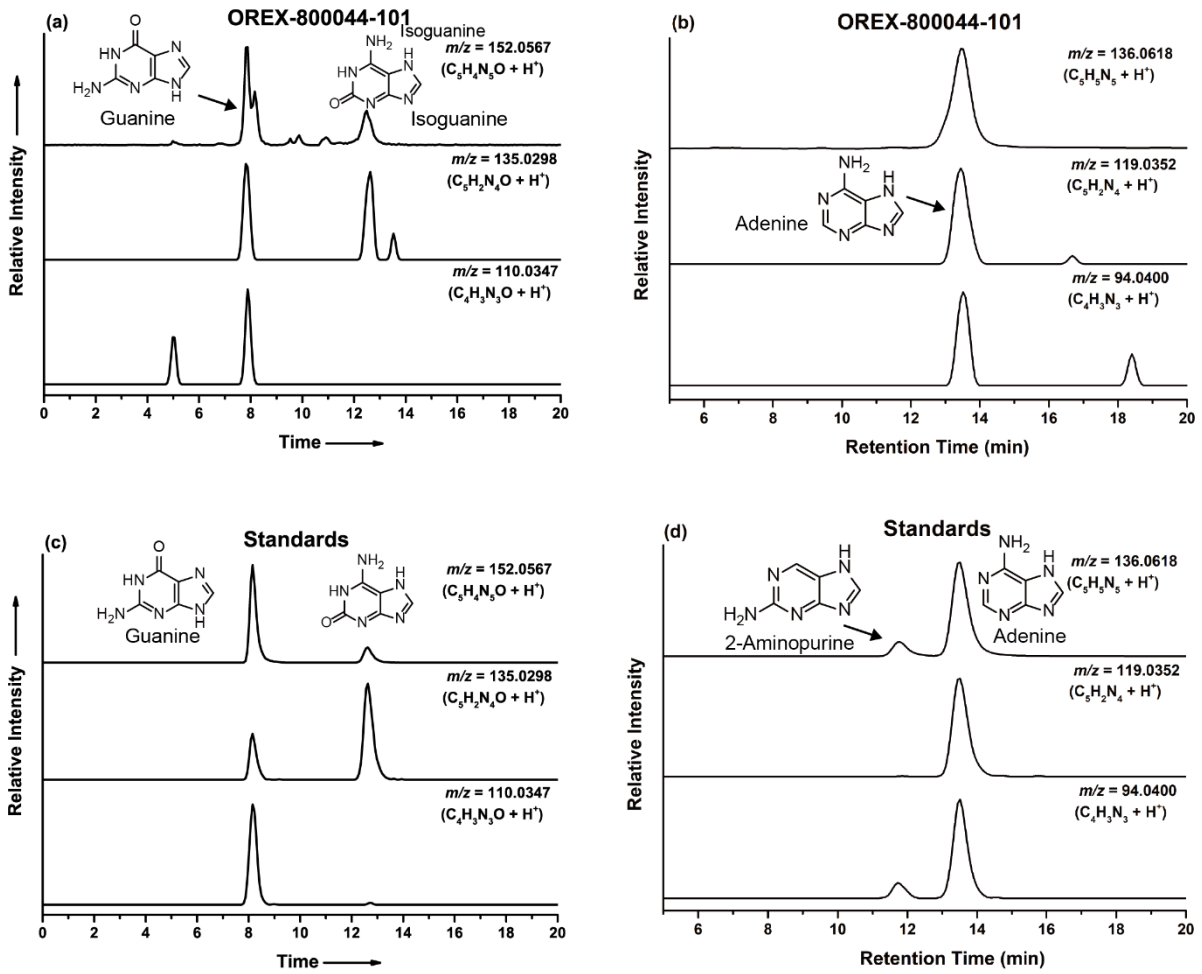

Supplementary Figure 13. High-resolution mass chromatograms of selected purines in the Bennu sample OREX-800044-101, the blanks, and standards. Mass chromatograms at the mass-to-charge (*m/z*) ratio corresponding to the parent ion of **a** guanine and isoguanine and **b** adenine and 2-aminopurine, as well as their daughter in the Bennu sample OREX-800044-101. Those for the **c** guanine and **d** adenine standards are also shown for comparison.

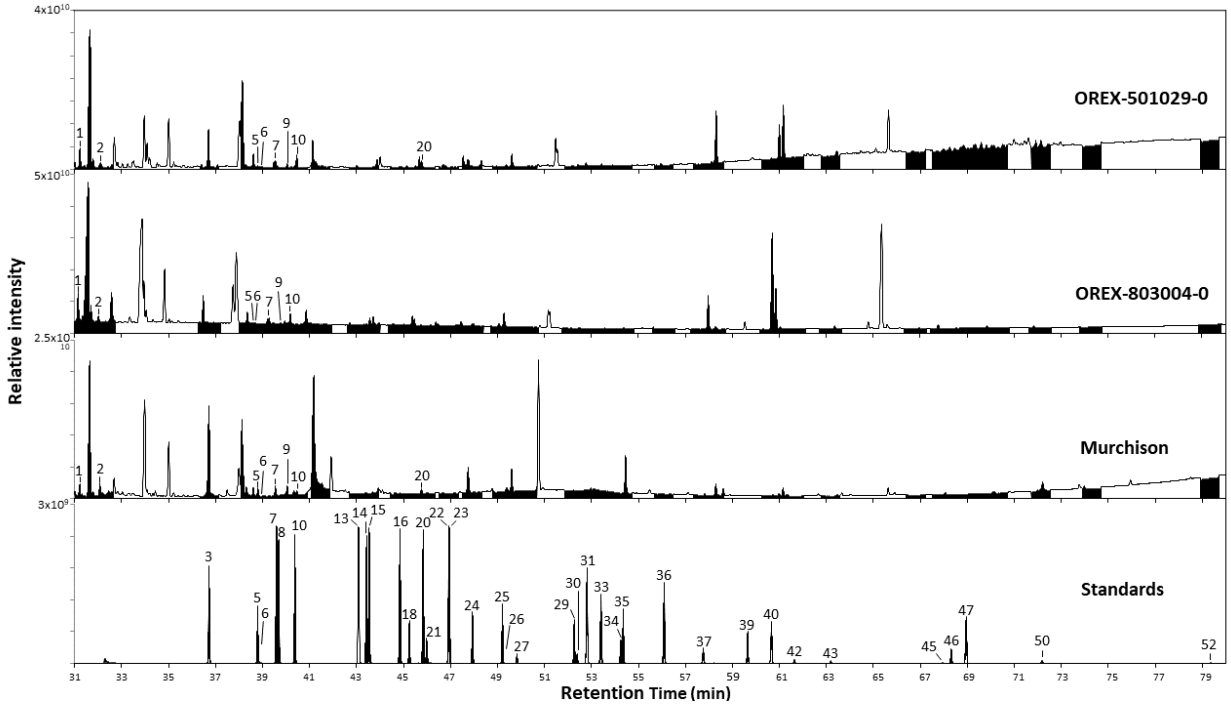

Supplementary Figure 14. Total-ion chromatograms (full scan and multiple reaction monitoring, MRM) showing the detection of amino acids and N-heterocycles after wet-chemistry pyrolysis GC-QqQ-MS analyses of OREX-501029-0, OREX-803004-0, the Murchison meteorite, and the standards. All samples were heated in a solution of MTBSFTA/DMF (4:1 v/v) at 85°C for 90 min prior to pyrolysis GC-QqQ-MS analyses. The amino acid and N-heterocycles in the samples were identified as their *tert*-butyldimethylsilyl (*t*BDMS) derivatives from the peak retention times and individual MRM scans compared to standards as described in Supplementary Table 2 and as follows: (1) 4(3*H*)-pyrimidinone, (2) imidazole, (3) 1-methyl-1*H*-pyrazole-5-carboxylic acid, (4) 2-ethyl-4-methylimidazole, (5) isonicotinic acid, (6) isocytosine, (7) alanine, (8) nicotinic acid/picolinic acid, (9) 2-methylalanine, (10) glycine, (11) 2-aminobutanoic acid, (12) β-alanine, (13) picolinamide, (14) urea, (15) valine, (16) leucine, (17) nicotinamide, (18) isonicotinamide, (19) 2,4-diaminopyrimidine, (20) isoleucine, (21) purine, (22) proline, (23) uracil, (24) 6-methyluracil, (25) thymine, (26) 1-methyluracil, (27) isocytosine, (28) 1*H*-imidazole-2-carboxylic acid, (29) cytosine, (30) pyroglutamic acid, (31) methionine, (32) 5-methylcytosine, (33) serine, (34) threonine, (35) 2,4-diaminopyrimidine, (36) phenylalanine, (37) aspartic acid, (38) 4-imidazole-carboxylic acid, (39) hypoxanthine, (40) glutamic acid, (41) asparagine, (42) adenine, (43) lysine, (44) 2,6-diaminopurine (2-*t*BDMS), (45) histidine, (46) xanthine, (47) tyrosine, (48) tryptophan (2-*t*BDMS), (49) guanine, (50) 2,6-diaminopurine (3-*t*BDMS), (51) tryptophan (3-*t*BDMS), and (52) cysteine.

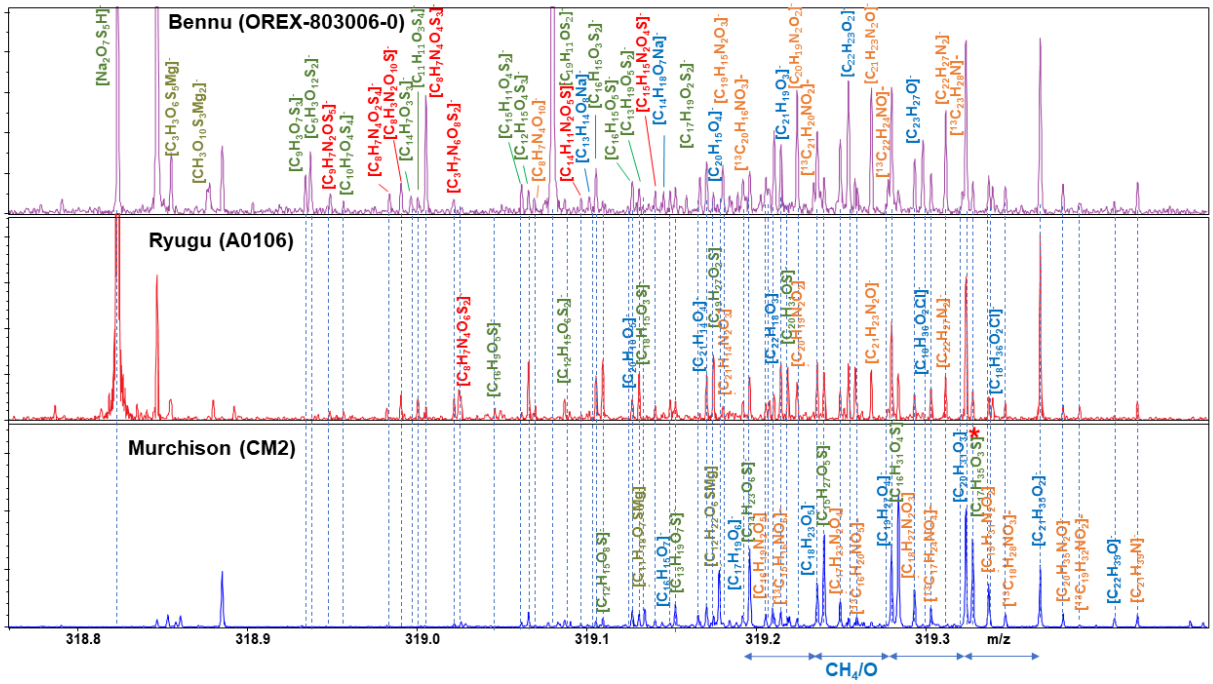

Supplementary Figure 15. FTICR-MS mass spectrum at nominal mass *m/z* 319 with annotated mass signals of Bennu (OREX-803006-0), Ryugu (A0106), and the Murchison (CM2) meteorite. The high signal density and systematic homologous series typical of complex organic mixtures is shown. Such a homologous series of sulfur-containing CHOS, for example, ends from 8 oxygen ($[C_{12}H_{15}O_8S]^-$) down to 3 oxygen ($[C_{17}H_{35}O_3S]^-$), indicating that these may be $-SO_3$ substituted molecules. Color code: blue, CHO; green, CHOS; orange, CHNO; and red, CHNOS.

Supplementary Tables

Supplementary Table 1. Description of the Bennu parent aggregate samples and subsamples and the sample preparation and analytical techniques used in this study.

Sample ID (mass) and Parent ID	Sample Description & Container	Subsample or split ID (mass)	Sample Preparation	Techniques Used
OREX-500002-0 (22 mg) Parent: OREX-500000-0 	Avionics deck aggregate mixture of mostly dark fines (<100 μm) and some intermediates (100–500 μm), some bright and highly reflective particles, others with a metallic luster, and numerous (>5) fibers; sealed under N_2 in concavity slide	OREX-501029-0 (1.1 mg)	Added 5 μl MTBSTFA:DMF (4:1 v/v) and heat at 85°C for 1.5 h; pyrolysis at 250°C	GC-QqQ-MS
		Multiple subsamples of OREX 500002-0: OREX-501034-0 to OREX-501041-0 (0.9–5.5 mg ea.)	Heated at 120°C for 24 h under Ar or under Ar at room temperature for 66 h	EA-IRMS
OREX-500005-0 (88 mg) Parent: OREX-500000-0 	Avionics deck aggregate mixture of mostly dark fines with average grain size <100 μm, with some particles up to 500 μm. Some bright and highly reflective particles mixed in; sealed under N_2 in glass vial with Viton stopper and crimped Al lid.	OREX-501006-0 (<1 mg)	Several <100 μm grains pressed onto a KBr window	Coordinated optical and UV fluorescence imaging and μ-L^2MS molecular analysis and mapping

OREX-800044-0 (109 mg) Parent: OREX-800013-0 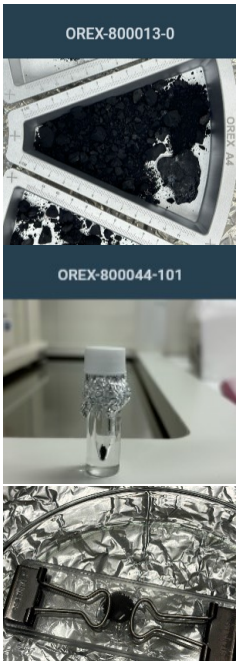 	Bulk aggregate parent sample removed from underneath the TAGSAM Mylar flap and placed in deep Tray OREX A4. Mixture of mostly dark fines (<100 μm) and intermediates (100–500 μm) with some coarse particles (>500 μm) and several mm-sized particles. This sample has mostly black particles, but rare light-colored particles are present; sealed under N_2 in glass concavity slide placed inside an Eagle Stainless.	OREX-800044-101 (17.75 mg)	110°C for 12 h extraction in 6 M HCl under N_2	LC-HRMS
OREX-800031-0 (52 mg) Parent: OREX-800013-0 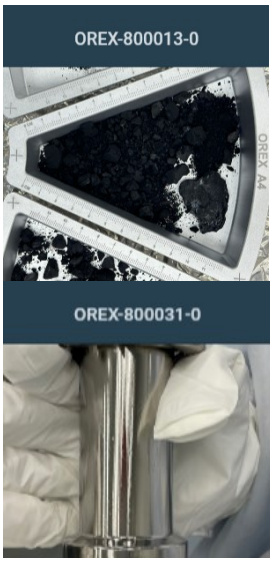 	Bulk aggregate parent sample removed from underneath the TAGSAM Mylar flap and placed in deep Tray OREX A4. Composed primarily of fine (<100 μm) and intermediate (100–500 μm) sized particles with some coarse particles (>500 μm). This sample includes mostly black particles with rare (but present in low abundance) light-colored particles; sealed under N_2 in a glass concavity slide placed in an Eagle Stainless container.	OREX-803001-0 (25.6 mg)	100°C for 24 h extraction in water, water extract split for coordinated SOM analyses	LC-MS, LC-HRMS, GC-QqQ-MS
		OREX-803001-112 (extract, n/a)	~2.6% split of water extract, added 2 μL 6 M HCl to water extract and dried under vacuum at room temperature in tin capsule	NanoEA-IRMS
		OREX-803001-103 (19.2 mg)	Dried residue after water extraction, heated at 120°C for 24 h under Ar	EA-IRMS
		OREX-803004-0 (1.0 mg)	Added 5 μL MTBSTFA:DMF (4:1 v/v) and heat at 85°C for 1.5 h; pyrolysis at 250°C under He	GC-QqQ-MS
		OREX-803006-0 (3.3 mg)	Sample crushing in methanol at room temperature	FTICR-MS
		OREX-803007-0 (23.6 mg)	Heated at 120°C for 24 h under Ar	EA-IRMS

Supplementary Table 2. Comparison of the bulk C, N, and H contents and their stable isotopic compositions of the individual subsamples of the Bennu aggregates. Measurement of the elemental abundances (wt.%) and stable isotopic compositions (‰ $\delta^{13}C$ vs. VPDB; $\delta^{15}N$ v. AIR; δD vs. VSMOW) of the bulk samples were conducted by using EA-IRMS at the Carnegie Institution for Science (CIS). The masses of each subsample used for the measurements are also shown. The reported errors are 1-sigma and correspond to the highest variability observed in the standards.

Bennu Aggregate Subsample	Mass (mg)	C (wt.%)	$\delta^{13}C$ (‰)	N (wt.%)	$\delta^{15}N$ (‰)	H (wt.%)	δD (‰)
Bennu (OREX-500002-0, Avionics Deck)							
OREX-501034-0[a] (fines, <0.1 mm)	0.877					0.84 ± 0.05	332 ± 2
OREX-501035-0[a] (fines, <0.1 mm)	0.878					0.86 ± 0.05	328 ± 2
OREX-501036-0[b] (fines, <0.1 mm)	0.930					0.90 ± 0.05	314 ± 2
OREX-501037-0[b] (fines, <0.1 mm)	0.934					0.89 ± 0.05	315 ± 2
OREX-501040-0[b] (intermediate, 0.2 mm)	0.992					0.93 ± 0.05	305 ± 2
OREX-501038-0[a] (fines, <0.1 mm)	5.238	4.7 ± 0.4	2.7 ± 0.1	0.24 ± 0.02	74.6 ± 0.1		
OREX-501039-0[b] (fines, <0.1 mm)	5.533	4.7 ± 0.4	3.2 ± 0.1	0.23 ± 0.02	75.5 ± 0.1		
OREX-501041-0[b] (intermediate, 0.2 mm)	2.281	4.7 ± 0.4	–0.5 ± 0.1	0.24 ± 0.02	57.1 ± 0.1		
Bennu (OREX-803007-0, TAGSAM aggregate, <0.5 mm)							
OREX-803040-0[a]	1.420					0.93 ± 0.03	325 ± 2
OREX-803041-0[a]	1.343					0.95 ± 0.03	359 ± 2
OREX-803042-0[a]	1.440					0.93 ± 0.03	344 ± 2
OREX-803043-0[a]	1.359					0.92 ± 0.03	365 ± 2
OREX-803002-0[a]	2.161					0.95 ± 0.03	327 ± 2
OREX-803044-0[a]	5.244	4.6 ± 0.2	4.4 ± 0.2	0.25 ± 0.01	70.4 ± 0.2		
OREX-803045-0[a]	5.411	4.4 ± 0.2	1.9 ± 0.2	0.25 ± 0.01	68.3 ± 0.2		
OREX-803046-0[a]	5.176	4.7 ± 0.2	3.5 ± 0.2	0.25 ± 0.01	106.0 ± 0.2		
OREX-803001-103 (residue after water extraction @ 100°C 24h)							
OREX-803001-104[a]	1.179					0.99 ± 0.03	288 ± 2
OREX-803001-105[a]	1.501					0.99 ± 0.03	295 ± 2
OREX-803001-106[a]	1.523					1.05 ± 0.03	297 ± 2
OREX-803001-107[a]	0.990					1.03 ± 0.03	295 ± 2
OREX-803001-108[a]	4.755	4.3 ± 0.2	–3.0 ± 0.2	0.20 ± 0.01	58.8 ± 0.2		
OREX-803001-109[a]	4.994	4.3 ± 0.2	–1.3 ± 0.2	0.20 ± 0.01	56.8 ± 0.2		
OREX-803001-110[a]	4.297	4.2 ± 0.2	–2.3 ± 0.2	0.20 ± 0.01	58.5 ± 0.2		

[a]Sample heated at 120°C for 48 h under Ar (<0.1 ppm H_2O and O_2) in a glovebox, and then kept there at room temperature for 66 hours without exposure to atmosphere prior to EA-IRMS analysis.
[b]Sample under Ar in glovebox at room temperature without any exposure to atmosphere prior to EA-IRMS analysis.

Supplementary Table 3. Summary of previously reported Ryugu bulk C, N, and H contents and stable isotopic compositions of aggregate samples and their calculated mass weighted average values. Measurement of the elemental abundances (wt.%) and stable isotopic compositions (‰ δ^{13}C vs. VPDB; δ^{15}N v. AIR; δD vs. VSMOW) of the samples were conducted by EA-IRMS. The masses of each sample used to calculate the weighted average values for each set of published data are also shown.

Ryugu Aggregate Sample	Mass (mg)[a]	C (wt.%)	δ^{13}C (‰)	N (wt.%)	δ^{15}N (‰)	Mass (mg)[b]	H (wt.%)	δD (‰)
Oba et al.[33]								
C0107	0.0450	3.36	-7.4	0.12		0.5276	1.12	255
C0107	0.1305	3.24	-1.3	0.13	39.0	0.3272	1.10	281
C0107	0.1600	3.47	-2.1	0.14	32.6	0.2642	0.94	270
C0107[c]	0.1696	4.27	15.7	0.15	38.8			
Weighted average		***3.67***	***4.6***	***0.14***	***36.7***		***1.07***	***266***
Naraoka et al.[20]								
A0106	0.1820	3.69	-2.7	0.16	39.1	0.1348	1.05	240
A0106	0.1019	3.93	1.4	0.17	53.2	0.0965	1.15	265
A0106	0.1279	3.68	-0.4	0.16	36.7	0.4241	1.22	250
Weighted average		***3.75***	***-0.9***	***0.16***	***42.0***		***1.17***	***250***
Okazaki et al.[70]								
A0105-07	0.118	6.8		0.070	1.7			
C0106-07	0.119	6.4		0.084	0.0			
A0105-05	0.140			0.089	18.1			
C0106-06	0.168			0.086	19.5			
Weighted average		***6.6***		***0.08***	***11.5***			
Yokoyama et al.[71]								
A0040	0.91	4.67				0.91	0.94	
Weighted average		***4.67***					***0.94***	
Grady et al.[69]								
A0219[d]	2	6	11	0.22	43			
C0208	1.7	2.9	0.0	0.0923	36.5			
C0209	2.5	3.8	-1.7	0.1491	29.4			
Weighted average		***3.44***	***-1.1***	***0.13***	***31.5***			
Nakamura et al.[68]								
A0022	0.557	4.02	14.1	0.12	40.5	0.137	1.11	178
A0033	0.532	5.39	-2.4	0.17	17.8	0.172	0.694	202
A0035	0.131	4.12	7.1	0.19	52.1	0.074	1.30	158
A0048	0.578	3.39	-10.3	0.13	35.0	0.119	1.12	218
A0073	0.113	3.40	-9.7	0.19	52.3			
A0078	0.757	3.48	-9.4	0.18	50.9	0.124	1.03	183
A0085						0.057	0.98	301
C0008	0.765	3.70	-3.0	0.16	46.2	0.317	0.974	341
C0019	0.583	3.17	-6.3	0.10	26.8	0.121	1.02	100
C0027	0.538	3.16	-7.3	0.10	22.7	0.147	1.07	123
C0039	0.173	3.34	-7.7	0.11				
C0047	0.103	2.79	-10.5	0.10				
C0053						0.135	1.22	210
C0079	0.571	3.24	-9.0	0.11	22.9	0.145	1.14	159
C0081	0.568	5.22	-9.8	0.22	53.0	0.130	1.07	345
C0082	0.650	5.34	-15.3	0.19	0.4	0.126	0.937	108
Weighted average		***3.95***	***-6.1***	***0.15***	***33.2***		***1.03***	***212***
Weighted average of all values		***3.81***	***-3.5***	***0.13***	***33.1***		***1.04***	***236***

[a]Sample mass used for C and N measurements.
[b]Sample mass used for H measurements.
[c]Carbonate-rich.
[d]Data excluded from mass weighted average due to large (± 30%) uncertainties in sample mass and measured abundances.

Supplementary Table 4. Comparison of the total C and N contents and their stable isotopic compositions of the Bennu aggregate and CM2 meteorite Murchison water extracts. All elemental abundances in nmol and stable isotopic compositions in ‰ (δ^{13}C vs. VPDB; δ^{15}N vs. AIR) were measured on the nano-EA-IRMS system at The Pennsylvania State University (PSU). The reported measured isotope values have been corrected for blank contribution using Equation 2, and the associated errors were determined using Equation 3. The Murchison nitrogen peak was below the detection limit. The calculated elemental abundances and stable isotope values were determined by mass balance using the elemental abundances and stable isotope values of Bennu and Murchison aggregate powder measured by EA-IRMS at CIS before and after hot-water extraction (see Extended Data Table 1). The amount of carbon lost is the difference between the calculated and measured values, and the δ^{13}C value of the carbon lost was calculated by mass balance using the measured and calculated abundances and isotope values. Uncertainties in the calculated values and carbon loss were determined by standard error propagation.

Subsample	δ^{13}C (‰, VPDB)		C (nmol)		Carbon lost	
	measured	calculated	measured	calculated	C (nmol)	δ^{13}C (‰, VPDB)
OREX-803001-112 (hot-water extract from aggregate, <0.5 mm)	–9 ± 3	80 ± 77	25 ± 53	166 ± 155	141 ± 164	96 ± 169
Murchison (CM2) (hot-water extract from powder)	23 ± 9	61 ± 35	28 ± 53	107 ± 62	79 ± 82	78 ± 109

Subsample	δ^{15}N (‰, AIR)		N (nmol)	
	measured	calculated	measured	calculated
OREX-803001-112 (hot-water extract from aggregate, <0.5 mm)	180 ± 47	178 ± 86	6 ± 35	24 ± 5
Murchison (CM2) (hot-water extract from powder)	55 ± 8[a]	80 ± 31	4 ± 35[a]	13 ± 4

[a]Below detection limit of nano-EA-IRMS system, therefore low confidence in value.

Supplementary Table 5. Uncorrected nitrogen and carbon peak areas and stable isotope values of the blanks and the dried water extracts of the Bennu aggregate (OREX-803001-112) and Murchison meteorite. All peak areas (Vs) and stable isotopic values (‰; uncorrected) were measured on the nano-EA-IRMS system at Pennsylvania State University. The mean peak area and mean isotope value of the capsule + water + acid blanks smaller than samples were used for data correction.

Sample	$\delta^{13}C$ (‰)	Peak Area (Vs)	$\delta^{15}N$ (‰)	Peak Area (Vs)
Empty Capsule Blank	–25.8	33.2	4.8	2.8
Empty Capsule Blank	–25.5	36.0	10.0	1.5
Capsule + Water + Acid	–25.9	32.2	0.7	2.0
Capsule + Water + Acid	–27.0	24.5	2.2	2.1
Capsule + Water + Acid	–26.0	31.0	9.4	0.6
Capsule + Water + Acid	–26.4	38.7	7.7	0.9
Capsule + Water + Acid	–25.9	31.8	2.8	2.1
Capsule + Water + Acid	–26.7	39.9	3.3	0.9
Capsule + Water + Acid	–25.9	27.6	4.0	3.1
Capsule + Water + Acid	–23.8	50.7	0.9	3.7
Capsule + Water + Acid	–26.5	24.3	1.7	1.7
Capsule + Water + Acid	–26.1	23.2	1.5	1.7
Fused silica FS120	–26.4	42.8	8.5	0.9
Procedural Blank	–26.6	26.6	4.3	0.7
Murchison (CM2) (hot-water extract of powder)	–11.8	42.2	26.4	1.3
OREX-803001-112 (hot-water extract from of aggregate, <0.5 mm)	–21.1	38.4	65.7	2.3

Supplementary Table 6. Detection metrics observed when analyzing a mixed amino acid standard using the analytical technique described in this study for hydrazine. After derivatization with AccQ·Tag, the mass shifted by either 171 or 171×2 Da.

	Molecular Weight of untagged analyte (g/mol)	Chemical Formula	Theoretical *m/z*	Experimental *m/z*
Hydrazine (Single Tag)	32.0452	$C_{10}H_{11}N_4O$	203.0928	203.0937
Hydrazine (Double Tag)	32.0452	$C_{20}H_{17}N_6O_2$	373.1408	373.1423

Supplementary Table 7. Multiple reaction monitoring (MRM) parameters used for the LC-QqQ-MS peak identifications and quantifications of the AccQ·Tag derivatives of amino acids. All three traces were used for compound identifications, and the first precursor ion to product ion (*m/z*) mass transition (Quant. Trace) was used for quantification.

RT (min)	Name	Quant. Trace (m/z)	1° Trace (m/z)	2° Trace
15.17	Histidine	326.10 > 156.10	326.13 > 155.97	An3 - FLR
16.01	Asparagine	303.10 > 171.10	303.10 > 116.10	An3 - FLR
17.09	Arginine	345.10 > 175.10	345.20 > 70.00	An3 - FLR
17.27	Glutamine	317.10 > 171.10	317.10 > 145.10	An3 - FLR
17.38	Serine	276.07 > 170.94	276.10 > 116.10	An3 - FLR
18.20	Glycine	246.10 > 171.10	246.10 > 89.10	An3 - FLR
18.72	Aspartic Acid	304.05 > 171.01	304.10 > 116.10	An3 - FLR
19.34	Glutamic Acid	318.10 > 171.00	318.10 > 116.20	An3 - FLR
19.86	Alanine	260.07 > 170.93	260.07 > 116.10	An3 - FLR
20.07	Threonine	290.13 > 170.95	290.13 > 115.96	An3 - FLR
21.20	β-Alanine	260.07 > 170.93	260.07 > 116.10	An3 - FLR
21.36	γ-Amino-*n*-butyric Acid	274.10 > 171.11	274.10 > 116.10	An3 - FLR
22.48	β- Amino-*n*-butyric Acid	274.10 > 171.11	274.10 > 116.10	An3 - FLR
22.85	Proline	286.13 > 170.90	286.13 > 115.91	An3 - FLR
23.15	β-Aminoisobutyric Acid	274.10 > 171.11	274.10 > 116.10	An3 - FLR
25.46	α-Aminoisobutyric Acid	274.10 > 171.11	274.10 > 116.10	An3 - FLR
26.97	α-Amino-*n*-butyric Acid	274.10 > 171.11	274.10 > 116.10	An3 - FLR
28.68	Cysteine	581.10 > 171.10	581.10 > 145.10	An3 - FLR
29.84	Lysine	487.13 > 171.04	487.13 > 116.17	An3 - FLR
33.84	Tyrosine	352.13 > 170.94	352.13 > 116.07	[a]
33.84	ε-Amino-*n*-caproic Acid	302.13 > 170.94	302.13 > 116.01	An3 - FLR
34.14	Isovaline	288.13 > 170.95	288.10 > 89.10	An3 - FLR
35.09	Methionine	320.13 > 170.93	320.13 > 116.01	An3 - FLR
35.83	Valine	288.13 > 170.95	288.10 > 116.10	An3 - FLR
43.07	Leucine	302.13 > 170.94	302.13 > 116.01	An3 - FLR
43.48	Isoleucine	302.13 > 170.94	302.13 > 116.01	An3 - FLR
44.06	Phenylalanine	336.10 > 171.10	336.10 > 116.10	An3 - FLR
44.50	Tryptophan	375.10 > 171.10	375.10 > 89.10	[a]

[a]AccQ·Tag derivative peak not observed at the UV detector excitation and emission wavelengths (λ_{ex} = 266 nm; λ_{em} = 473 nm). FLR = fluorescence signal.

Supplementary Table 8. Multiple reaction monitoring (MRM) parameters used for the LC-QqQ-MS peak identifications and quantifications of the AccQ·Tag derivatives of ammonia and the amines. All three traces were used for compound identifications, and the first precursor ion to product ion (*m/z*) mass transition (Quant. Trace) was used for quantification.

RT (min)	Name	Quant. Trace (*m/z*)	1° Trace (*m/z*)	2° Trace
15.01	Ammonia	188.07 > 115.96	188.07 > 89.02	An3 - FLR
18.91	Methylamine	202.13 > 170.91	202.13 > 115.97	An3 - FLR
22.31	Ethylamine	216.20 > 115.95	216.20 > 89.00	An3 - FLR
30.33	Isopropylamine	230.20 > 170.89	230.20 > 115.96	An3 - FLR
31.56	Propylamine	230.20 > 170.89	230.20 > 115.96	An3 - FLR
36.44	*sec*-Butylamine	244.20 > 170.91	244.20 > 115.97	[a]
40.68	Isobutylamine	244.20 > 170.91	244.20 > 115.97	An3 - FLR
42.04	*n*-Butylamine	244.20 > 170.91	244.20 > 115.97	An3 - FLR
42.39	*tert*-Butylamine	244.20 > 170.91	244.20 > 115.97	An3 - FLR
44.28	3-Aminopentane	258.20 > 170.94	258.20 > 115.95	An3 - FLR
44.54	2-Amino-3-methylbutylamine	258.20 > 170.94	258.20 > 115.95	An3 - FLR
45.20	*sec*-Pentylamine	258.20 > 170.94	258.20 > 115.95	An3 - FLR
45.48	2-Methylbutylamine	258.20 > 170.94	258.20 > 115.95	An3 - FLR
45.80	*tert*-Pentylamine	258.20 > 170.94	258.20 > 115.95	An3 - FLR
45.81	Isopentylamine	258.20 > 170.94	258.20 > 115.95	An3 - FLR
46.32	*n*-Pentylamine	258.20 > 170.94	258.20 > 115.95	An3 - FLR
51.64	*n*-Hexylamine	272.13 > 170.95	272.13 > 115.96	An3 - FLR

[a]AccQ·Tag derivative peak not observed at the UV detector excitation and emission wavelengths (λ_{ex} = 266 nm; λ_{em} = 473 nm). FLR = fluorescence signal.

Supplementary Table 9. Detection metrics observed for selected C2 to C6 amino acids using the LC-FD/ToF-MS analytical technique. As a result of derivatization with OPA/NAC, 261 Da is added to the measured mass of each amino acid. Mass error was calculated using the following equation:

$$mass\ error = \frac{experimental\ mass - theoretical\ mass}{theoretical\ mass} * 1e^6$$

Analyte	FD RT (min)	MS RT (min)	$[M+H]^+$ Chemical Formula	Theoretical *m/z*	Experimental *m/z*	Mass Error (ppm)
D-Aspartic acid	4.55	4.69	$C_{17}H_{19}N_2O_7S$	395.0913	395.0916	0.7593
L-Aspartic acid	4.92	5.06	$C_{17}H_{19}N_2O_7S$	395.0913	395.0915	0.5062
L-Glutamic acid	7.08	7.23	$C_{18}H_{21}N_2O_7S$	409.1069	409.1068	0.2444
D-Glutamic acid	7.52	7.65	$C_{18}H_{21}N_2O_7S$	409.1069	409.1072	0.7333
D-Serine	13.25	13.4	$C_{16}H_{19}N_2O_6S$	367.0964	367.0962	0.5448
L-Serine	13.58	13.73	$C_{16}H_{19}N_2O_6S$	367.0964	367.0966	0.5448
D-Threonine	16.83	16.98	$C_{17}H_{21}N_2O_6S$	381.1120	381.1117	0.7872
L-Threonine	17.87	18.01	$C_{17}H_{21}N_2O_6S$	381.1120	381.1118	0.5248
Glycine	18.53	18.67	$C_{15}H_{17}N_2O_5S$	337.0858	337.0845	3.8565[a]
β-Ala	19.67	19.81	$C_{16}H_{19}N_2O_5S$	351.1015	351.1014	0.2848
γ-ABA	21.88	22.03	$C_{17}H_{21}N_2O_5S$	365.1171	365.1179	2.1911[a]
D-Alanine	22.42	22.56	$C_{16}H_{19}N_2O_5S$	351.1015	351.1023	2.2785[a]
L-Alanine	23.2	23.35	$C_{16}H_{19}N_2O_5S$	351.1015	351.1021	1.7089
D-β-ABA	24.23	24.38	$C_{17}H_{21}N_2O_5S$	365.1171	365.1172	0.2739
L-β-ABA	25.22	25.37	$C_{17}H_{21}N_2O_5S$	365.1171	365.1172	0.2739
α-AIB	25.5	25.64	$C_{17}H_{21}N_2O_5S$	365.1171	365.1168	0.8217
D,L-α-ABA	27.98	28.13	$C_{17}H_{21}N_2O_5S$	365.1171	365.1166	1.3694
ε-ACA	29.28	29.46	$C_{19}H_{25}N_2O_5S$	393.1484	393.1484	0.0000
L-Isoleucine	35.15	35.3	$C_{19}H_{25}N_2O_5S$	393.1484	393.1477	1.7805
D-Isoleucine	36.6	36.76	$C_{19}H_{25}N_2O_5S$	393.1484	393.1478	1.5261
D-Leucine	37.7	37.85	$C_{19}H_{25}N_2O_5S$	393.1484	393.1477	1.7805
L-Leucine	38.1	38.27	$C_{19}H_{25}N_2O_5S$	393.1484	393.1477	1.7805

[a]Glycine, D-alanine, and γ-ABA all have peaks in the mass spectra that are leading to higher mass errors. These peaks are fully separated by the Xevo G2 XS time of flight in the mass spectra and in all FWHM resulting chromatograms, but the mass experimental *m/z* calculation completed by the Masslynx software takes these smaller peaks into account.

Supplementary Table 10. Detection metrics observed for the C5 amino acids using the LC-FD/ToF-MS analytical technique. After derivatization with OPA/NAC, 261 Da is added to the measured mass of each amino acid. Mass error was calculated using the following equation:

$$mass\ error = \frac{experimental\ mass - theoretical\ mass}{theoretical\ mass} * 1e^6$$

Analyte	FD RT (min)	MS RT (min)	$[M+H]^+$ Chemical Formula	Theoretical *m/z*	Experimental *m/z*	Mass Error (ppm)
3-A-2,2-DMPA	20.47	20.59	$C_{18}H_{23}N_2O_5S$	379.1328	379.1330	0.5275
D,L-4-APA	24.22	24.36	$C_{18}H_{23}N_2O_5S$	379.1328	379.1326	0.5275
D,L-4-A-3-MBA	24.78	24.95	$C_{18}H_{23}N_2O_5S$	379.1328	379.1333	1.3188
D,L-and *allo*-3-A-2-MBA	25.45	25.60	$C_{18}H_{23}N_2O_5S$	379.1328	379.1324	1.0550
D,L-3-A-2-EPA	26.50	26.50	$C_{18}H_{23}N_2O_5S$	379.1328	n.d.	-
δ-AVA	28.33	28.51	$C_{18}H_{23}N_2O_5S$	379.1328	379.1324	1.0550
D,L-4-A-2-MBA	29.40	29.57	$C_{18}H_{23}N_2O_5S$	379.1328	379.1325	0.7913
3-A-3-MBA	30.82	30.98	$C_{18}H_{23}N_2O_5S$	379.1328	379.1327	0.2638
D-Iva	33.03	33.20	$C_{18}H_{23}N_2O_5S$	379.1328	379.1325	0.7913
L-3-APA	33.48	33.65	$C_{18}H_{23}N_2O_5S$	379.1328	379.1321	1.8463
L-Iva	33.85	34.00	$C_{18}H_{23}N_2O_5S$	379.1328	379.1322	1.5826
D-3-APA	35.27	35.42	$C_{18}H_{23}N_2O_5S$	379.1328	379.1321	1.8463
L-Val	36.05	36.25	$C_{18}H_{23}N_2O_5S$	379.1328	379.1326	0.5275
D-Val	38.82	39.01	$C_{18}H_{23}N_2O_5S$	379.1328	379.1321	1.8463
D-Nva	40.95	41.12	$C_{18}H_{23}N_2O_5S$	379.1328	379.1321	1.8463
L-Nva	41.28	41.46	$C_{18}H_{23}N_2O_5S$	379.1328	379.1325	0.7913

n.d. = not determined due to degradation of the standard which is not commercially available. Therefore, the neighboring peak consisting of D,L- and *allo*-3-A-2-MBA analyte was used for quantitation of this amino acid in the samples.

Supplementary Table 11. Summary of the wet-chemistry pyrolysis GC-QqQ-MS peak identifications of the amino acid and N-heterocycles identified in the Bennu samples and Murchison. Identification of the *tert*-butyldimethylsilyl (tBDMS) derivatives was made based on retention times (min) and precursor to product ion (*m/z*) mass transitions used in multiple reaction monitoring (MRM) mode for the Murchison meteorite, reagent blank, and Bennu aggregate samples (OREX-803004-0 and OREX-501029-0).

Peak #	Analyte	Retention Time (min)	Precursor Mass *m/z*	Product Mass *m/z*	Murchison	Reagent Blank	Blank	OREX-803004-0	OREX-501029-0
1	4(3H)-Pyrimidinone, 1-tBDMS	31.5 ± 0.8	99.1	45.0	+	+	-	+	+
			153.1	99.0	+	+	-	+	+
			154.1	100.1	+	+	-	+	+
2	Imidazole, 1-tBDMS	32.3 ± 0.8	125.1	98.1	+	-	-	+	+
			155.2	140.1	+	-	-	+	+
			182.2	126.1	-	-	-	+	+
3	1-Methyl-1H-pyrazole-5-carboxylic acid, 1-tBDMS	36.7 ± 0.8	109.1	54.1	n.d.	+	-	n.d.	n.d.
			139.1	59.1	n.d.	+	-	n.d.	n.d.
			183.1	139.1	n.d.	+	-	n.d.	n.d.
4	2-ethyl-4-methylimidazole, 1-tBDMS	38.5 ± 0.8	167.1	109.1	-	-	-	+	+
			168.1	113.1	+	-	-	-	-
			224.2	168.2	+	-	-	+	-
5	Isonicotinic acid, 1-tBDMS	38.8 ± 0.8	106.0	78.1	+	+	-	+	+
			180.1	106.0	+	+	-	+	+
			180.1	136.1	+	+	-	+	+
6	Isocytosine, 1-tBDMS	38.8 ± 0.8	168.1	74.1	n.d.	-	-	+	n.d.
			168.1	99.1	n.d.	-	-	+	n.d.
			168.1	126.1	n.d.	-	-	+	n.d.
7	Alanine, 2-tBDMS	39.6 ± 0.8	158.2	73.1	+	+	-	+	+
			260.2	158.2	+	+	-	+	+
			260.2	232.2	+	+	-	+	+
8	Nicotinic acid+Picolinic acid, 1-tBDMS	39.7 ± 0.8	136.1	94.1	+	-	-	+	+
			180.1	106.0	+	-	-	+	+
			180.1	136.1	+	-	-	+	+
9	2-Methylalanine, 2-tBDMS	40.3 ± 0.8	246.2	147.1	+	+	-	+	+
			274.2	147.1	+	+	-	+	+
			274.2	246.2	+	+	-	+	+
10	Glycine, 2-tBDMS	40.4 ± 0.8	218.2	147.1	+	+	-	+	+
			246.1	147.1	+	+	-	+	+
			246.1	218.2	+	+	-	+	+
11	2-Aminobutanoic acid, 2-tBDMS	40.5 ± 0.8	246.2	147.1	+*	-	-	+	+*
			274.2	147.1	+*	-	-	+	+*
			274.2	246.2	+*	-	-	+	+*
12	β-Alanine, 2-tBDMS	41.5 ± 0.8	218.2	147.1	-	+	-	+	-
			260.2	117.1	-	+	-	-	-
			260.2	218.2	-	+	-	+	-
13	Picolinamide, 1-tBDMS	43.1 ± 0.8	179.1	75.1	+	+	-	+	+
14	Urea, 2-tBDMS	43.4 ± 0.8	147.1	131.1	n.d.	-	-	n.d.	n.d.
			231.1	147.0	n.d.	-	-	n.d.	n.d.
15	Valine, 2-tBDMS	43.5 ± 0.8	186.2	130.1	-	+	-	-	+
			260.2	147.1	-	+	-	-	+
			288.2	260.2	-	+	-	-	+
16	Leucine, 2-tBDMS	44.9 ± 0.8	274.2	147.1	+	+	-	+	+
			302.2	200.2	+	+	-	+	+
			302.2	274.2	+	+	-	+	+
17	Nicotinamide, 1-tBDMS	44.9 ± 0.8	136.1	108.1	-	-	-	-	-
			179.1	105.1	-	-	-	-	-
			179.1	136.1	-	-	-	-	-
18	Isonicotinamide, 1-tBDMS	45.3 ± 0.8	136.1	108.0	-	-	-	-	-
			179.1	136.1	-	-	-	-	-
			180.1	137.1	-	-	-	-	-
19	2,4-Diaminopyrimidine, 1-tBDMS	45.7 ± 0.8	167.1	98.1	-	-	-	-	-
			167.1	125.1	-	-	-	-	-

			167.1	150.1	-	-	-	-	-
20	Isoleucine, 2-tBDMS	45.8 ± 0.8	274.2	147.1	+	+	-	+	+
			302.2	147.1	+	+	-	+	+
			302.2	274.2	+	+	-	+	+
21	Purine, 1-tBDMS	46.0 ± 0.8	177.1	123.1	-	-	-	-	-
			178.1	136.0	-	-	-	-	-
			178.1	163.1	-	-	-	-	-
22	Proline, 2-tBDMS	46.9 ± 0.8	184.2	73.1	-	-	-	+	+
			258.2	147.1	-	-	-	n.d.	+
23	Uracil, 2-tBDMS	46.9 ± 0.8	283.1	73.0	-	+	-	+	+
			283.1	99.1	-	+	-	+	+
			283.1	147.1	-	+	-	+	+
24	6-Methyluracil, 3-tBDMS	47.9 ± 0.8	297.2	147.1	+	+	-	+	+
			298.2	148.1	+	+	-	+	+
			298.2	241.1	-	-	-	+	n.d.
25	Thymine, 2-tBDMS	49.2 ± 0.8	297.1	113.0	-	-	-	+	+
			297.1	147.1	-	-	-	+	+
			297.1	255.2	-	-	-	+	+
26	1-Methyluracil, 1-tBDMS	49.2 ± 0.8	100.0	72.0	-	-	-	n.d.	-
			183.1	72.0	-	-	-	n.d.	-
			183.1	100.0	-	-	-	n.d.	-
27	Isocytosine, 2-tBDMS	49.8 ± 0.8	282.1	125.1	-	-	-	+	+
			282.1	171.1	-	-	-	+	+
			283.2	172.1	-	-	-	+	+
28	2-imidazole-carboxylic acid, 2-tBDMS	50.3 ± 0.8	283.2	73.1	-	+	-	+	+
			283.2	239.2	-	-	-	+	+
29	Cytosine, 2-tBDMS	52.3 ± 0.8	282.1	170.1	-	-	-	-	+
			282.1	212.2	-	-	-	-	+
			283.2	213.2	-	-	-	-	+
30	Pyroglutamic acid, 2-tBDMS	52.4 ± 0.8	147.1	131.1	-	-	-	+	+
			272.2	147.1	-	-	-	+	+
			300.1	272.2	-	-	-	+	+
31	Methionine, 2-tBDMS	52.8 ± 0.8	218.1	170.2	-	-	-	-	+
			292.2	147.1	-	-	-	-	+
			320.2	292.2	-	-	-	-	+
32	5-Methylcytosine, 2-tBDMS	53.1 ± 0.8	296.2	112.1	-	-	-	-	+
			296.2	182.1	-	-	-	-	+
			296.2	226.2	-	-	-	-	+
33	Serine, 3-tBDMS	53.4 ± 0.8	362.2	147.1	-	-	-	+	+
			390.2	230.2	-	-	-	+	+
			390.2	362.2	-	-	-	+	+
34	Threonine, 3-tBDMS	54.3 ± 0.8	303.2	148.1	-	-	-	-	+
			303.2	202.1	-	-	-	-	+
			303.2	287.2	-	-	-	-	+
35	2,4-Diaminopyrimidine, 2-tBDMS	54.4 ± 0.8	281.2	125.1	-	-	-	-	-
			281.2	170.1	-	-	-	+	+
			281.2	212.2	+	-	-	+	+
36	Phenylalanine, 2-tBDMS	56.1 ± 0.8	234.2	178.1	-	-	-	-	+
			308.2	147.1	-	-	-	-	+
			336.2	308.2	-	-	-	-	+
37	Aspartic acid, 3-tBDMS	57.8 ± 0.8	302.2	147.1	-	-	-	-	+
			390.2	147.1	-	-	-	-	+
			390.2	346.3	-	-	-	-	+
38	4-imidazole-carboxylic acid, 2-tBDMS	58.3 ± 0.8	169.1	75.1	-	-	-	+	+
			169.1	125.1	-	-	-	+	+
			283.2	73.1	-	+	-	+	+
39	Hypoxanthine, 2-tBDMS	69.7 ± 0.8	193.1	111.0	-	-	-	-	-
			307.2	193.1	-	-	-	-	-
			307.2	251.1	-	-	-	-	-
40	Glutamic acid, 3-tBDMS	60.7 ± 0.8	272.2	147.1	-	-	-	+	+
			330.2	170.1	-	-	-	-	+
			432.3	272.2	-	-	-	+	+
41	Asparagine, 2-tBDMS	61.5 ± 0.8	302.2	147.1	-	-	-	+	-
			417.2	147.1	-	-	-	+	+
			417.2	400.2	-	-	-	-	-
42	Adenine, 2-tBDMS	61.6 ± 0.8	192.1	165.1	-	-	-	-	-
			306.2	192.1	-	-	-	-	-
			307.2	193.1	-	-	-	-	-

43	Lysine, 3-tBDMS	63.2 ± 0.8	300.2	147.1	-	-	-	-	-
			300.2	168.1	-	-	-	-	-
			300.2	272.2	-	-	-	-	-
44	2,6-Diaminopurine, 2-tBDMS	66.8 ± 0.8	321.2	73.1	-	-	-	-	-
			321.2	263.1	-	-	-	-	-
			321.2	305.2	-	-	-	-	-
45	Histidine, 2-tBDMS	67.9 ± 0.8	338.3	197.2	-	-	-	-	-
			440.3	280.1	-	-	-	-	-
			440.3	412.2	-	-	-	-	-
46	Xanthine, 3-tBDMS	68.3 ± 0.8	437.2	147.1	-	-	-	-	-
			437.2	363.2	-	-	-	-	-
			437.2	436.1	-	-	-	-	-
47	Tyrosine, 3-tBDMS	69.0 ± 0.8	302.2	147.1	-	-	-	-	-
			302.2	218.2	-	-	-	-	-
			302.2	245.1	-	-	-	-	-
48	Tryptophan, 2-tBDMS	69.9 ± 0.8	302.2	73.1	-	-	-	-	-
			302.2	147.1	-	-	-	-	-
			302.2	218.2	-	-	-	-	-
49	Guanine, 3-tBDMS	70.4 ± 0.8	436.3	264.1	-	-	-	-	-
			436.3	322.1	-	-	-	-	-
			436.3	435.4	-	-	-	-	-
50	2,6-Diaminopurine, 3-tBDMS	72.2 ± 0.8	435.3	263.1	+	-	-	-	-
			435.3	377.1	+	-	-	-	+
			435.3	419.2	+	-	-	-	-
51	Tryptophan, 3-tBDMS	74.3 ± 0.8	244.2	73.1	-	-	-	-	-
			244.2	188.1	-	-	-	-	-
			245.2	189.2	-	-	-	-	-
52	Cystine, 4-tBDMS	79.4 ± 0.8	348.2	106	-	-	-	-	-
			348.2	188.1	-	-	-	-	-
			348.2	302.2	-	-	-	-	-

n.d. = not determined due to MRM crosstalk from analogous ions.
*scan window insufficient to capture the entire peak.

Supplementary Table 12. A comparison of the standard protein amino acids detected in the Bennu aggregate samples compared to those reported in the meteorite literature. Amino acids with a green check mark indicate they were detected. The red X indicates the amino acid was not detected in the current study or has not been published in the literature[13].

Standard Protein Amino Acids	Meteorite Literature	OREX-803004-0 (TAGSAM) MTBSTFA PyGC-MS	OREX-501029-0 (Avionics Deck) MTBSTFA PyGC-MS	OREX-803001-0 (TAGSAM) OPA/NAC LC-MS	OREX-803001-0 (TAGSAM) AccQ·TAG LC-MS
glycine	✓	✓	✓	✓	✓
alanine	✓	✓	✓	✓	✓
proline	✓	✓	✓	n/a	✓
valine	✓	X	✓	✓	✓
leucine	✓	X	✓	✓	✓
isoleucine	✓	X	✓	✓	✓
methionine	✓[a]	X	tentative	n.d.	X
phenylalanine	✓	X	✓	n.d.	✓
threonine	✓	✓	✓	✓	✓
serine	✓	✓	✓	✓	✓
aspartic acid	✓	X	✓	✓	✓
glutamic acid	✓	✓	✓	✓	✓
asparagine	✓[b]	✓	✓	n.d.[c]	tentative[c]
glutamine	X	X	X	n.d.[c]	X[c]
tyrosine	✓	X	X	n.d.	tentative
tryptophan	X	X	X	n.d.	X
lysine	X	X	X	n.d.	X
arginine	X	X	X	n.d.	X
histidine	X	X	X	n.d.	X
cysteine	X	X	X	n.d.[c]	X[c]

[a]Single report of a weak identification in the CM2 carbonaceous chondrites ALHA 77306 and Murchison meteorite[102].
[b]First reported detection in the CM2 Murchison meteorite[54].
[c]Unstable in hot water and may have decomposed during extraction.
n.d. = not determined.
n/a = not detectable with the OPA/NAC derivatization method that does not label secondary amines.
Tentative = peak observed above background levels, but near limit of detection.

Supplementary Table 13. Qualitative comparison of the N-heterocycle detections in Bennu aggregate samples. Detections are indicated by a green check mark, and a red x indicates the compound was not detected. Previously published data from Ryugu (A0106 and C0107) and the CM2 Murchison meteorite are also shown for comparison.

Compound	OREX-501029-0	OREX-803004-0	OREX-800044-101	Ryugu[a]	Murchison[b]
Uracil	✓	✓	✓	✓	✓
Thymine	✓	✓	✓	X	✓
Cytosine	✓	X	✓	X	✓
1-Methyluracil	X	tentative	✓	X	✓
6-Methyluracil	✓	✓	✓	X	✓
5-Methylcytosine	✓	X	X	X	X
Isocytosine	✓	✓	X	X	X
2,4-Diaminopyrimidine	tentative	tentative	X	X	X
Adenine	X	X	✓	X	✓
Guanine	X	X	✓	X	✓
Purine	X	X	✓	X	✓
Hypoxanthine	X	X	✓	X	✓
Xanthine	X	X	✓	X	✓
Isoguanine	n.d.	n.d.	✓	X	✓
Diaminopurine (2,6- or 6,8-)	tentative	X	X	X	✓
Nicotinic acid	tentative	tentative	✓	✓	✓
Isonicotinic acid	✓	✓	✓	✓	✓
2-Methylnicotinic acid	n.d.	n.d.	✓	X	X
5-Methylnicotinic acid	n.d.	n.d.	✓	X	X
6-Methylnicotinic acid	n.d.	n.d.	✓	X	X
Picolinamide	tentative	tentative	tentative	X	tentative
Imidazole	✓	✓	tentative	n.d.	tentative
2-Imadazole carboxylic acid	✓	✓	✓	✓	✓
4-Imadazole carboxylic acid	✓	✓	✓	✓	✓
2-Methyl-1H-imidazole carboxylic acid	n.d.	n.d.	✓	n.d.	n.d.

[a]Data from ref. [33].
[b]Data from refs. [33,34,63].
n.d. = not determined.
Tentative = peak observed above background levels, but near limit of detection.

Supplementary Table 14. List of the measurement data products from the Bennu samples analyzed in this study and corresponding DOIs available at https://astromat.org.

EA-IRMS Data

DOI	Product Name	Product Type
EA-IRMS	OREX-501033-0, OREX-501034-0, OREX-501035-0, OREX-501036-0, OREX-501037-0, OREX-501038-0, OREX-501039-0, OREX-501040-0, OREX-501041-0, OREX-803002-0, OREX-803040-0, OREX-803041-0, OREX-803042-0, OREX-803043-0, OREX-803044-0, OREX-803045-0, OREX-803046-0, OREX-803001-104, OREX-803001-105, OREX-803001-106, OREX-803007-108, OREX-803001-109, OREX-803001-110	
10.60707/g1fx-9s05	20231210_EAIRMS_CIS_multiSample_2_EAIRMSCollection_1.zip	EAIRMSCollection
10.60707/ndf3-qn80	20231210_EAIRMS_CIS_multiSample_1_EAIRMSCollection_1.zip	EAIRMSCollection
10.60707/0g1m-4v39	20231209_EAIRMS_CIS_multiSample_1_EAIRMSCollection_1.zip	EAIRMSCollection
10.60707/m5mw-kj32	20231208_EAIRMS_CIS_multiSample_1_EAIRMSCollection_1.zip	EAIRMSCollection
10.60707/6c5n-e486	20231005_EAIRMS_CIS_multiSample_1_EAIRMSCollection_1.zip	EAIRMSCollection
10.60707/wg35-6e70	20231005_EAIRMS_CIS_OREX-501033-0_1_EAIRMSCollection_1.zip	EAIRMSCollection
10.60707/t5ac-es57	20231004_EAIRMS_CIS_multiSample_2_EAIRMSCollection_1.zip	EAIRMSCollection
Nano EA-IRMS	OREX-803001-112	
10.60707/7h3b-xk29	20240423_EA-IRMS_PSU_OREX-803001_112_1_EAIRMSCollection_1.zip	EAIRMSCollection

VIS-UV imaging/μL^2MS Data

DOI	Product Name	Product Type
VIS-UV imaging	OREX-501006-0	
10.60707/wspc-wg10	20231002_UVFM_JSC-ARES_OREX-501006-0_1_UVFMImage_1.tif	UVFMImage
μL^2MS	OREX-501006-0	
10.60707/srdv-7b95	20231127_uL2MS_JSC-ARES_OREX-501006-0_1_L2MSCube_11.h5	L2MSCube

GCMS Data

DOI	Product Name	Product Type
PyGCMS	OREX-501028-0, OREX-501029-0, OREX-803003-0, OREX-803004-0	
10.60707/579m-1256	20231003_GC-MS_GSFC_OREX-501028-0_1_GCMSCollection_1.zip	GCMSCollection
10.60707/me36-7c97	20231003_GC-MS_GSFC_OREX-501029-0_1_GCMSCollection_1.zip	GCMSCollection
10.60707/yv1f-jb20	20231121_GC-MS_GSFC_OREX-803003-0_1_GCMSCollection_1.zip	GCMSCollection
10.60707/9ww1-7a05	20231109_GC-MS_GSFC_OREX-803004-0_1_GCMSCollection_1.zip	GCMSCollection
GCMS	OREX-803001-0	
10.60707/5me5-cm54	20231201_GC-MS_GSFC_OREX-803001-0_1_GCMSCollection_315.zip	GCMSCollection

LCMS Data

DOI	Product Name	Product Type
LCMS	OREX-803001-0	
10.60707/3gcb-z762	20240131_LC-MS_GSFC_OREX-803001-0_1_LCMSCollection_1.zip	LCMSCollection
10.60707/cw79-c829	20231219_LC-MS_GSFC_OREX-803001-0_1_LCMSCollection_1.zip	LCMSCollection
10.60707/dt7a-vp76	20240201_LC-MS_GSFC_OREX-803001-0_1_LCMSCollection_1.zip	LCMSCollection
10.60707/81ff-sx95	20231114_LC-MS_GSFC_OREX-803001-0_1_LCMSCollection_1.zip	LCMSCollection
10.60707/q6zw-mb66	20231115_LC-MS_GSFC_OREX-803001-0_1_LCMSCollection_1.zip	LCMSCollection
10.60707/pwm6-na19	20231116_LC-MS_GSFC_OREX-803001-0_1_LCMSCollection_1.zip	LCMSCollection
10.60707/bt5a-4e54	20231117_LC-MS_GSFC_OREX-803001-0_1_LCMSCollection_1.zip	LCMSCollection
10.60707/c0v3-d379	20240123_LC-MS_GSFC_OREX-803001-0_1_LCMSCollection_1.zip	LCMSCollection
10.60707/gyq2-mq38	20240124_LC-MS_GSFC_OREX-803001-0_1_LCMSCollection_1.zip	LCMSCollection
LCMS	OREX-800044-101	
10.60707/m53m-r760	20240301_LC-MS_KU_OREX-800044-101_1_LCMSCollection_10.zip	LCMSCollection
10.60707/xafm-3b57	20240301_LC-MS_KU_OREX-800044-101_1_LCMSCollection_1.zip	LCMSCollection
10.60707/m48s-xe07	20240301_LC-MS_KU_OREX-800044-101_1_LCMSCollection_11.zip	LCMSCollection
10.60707/92y7-at49	20240301_LC-MS_KU_OREX-800044-101_1_LCMSCollection_12.zip	LCMSCollection
10.60707/nz85-cr04	20240301_LC-MS_KU_OREX-800044-101_1_LCMSCollection_13.zip	LCMSCollection
10.60707/s4e0-tk28	20240301_LC-MS_KU_OREX-800044-101_1_LCMSCollection_14.zip	LCMSCollection
10.60707/1h12-7408	20240301_LC-MS_KU_OREX-800044-101_1_LCMSCollection_15.zip	LCMSCollection

10.60707/3mpq-xb27	20240301_LC-MS_KU_OREX-800044-101_1_LCMSCollection_2.zip	LCMSCollection
10.60707/vswb-pw60	20240301_LC-MS_KU_OREX-800044-101_1_LCMSCollection_4.zip	LCMSCollection
10.60707/3brh-2b78	20240301_LC-MS_KU_OREX-800044-101_1_LCMSCollection_5.zip	LCMSCollection
10.60707/b9mm-0r98	20240301_LC-MS_KU_OREX-800044-101_1_LCMSCollection_6.zip	LCMSCollection
10.60707/jyjn-yh28	20240301_LC-MS_KU_OREX-800044-101_1_LCMSCollection_7.zip	LCMSCollection
10.60707/2x5w-0w88	20240301_LC-MS_KU_OREX-800044-101_1_LCMSCollection_8.zip	LCMSCollection
10.60707/1f3g-x731	20240301_LC-MS_KU_OREX-800044-101_1_LCMSCollection_9.zip	LCMSCollection

FTICR-MS Data

DOI	Product Name	Product Type
FTICR-MS	OREX-803006-0	
10.60707/tc63-1847	20240530_FTICR-MS_HMGU_OREX-803006-0_1_FTICRMSCube_1.mzml	FTICRMSCube
10.60707/ff9b-4j27	20240530_FTICR-MS_HMGU_OREX-803006-0_1_FTICRMSCube_2.mzml	FTICRMSCube
10.60707/4ceq-2x52	20240530_FTICR-MS_HMGU_OREX-803006-0_1_FTICRMSCube_3.mzml	FTICRMSCube
10.60707/gk8m-0h97	20240530_FTICR-MS_HMGU_OREX-803006-0_1_FTICRMSCube_4.mzml	FTICRMSCube
10.60707/1knn-kw48	20240530_FTICR-MS_HMGU_OREX-803006-0_1_FTICRMSCube_5.mzml	FTICRMSCube
10.60707/f6fk-dt75	20240530_FTICR-MS_HMGU_OREX-803006-0_1_FTICRMSCube_6.mzml	FTICRMSCube
10.60707/66gm-xn41	20240530_FTICR-MS_HMGU_OREX-803006-0_1_FTICRMSCube_7.mzml	FTICRMSCube
10.60707/q8jg-v633	20240530_FTICR-MS_HMGU_OREX-803006-0_1_FTICRMSCube_8.mzml	FTICRMSCube
10.60707/r8hy-7y50	20240530_FTICR-MS_HMGU_OREX-803006-0_1_FTICRMSTabular_1.csv	FTICRMSTabular
10.60707/ampq-z880	20240530_FTICR-MS_HMGU_OREX-803006-0_1_FTICRMSTabular_2.csv	FTICRMSTabular
10.60707/7aye-1h38	20240530_FTICR-MS_HMGU_OREX-803006-0_1_FTICRMSTabular_5.csv	FTICRMSTabular
10.60707/4jp0-cb92	20240530_FTICR-MS_HMGU_OREX-803006-0_1_FTICRMSTabular_4.csv	FTICRMSTabular
10.60707/48ne-8t35	20240530_FTICR-MS_HMGU_OREX-803006-0_1_FTICRMSTabular_3.csv	FTICRMSTabular
10.60707/5pt4-kr47	20240530_FTICR-MS_HMGU_OREX-803006-0_1_FTICRMSTabular_6.csv	FTICRMSTabular
10.60707/jk2s-6k42	20240530_FTICR-MS_HMGU_OREX-803006-0_1_FTICRMSTabular_7.csv	FTICRMSTabular
10.60707/3290-8d50	20240530_FTICR-MS_HMGU_OREX-803006-0_1_FTICRMSTabular_8.csv	FTICRMSTabular